ASSESSING THE INCREASED RISK OF MICROBIAL CORROSION DUE TO HYDROGEN TRANSPORTATION: PHASE 2

CLIENT: National Gas Transmission

PROJECT NUMBER: 21072

REVISION: 0

ROSEN

empowered by technology

Rev.	Date	Description	Prepared by	Reviewed by	Approved by
0	20/03/2026	Phase 2 report: Methods, Results and Conclusions	Jacqueline Penn-Morley Aidan Jaques	Ian Head	Ian Laing

© ROSEN GROUP

CONFIDENTIALITY AND COPYRIGHT

This report (including any enclosures and attachments) (the "Report") has been prepared for the exclusive use and benefit of the addressee(s) and solely for the purpose for which it is provided. Nothing in this Report should be considered a guarantee or warranty of the correctness or completeness of data or conclusions or recommendations contained herein. Unless ROSEN provides express prior written consent, no part of this Report should be reproduced, distributed or otherwise communicated to any third party. ROSEN does not accept any liability if this Report is used for an alternative purpose from which it is intended, nor shall ROSEN have any liability to any third party in respect of this Report.

EXECUTIVE SUMMARY

National Gas Transmission commissioned ROSEN to provide a two-phase project investigating whether elevated hydrogen concentrations in soil surrounding buried hydrogen pipelines could increase the risk of microbiologically influenced corrosion (MIC). Phase 1 comprised a comprehensive literature review of existing knowledge regarding MIC, the effect of hydrogen on microbial activity, and a review of MIC control measures in relevant hydrogen pipeline standards. The finding of this study informed the design of the research carried out in Phase 2. This Phase 2 report details the experimental methods, results, discussion and conclusions of this research.

This research used soils collected from three geochemically diverse pipeline excavations: [redacted] and [redacted] chosen to provide varying microbial communities. Microcosms containing steel coupons were incubated under different conditions to promote different metabolic pathways associated with MIC under a gas headspace with or without hydrogen. Incubation conditions were designed to maximise microbial activity rather than replicate in-situ conditions, allowing the influence of hydrogen on MIC-relevant processes to be studied within a limited timeframe.

Microbial activity was monitored through the uptake and production of gases including hydrogen and methane, the change in pH over the incubation period, and through analysis of the microbial community profile with 16S rRNA sequencing. Corrosion was investigated through calculation of the corrosion rate from mass loss during the incubation period, and with spectroscopic analysis of the steel coupons using scanning electron microscopy (SEM) and energy dispersive x-ray spectroscopy (EDS).

Across all three soils, hydrogen consistently stimulated microbial activity. Hydrogen consumption occurred in every live microcosm, with [redacted] and [redacted] soils exhibiting rapid depletion across most electron-acceptor treatments. Correspondingly, microcosms containing hydrogen typically demonstrated larger increases in pH than their nitrogen controls, consistent with increased proton consumption due to anaerobic respiration. Metabolic products of MIC-relevant pathways were also detected: methane production was measured only in microcosms with hydrogen in the gas headspace, and sulphur-containing deposits indicative of sulphate-reduction were identified on coupons. Sequencing revealed substantial restructuring of microbial communities in hydrogen microcosms, with clear enrichment of taxa commonly associated with MIC, including sulphate reducing bacteria *Desulfovibrionaceae*, and methanogens *Methanobacteriaceae*. In contrast, nitrogen-only treatments generally selected for fewer organisms associated with MIC compared to hydrogen microcosms.

Measured corrosion rates were relatively low (<0.03 mm yr^{-1}) across all soils and conditions, reflecting the short exposure period and small mass-loss values. However, in [redacted] and [redacted] soils, corrosion rates were generally higher in live microcosms with hydrogen than in equivalent nitrogen controls or abiotic killed-controls, and SEM imaging identified metastable pitting in several hydrogen-exposed samples.

Overall, the evidence of enhanced microbial activity, production of MIC-related metabolic products, sulphur-containing deposits, and the enrichment of microorganisms known to contribute to MIC collectively indicates that hydrogen can create conditions more susceptible to MIC. The study further demonstrates that hydrogen availability can, under certain conditions, increase corrosion rates even over short experimental timeframes.

While absolute corrosion rates measured in this study were low, the consistent enrichment of MIC associated taxa under hydrogen conditions highlights the potential for longer-term, hydrogen-driven

© ROSEN
This document is classified as confidential

MIC risk particularly in soils with favourable geochemical and microbial characteristics. These findings emphasise the importance of continued investigation into hydrogen-induced changes in soil microbial communities and their implications for pipeline integrity.

To reduce uncertainty and better reflect real-world pipeline environments, further work should include long-duration incubations, temperature-specific testing, experiments at higher hydrogen concentrations, and studies without supplemental growth media. It is also recommended that future investigations include tests both with and without cathodic protection (CP) to determine whether CP influences, or is influenced by, hydrogen-driven MIC risk.

© ROSEN
This document is classified as confidential

TABLE OF CONTENTS

EXECUTIVE SUMMARY **3**

TABLE OF CONTENTS **5**

LIST OF TABLES **7**

LIST OF FIGURES **7**

1 INTRODUCTION **9**

1.1 Scope 9

2 METHODOLOGY **10**

2.1 Introduction 10

2.2 Soil Sample Collection and Analysis 11

2.2.1 Soil Sample Collection 11

2.2.2 Soil Analysis 13

2.3 Metal Coupons 13

2.4 Incubation Conditions 14

2.4.1 Headspace Gas Analysis 15

2.5 pH measurement 16

2.6 General Corrosion Rate Calculation 16

2.7 Scanning Electron Microscopy (SEM) and Energy Dispersive X-Ray Spectroscopy (EDS) 17

2.8 Microbial Community Analysis 17

2.8.1 DNA Extraction 17

2.8.2 PCR Amplification and Gel Electrophoresis 17

2.8.3 Sequencing 18

3 RESULTS **19**

3.1 Soil Analysis 19

3.2 Headspace Gas Analysis 19

3.2.1 H_2 Consumption 19

3.2.2 Methane, Nitrous Oxide and Carbon Dioxide Production 21

3.2.3 pH Change 25

3.3 General Corrosion Rate 27

3.4 Scanning Electron Microscopy and Spectroscopic Analysis of Steel Coupons 30

3.4.1 Iron-treated microcosms 30

3.4.2 Sulphate-treated microcosms 31

3.4.3 CO_2-treated microcosms 32

3.4.4 Nitrate-treated microcosms 32

© ROSEN
This document is classified as confidential

3.4.5 Summary of SEM and EDS analysis 32
3.5 Microbial Community Analysis 33
3.5.1 Microbial Communities from [redacted] Soil inoculated microcosms 33
3.5.2 Microbial Communities from [redacted] Soil Inoculated Microcosms 37
3.5.3 Microbial Communities from [redacted] Soil Inoculated Microcosms 40
4 DISCUSSION 43
4.1 [redacted] 43
4.2 [redacted] 43
4.3 [redacted] 44
5 CONCLUSIONS AND FUTURE WORK 46
5.1 Conclusions 46
5.2 Limitations and Future Work 46
6 REFERENCES 49
APPENDIX A TOTAL ORGANIC AND INORGANIC CARBON 52
APPENDIX B MATERIALS CERIFICATES 53
B.1 Steel Data Sheet 53
B.2 Laser Cutting Data Sheet 54
B.3 Pipeline Material Chemical Analysis 55
APPENDIX C CHEMICAL COMPOSITION OF BAK AND WIDDEL GROWTH MEDIUM 56
APPENDIX D SEQUENCING COUNTS 58
APPENDIX E SEM AND EDS ANALYSIS 59
APPENDIX F PRINCIPAL COORDINATE ANALYSIS ON SOIL TREATMENTS 77
F.1 [redacted] PCoA 77
F.2 [redacted] PCoA 78
F.3 [redacted] PCoA 78

© ROSEN
This document is classified as confidential

LIST OF TABLES

Table 1: Overview of key hydrogen-consuming reactions from anaerobic hydrogenotrophic microorganisms 10

Table 2: ICP-OES Chemical analysis of BS EN 10025:2004 Grade S355JR carbon steel used as test coupons 14

Table 3: ICP-OES Chemical analysis of pipeline samples, cut from 14" X52 carbon steel fuel pipeline 14

Table 4: Experimental Conditions completed in triplicate. 15

Table 5: Soil analysis - TOC and pH. 19

LIST OF FIGURES

Figure 1: Map overview of pipeline-adjacent soil sample locations. 11

Figure 2: Pipeline excavation in [redacted] 12

Figure 3: Pipeline excavation at [redacted] gas compressor station. 13

Figure 4: Total hydrogen (mmol) consumption across microcosms under Iron-, Sulphate-, CO_2 -and Nitrate-reducing conditions. Solid lines show data from live microcosms and dashed lines show data from abiotic microcosms sterilised with 2% formaldehyde to inhibit microbial activity. 20

Figure 5: Methane (mmol) measured in the headspace of microcosms that initially contained 10% H_2 (left) or 100% N_2 (right). Solid lines show data from live microcosms and dashed lines show data from abiotic microcosms sterilised with 2% formaldehyde to inhibit microbial activity. 22

Figure 6: Nitrous oxide (mmol) measured in nitrate-treated microcosms. Solid lines show data from microcosms with hydrogen in the headspace and dashed lines show data from microcosms with no added hydrogen in the headspace. 23

Figure 7: Carbon dioxide (mmol) measurement in gas headspace across the experiment period. Hydrogen headspace microcosms on the left with nitrogen on the right. The hydrogen CO_2 treatment started with 10% CO_2 in the headspace. Solid lines show data from live microcosms and dashed lines show data from abiotic microcosms sterilised with 2% formaldehyde to inhibit microbial activity. 24

Figure 8: Microcosm Day 0 pH recorded prior to incubation and Day 28 recorded post-incubation. Average of three microcosms at the same conditions, with standard deviation shown as error bars. Soil pH for each sample location given in yellow box. 26

Figure 9: Corrosion rate of steel coupons in microcosms inoculated with different soils under four different electron accepting conditions. 28

© ROSEN
This document is classified as confidential

Figure 10: Comparison of corrosion rates of carbon steel test coupons (left) to coupons prepared from X52 pipeline material (right) in [redacted] soil under iron- and sulphate-reducing conditions with and without hydrogen in the headspace. 29

Figure 11: SEM and EDS analysis of steel coupon (a – c) and pipeline samples (d-f) prior to incubation. a) Coupon under 200x magnification, b) Coupon under 1000x magnification and c) EDS map and composition analysis of coupon. d) Pipeline sample under 200x magnification. 30

Figure 12: SEM Images of steel coupons under 200x magnification in live microcosm (a, b) and killed control (c), incubated with hydrogen in the headspace (a) or 100% nitrogen (b, c). 31

Figure 13: SEM and EDS of a) carbon steel coupons from microcosms inoculated with [redacted] soil and incubated under a 100% nitrogen headspace, and b) pipeline material sample from microcosms inoculated with [redacted] soil and incubated under a gas headspace initially containing 10% hydrogen 31

Figure 14: SEM and EDS analysis of steel coupon from microcosm inoculated with [redacted] soil incubated under a gas headspace initially containing 10% hydrogen. a) SEM image 200x magnification, b) SEM image 1000x magnification, c) EDS map showing sulphur-containing deposit 32

Figure 15: PCoA of microbial communities from [redacted] soil (green circles) and microcosms inoculated with [redacted] soil under different electron accepting conditions. Microbial communities from microcosms incubated with 10% hydrogen in the headspace are coloured red and those incubated under a nitrogen headspace are coloured blue. The changes in community composition from that of the soil prior to incubation is illustrated for microcosms incubated under (A) iron-reducing conditions in the presence of carbon steel coupons, (B) under iron-reducing conditions in the presence of coupons of X52 pipeline material (C) under sulphate-reducing and CO_2-reducing conditions in the presence of carbon steel coupons and under sulphate-reducing conditions in the presence of coupons of X52 pipeline material, and (D) under nitrate-reducing conditions. 34

Figure 16: Microbial community composition in [redacted] soil prior to incubation and following incubation under iron-, sulphate-, CO_2- and nitrate-reducing conditions with nitrogen or 10% hydrogen gas headspace. Data represent the 20 most abundant taxa categorized at Family level. 35

Figure 17: Microbial community composition in [redacted] soil prior to incubation and following incubation under iron-, sulphate-, CO_2- and nitrate-reducing conditions with nitrogen or 10% hydrogen gas headspace. Data represent the 20 most abundant taxa categorized at Family level. 38

Figure 18: Microbial community composition in [redacted] soil microcosms after 28 days of incubation with a 10% hydrogen headspace, under iron-, sulphate- and nitrate-reducing conditions. Data represent the 20 most abundant taxa categorized at Family level. 41

© ROSEN
This document is classified as confidential

1 INTRODUCTION

Hydrogen is expected to play a significant role in the energy transition towards net-zero, as a low-carbon alternative to natural gas. However, hydrogen's unique properties present significant challenges to pipeline integrity. Hydrogen's small molecular size increases the risk of leaks through small gaps in pipeline fixtures and fittings, and atomic hydrogen permeates through pipeline materials. There is, therefore, the potential for increased concentrations of hydrogen in adjacent soil environments which may promote microbial growth and increase the risk of microbiologically influenced corrosion (MIC) on external pipeline surfaces.

MIC is a well-documented corrosion mechanism capable of causing severe localised pitting, with rates often exceeding 1 – 2 mm/year in aggressive environments. Hydrogen can exacerbate these risks by serving as an energy source for hydrogenotrophic microorganisms such as sulphate-reducing bacteria (SRB), methanogens, and acetogens. These microorganisms can oxidise hydrogen and produce corrosive by-products, including hydrogen sulphide (H_2S), which accelerates corrosion and can contribute to stress corrosion cracking (SCC), posing serious threats to pipeline integrity, safety, and operational reliability.

This project studies the influence of hydrogen on soil microbial communities adjacent to pipelines, focusing on monitoring hydrogen consumption, microbial growth dynamics, community composition shifts, and the production of corrosive metabolites. Additionally, the study will characterise corrosion mechanisms by investigating MIC initiation on representative carbon steel coupons exposed to hydrogen-enhanced microbial activity under controlled conditions.

To achieve this, the project has been divided into two phases:

- Phase 1: Comprehensive literature review and baseline study, including analysis of existing standards, regulations, and best practices. This phase identified knowledge gaps and informed the experimental design for Phase 2.

- Phase 2: Laboratory based investigation of microbial activity and corrosion behaviour under simulated conditions, incorporating advanced monitoring techniques to quantify microbial metabolism, byproduct formation, and corrosion kinetics.

1.1 Scope

This Phase 2 report details the methodology of the laboratory-based research including soil sample collection (the microbial inoculum), incubation conditions, and analysis of the impact of hydrogen on microbial communities and metal coupons, with discussion and conclusions. Finally the limitations of the study and areas to focus future work are discussed.

© ROSEN
This document is classified as confidential

2 METHODOLOGY

2.1 Introduction

The Phase 1 literature review found that there may be an increased risk of MIC during hydrogen pipeline transport, due to the potential for elevated hydrogen concentrations in soil surrounding buried pipelines to enhance the growth and activity of hydrogenotrophic microorganisms. The reactions of key hydrogen-consuming microbial processes relevant to MIC are shown in Table 1.

Table 1: Overview of key hydrogen-consuming reactions from anaerobic hydrogenotrophic microorganisms

H_2 consuming process	Microbial Reaction	Free Energy $\Delta G^{0'}$ / kJ mol^{-1} H_2
Sulphate reduction	$\frac{1}{4}\ SO_4^{2-} + H_2 + \frac{1}{2}\ H^+ \rightarrow \frac{1}{4}\ HS^- + H_2O$	-38.0
Methanogenesis	$\frac{1}{4}\ HCO_3^- + H_2 + \frac{1}{4}\ H^+ \rightarrow \frac{1}{4}\ CH_4 + \frac{3}{4}\ H_2O$	-33.9
Acetogenesis	$\frac{1}{4}\ HCO_3^- + H_2 + \frac{1}{4}\ H^+ \rightarrow \frac{1}{4}\ CH_3COO^- + \frac{3}{4}\ H_2O$	-26.1
Iron reduction	$2\ FeOOH + H_2 + 4\ H^+ \rightarrow 2\ Fe^{2+} + 4\ H_2O$	−228.3
Nitrate reduction	$\frac{2}{5}\ NO_3^- + H_2 + \frac{2}{5}\ H^+ \rightarrow \frac{1}{5}\ N_2 + 1\frac{1}{5}\ H_2O$	−240.1

This Phase 2 research investigates the effect of hydrogen on the growth and metabolism of representative microbial communities likely to be found in the soil surrounding buried onshore hydrogen pipelines. It also investigates the corrosion of carbon steel by these microorganisms, and how the corrosion is affected by the addition of hydrogen.

Based on the time constraints of the research project, conditions were optimised to support microbial growth and metabolism rather than to reflect in-situ conditions. The microorganisms were supplied with the medium of Widdel and Bak, a well-established growth medium for cultivation of SRB, methanogens and acetogens containing the required nutrients to support growth and metabolism. This facilitated the study of MIC in a soil environment, without limitation of nutrients to accommodate the short timescale of the project. In addition to the growth medium, common electron acceptors that support anaerobic microbial respiration including nitrate, sulphate, ferric iron and CO_2, were added to different incubations to simulate different environmental conditions and promote different metabolic pathways [Table 1].

The soil, growth medium, electron acceptor and carbon steel coupons were incubated for a period of 4 weeks under anoxic conditions, as MIC is frequently associated with anaerobic microorganisms. Incubations with the different electron acceptors were carried out with and without hydrogen in the headspace of the sample bottle, to investigate the effect of hydrogen on MIC under these different conditions. Incubations were carried out at 30 ºC to simulate optimal mesophilic conditions, allowing for the investigation of MIC within the relatively short timescales of the project. Higher concentrations of hydrogen were used in this research than would be expected to occur in soil environments as a result of hydrogen pipeline transport, as the primary objectives of this study are to determine whether there is a risk of hydrogen increasing the rate of MIC rather than to replicate in-situ conditions given the time constraints of the research project.

© ROSEN
This document is classified as confidential

The headspace gas was sampled regularly to monitor the uptake and production of gases. The pH was measured at the start and end of the incubation period to monitor changes as a result of microbial activity. To study corrosion, the weight of carbon steel coupons was measured at the start and end of the incubation, and a corrosion rate calculated. Corrosion was also studied using SEM imaging of the samples. Controls with sterilized soil were included to distinguish corrosion, or changes in the gas headspace or pH, that occur without the influence of microbial activity from MIC. All incubations will be prepared in triplicate to facilitate statistical analysis of the results. Following the incubation period, complementary 16S rRNA gene sequencing was conducted to examine community composition differences associated with indicators of corrosion.

2.2 Soil Sample Collection and Analysis

2.2.1 Soil Sample Collection

Samples of pipeline-adjacent soil were taken from three pipeline excavation sites and used as an inoculum for laboratory incubation experiments to provide representative soil microbial communities. Locations with varied geological conditions, along with differing pipeline excavation depths between 1 and 3 m, were chosen from available locations to maximise microbial community diversity. At greater depths, soils generally have less oxygen and are therefore more likely to contain anaerobic microorganisms associated with MIC. The sample locations were [redacted] and [redacted] shown on Figure 1. Samples were collected in sterile sample bags, vacuum sealed and refrigerated at 4ºC. Soils were thoroughly mixed prior to use to increase homogeneity in the sample.

Figure 1: Map overview of pipeline-adjacent soil sample locations.

2.2.1.1 [redacted]

Soil was collected from a pipeline excavation in [redacted] West Lothian, at a depth of approximately 2.5 m. The sampling location coordinates were 55°54.687' N, 003°41.197' W. According to British Geological Survey data, the soil parent material at this site is classified as Glacial Till, a mixture of clay, sand, and gravel that typically forms dense, poorly structured soils with limited drainage [1] [Figure 2].

Figure 2: Pipeline excavation in [redacted]

2.2.1.2 [redacted]

Soil was collected from a pipeline excavation on the [redacted] pipeline in the Bannau Brycheiniog (Brecon Beacons) National Park, South Wales. The pipeline-adjacent sample was taken from a depth of approximately 1 m, the coordinates of the sample location are: 51°49′28″N, 003°11′24″W. According to LandIS® data, soils in this area are highly variable due to the complex underlying geology; however, the sampling location is classified as blanket bog peat soil [2]. This soil type is typically waterlogged (anaerobic), slightly acidic, and rich in organic carbon.

2.2.1.3 [redacted]

Soil was collected from an excavation at [redacted] gas compressor station, Cambridgeshire. The pipeline-adjacent soil sample was taken at a depth of approximately 3 m. Coordinates of the sample location are: 52°18′41″N, 000°21′45″W. Data from LandIS® categorises the soil in the sample location as lime-rich (alkaline), loamy, and clayey with impeded drainage [2].

© ROSEN
This document is classified as confidential

Figure 3: Pipeline excavation at [redacted] gas compressor station.

2.2.2 Soil Analysis

Total Organic Carbon (TOC) was measured for each sample location to provide information about the soil conditions. A higher TOC is generally associated with a more active and diverse microbial community. TOC was measured using a Leco RC612 multiphase carbon analyser. Two samples were analysed from each soil location and an average value taken. Raw data from TOC analysis is provided in Appendix A.

2.3 Metal Coupons

A complete set of experiments was carried out using carbon steel coupons, which were laser cut from a plate of BS EN 10025:2004 Grade S355JR carbon steel. The dimensions of the coupons were 8 x 8 x 4 mm. The material test certificate is given in Appendix B.1. The laser cutting datasheet is given in Appendix B.2. Inductively Couple Plasma-Optical Emission Spectroscopy (ICP-OES) Chemical composition of the steel, provided by the manufacturer, is given in Table 2.

Carbon steel plate was used as a test material to represent X52 carbon steel pipeline, as it was not feasible to use pipeline samples due to the quantity required for this research and the relatively short project timescale. Both S355JR carbon steel and X52 carbon steel are low-alloy carbon-manganese steels, and MIC mechanisms depend primarily on environmental and microbiological factors across carbon–manganese steels of comparable composition. Trends in MIC observed across the range of conditions tested, with and without hydrogen, will therefore be applicable to all grades of carbon steel pipeline that may be used to transport hydrogen.

© ROSEN
This document is classified as confidential

Table 2: ICP-OES Chemical analysis of BS EN 10025:2004 Grade S355JR carbon steel used as test coupons

Element	C	Si	Mn	P	S	Cr	Mo	Ni	Cu	V	Al	Nb	N	Ce
%	.13	.020	1.16	.012	.009	.04	.002	.010	.020	.072	.032	.001	.005	.348

A small number of duplicate experiments were also carried out using carbon steel samples cut from an excavated section of a 14" fuel pipeline, determined to be grade X52. This was to observe any differences in corrosion between the test coupons and pipeline material. The dimensions of the pipeline samples were 8 x 8 x 8 mm. Chemical analysis of the pipeline using ICP-OES is given in Table 3. The carbon equivalent value (CEV) of the material was calculated to be 0.39. The material test certificate is given in Appendix B.3.

Table 3: ICP-OES Chemical analysis of pipeline samples, cut from 14" X52 carbon steel fuel pipeline

Element	C	Si	Mn	P	S	Cr	Mo	Ni	Cu	V	Al	Nb	Ti	V
%	.20	.13	1.00	.020	.021	.03	< .01	.08	.16	< .01	< .01	< .01	< .01	< .01

2.4 Incubation Conditions

The primary objectives of this study are to determine whether there is a risk of hydrogen increasing the rate of MIC, rather than to replicate in-situ conditions due to the time constraints of the research project. Conditions were therefore optimised to support microbial growth, in terms of nutrient availability and incubation temperature.

All incubations were carried out for 28 days at 30 ºC in sealed 250 ml borosilicate glass serum bottles closed with thick, gas-impermeable butyl rubber stoppers and crimp sealed. Incubations contained 5 g of soil and 100 ml of Bak and Widdel growth medium [3] containing different chemical electron acceptors: nitrate, ferric iron, sulphate and carbon dioxide. These electron acceptors were chosen to promote four common metabolic pathways commonly associated with MIC: nitrate reduction, iron reduction, sulphate reduction and methanogenesis. The incubations are referred to as microcosms hereafter. The chemical composition of the Bak and Widdel growth medium is given in Appendix C.

Electron acceptors nitrate (sodium nitrate, $NaNO_3$), iron (iron(III) citrate, $C_6H_5FeO_7$), and sulphate (sodium sulphate, Na_2SO_4) were provided in solution at a concentration of 5 mmol L^{-1}, carbon dioxide (CO_2) was provided in the gas headspace at a concentration of 10% (v/v).The headspace gas of the sealed serum bottles with hydrogen contained 10% (v/v) hydrogen (H_2) in a balance of nitrogen (N_2), except for incubations with carbon dioxide and hydrogen, which contained 10% (v/v) hydrogen and 10% (v/v) carbon dioxide in a balance of nitrogen. Corresponding incubations without hydrogen were set up in parallel for comparison containing 100% nitrogen in the gas headspace. Higher initial concentrations of hydrogen were used than would be expected to occur in soil due to the primary objective of the research being to determine whether hydrogen can increase the risk of MIC rather than to replicate soil conditions.

© ROSEN
This document is classified as confidential

To minimise gas leakage, the microcosms were inverted so the liquid phase was in contact with the stopper. Killed control incubations with sterilized soil were set up to distinguish MIC from corrosion that occurs without the influence of microbial activity. Blank incubations were set up, containing Bak and Widdel medium without soil as a control.

Each incubation contained two carbon steel coupons; one used for weight loss measurement and the other preserved for further analysis. Four additional experiments were set up containing coupons cut from a sample of excavated pipeline at the conditions that were expected to be most aggressive, for comparison of corrosion between the test coupons and pipeline material.

Three replicate incubations were set up at each condition to facilitate statistical analysis of the results. A table of experimental conditions and associated sample ID is shown in Table 4.

Table 4: Experimental Conditions completed in triplicate.

Electron Acceptor	Iron		Sulphate		Carbon Dioxide		Nitrate	
Headspace Gas	**10% H_2 90% N_2**	**100% N_2**	**10% H_2 90% N_2**	**100% N_2**	**10% H_2 10% CO_2 80% N_2**	**100% N_2**	**10% H_2 90% N_2**	**100% N_2**
[redacted]	HIH	NIH	HSH	NSH	HCH	NCH	HNH	NNH
[redacted]	HIF	NIF	HSF	NSF	HCF	NCF	HNF	NNF
[redacted]	HIW	NIW	HSW	NSW	HCW	NCW	HNW	NNW
[redacted] Killed	HIHK	NIHK	HSHK	NSHK	HCHK	NCHK	HNHK	NNHK
[redacted] Killed	HIFK	NIFK	HSFK	NSFK	HCFK	NCFK	HNFK	NNFK
[redacted] Killed	HIWK	NIWK	HSWK	NSWK	HCWK	NCWK	HNWK	NNWK
Blank	IB		SB		CB		NB	
Pipeline Sample + [redacted] soil	HIPM	NIPM	HSPM	NSPM				

2.4.1 Headspace Gas Analysis

The headspace was sampled regularly to monitor the uptake and production of gases by microorganisms in the microcosms. A 4.5 ml sample of headspace gas was taken weekly using a 5 ml syringe and 22G needle (Terumo Agani). These samples were transferred to pre-evacuated exetainers. Needles and syringes were flushed with nitrogen prior to use. Gas was sampled in 1.5 ml aliquots from the exetainers using a 2.5 ml gastight 1002SL syringe and 26S needle (Hamilton).

The concentration of hydrogen in the gas headspace was measured to monitor microbial hydrogen consumption in different conditions. This was conducted using a SRI 8610C Gas Chromatograph with Thermal Conductivity Detector (GC -TCD). Before sample injection, the GC-TCD was heated at 300°C for 2.5 hours to remove any residual contaminants from the column. Gases were injected via a 0.5 mL sample loop onto a 6 ft long packed molecular sieve 5 Å column at a constant pressure of 30 psi with nitrogen carrier gas, column temperature of 40°C, and TCD temperature of 100°C. After every nine samples run, a standard of 1.5 ml of 1% hydrogen, 99% nitrogen was run to correct for any drift. Each sample's peak area was manually integrated. Peak areas were calibrated through two control standards of 1% hydrogen and 10% hydrogen in a balance of nitrogen. Gas concentrations (%) were converted to mmol using the ideal gas law.

© ROSEN
This document is classified as confidential

Concentrations of methane (CH_4), carbon dioxide (CO_2), and nitrous oxide (N_2O) were analysed on a Gas Chromatograph – Mass Spectrometer (GC-MS) (Agilent 5977B). This used helium gas as a carrier at 49.5 ml min^{-1} and 6.181 psi with oven temperature at 35°C and heat at 150°C. Standards of 1% methane, 1% carbon dioxide in 98% nitrogen and 10% methane, 10% carbon dioxide in 80% nitrogen were run at 20 µl, 40 µl, 60 µl, 80 µl, and 100 µl, respectively prior to manual injection of 100 µl from exetainer samples. Peak areas were automatically calculated by the GCMS software. A linear calibration curve was generated from the standards. Peak areas were converted into mmol using the ideal gas law.

2.5 pH measurement

Soil pH was measured to provide information about the soil condition in each of the sample locations. This was measured by mixing a 1:1 ratio of soil with distilled water, stirring and leaving for 5 minutes before taking a pH measurement in triplicate.

The pH of the microcosms was measured before and after incubation, as changes in microcosm pH can indicate microbial activity. Microorganisms can produce or consume acidic or basic metabolites or substrates. Sulphate reduction, methanogenesis, nitrate reduction and iron reduction can all increase pH through the consumption of H+ ions.

pH was recorded using a Mettler Toledo Micro pH electrode in triplicate following a triple-point calibration (4.01/7.00/10.00 respectively).

2.6 General Corrosion Rate Calculation

The general corrosion rate was calculated from the mass loss of the coupons over the incubation period, to allow comparison of corrosion rates under different conditions.

Prior to being added to the microcosms, all metal coupons were cleaned with 70% ethanol, dried with a paper towel, and weighed. After the incubation period, one of the two coupons per microcosm was cleaned with 70% ethanol, lightly scrubbed with a wire brush (non-iron wire) to remove corrosion products, dried with paper towel and re-weighed. The other coupon in each microcosm was preserved in 50% ethanol for further analysis.

The general corrosion rate (*CR*) in mm yr^{-1} was calculated using Equation 1 where M_x is the mass of the coupon pre-incubation in g, M_y is the mass of the coupon post-incubation in g, *A* is the surface area of the coupon in mm^2, *t* is the incubation time in yr, and ρ is the density in g mm^{-3}. As three incubations were carried out at each test condition, a mean corrosion rate (mm yr^{-1}) and standard deviation was calculated for each test condition, for comparison between the different conditions and soils.

$$CR = \frac{M_x - M_y}{A \times t \times \rho} \qquad Equation\ 1$$

© ROSEN
This document is classified as confidential

2.7 Scanning Electron Microscopy (SEM) and Energy Dispersive X-Ray Spectroscopy (EDS)

SEM Imaging was used to analyse the corrosion morphology of the coupons, and EDS to identify any corrosion products. The metal coupons were analysed using a JEOL JSM-IT510 InTouchScope™ Scanning Electron Microscope with integrated EDS. SEM images and EDS spectra were taken under high vacuum with secondary electron detection using an accelerator voltage of 20 kV and a working distance of 10 mm.

2.8 Microbial Community Analysis

The microbial community composition was analysed in the original soil sampled from pipeline excavations, and in microcosms incubated under the various different conditions, using complementary 16S rRNA gene sequencing. This allowed examination of how community profiles changed in response to each condition and enabled the identification of microbial groups associated with MIC. First DNA was extracted from the samples, then the viability of the extracted DNA was determined with gel electrophoresis testing. Viable samples were then sequenced.

2.8.1 DNA Extraction

DNA was extracted using the Qiagen DNeasy® PowerSoil® Pro Kit. The standard protocol recommended by the kit manufacturer was followed, outlined in the DNeasy® PowerSoil® Pro Kit Handbook [4].

2.8.2 PCR Amplification and Gel Electrophoresis

The viability of extracted DNA for sequencing was determined using polymerase chain reaction (PCR) amplification and gel electrophoresis testing.

16S rRNA PCR amplification was performed using Earth Microbiome Project (EMP) primers (V4F: 5'-GTG YCA GCM GCC GCG GTA A -3'; V4R: 5'-GGA CTA CNV GGG TWT CTA AT-3'). 2 µl of purified DNA solution (prepared as described in section 2.8.1), 22 µl of MegaMix blue reaction mix (Microzone, UK) containing 0.50 µl of each EMP primer, dNTP (220 µM), $MgCl_2$ (2.75 mM), and Taq DNA polymerase, were added to a 25 µl PCR amplification reaction tube. The amplification was carried out in a Techne thermocycler (Bibby Scientific, UK) with the following PCR cycling conditions: 40 cycles at Denature (95°C) for 1 min, Annealing (55 °C) for 1 min and Extension (72 °C) for 1 min; and final extension at 72 °C for 5 min.

To conduct gel electrophoresis testing, a 1% agarose gel (using 0.8 g of ultrapure agarose per 80 ml of 1x Tris-Acetate EDTA (TAE) buffer, pH 8.0) was prepared by dissolving the agarose in TAE buffer in a 250 ml conical flask. The agarose the solution was heated in a microwave oven for 10-seconds at a time, until the agarose was fully dissolved. The agarose solution was left to cool slightly before adding 8 µl of SYBR Safe DNA Gel Stain and pouring into a gel casting tray fitted with a 20-well comb. After the gel cooled and solidified, the well-forming comb was removed before placing it in a gel tank, which was filled with TAE buffer to submerge the gel. 5 µL of each PCR reaction was transferred to separate wells. An electrical current of 110 V at 400 amps was run for 50 minutes to separate the DNA. The electrophoresis results of each PCR product were visualized and images captured using VisionWorks

© ROSEN
This document is classified as confidential

image analysis system (Ultra-Violet Products, USA). Samples that showed successful PCR amplification of 16S rRNA genes were used for 16S rRNA sequencing.

2.8.3 Sequencing

16S rRNA genes were amplified from total DNA, and the V4 variable region was sequenced following the Illumina 16S rRNA gene Amplicon Protocol using primers 515F :GTGCCAGCMGCCGCGGTAA; and 806R:GGACTACHVGGGTWTCTAAT) from the Earth Microbiome Project [5]. Sequencing was conducted by the NU-Omics facility, Northumbria University.

Raw sequence data (FastQ files) obtained from the Illumina sequencing platform were demultiplexed and analysed using QIIME2 and DADA2, against the SILVA132 reference database of 16S rRNA sequences [5, 6, 7]. QIIME2 is an open-source bioinformatics platform used to analyse, visualise and interpret microbiome data.

The QIIME2 feature table output consisted of count data for different amplicon sequence variants (ASVs, are unique DNA sequences recovered from sequencing data and in a general sense correspond to microbial species) [Appendix E]. For taxonomic visualisation, ASV count data were normalised to relative abundance within each sample. To reduce noise from rare taxa and improve interpretability of the bar plots, taxa with a relative abundance below 0.5% were filtered and grouped to form “Others”, and the top 20 most abundant taxa in each sample were were displayed in stacked bar charts.

Beta diversity analysis (comparative analysis of the microbial community composition in different samples) was performed by calculating pair-wise Bray-Cutris dissimilarity of microbial communities in all samples. The Bray-Curtis distance matrix was analysed using Principal Coordinate Analysis (PCoA). PCoA reduces the dimensionality of the distance matrix by calculating eigenvalues and eigenvectors, allowing patterns of similarity or dissimilarity among samples to be visualised in 2D/3D space [Appendix F].

© ROSEN
This document is classified as confidential

3 RESULTS

3.1 Soil Analysis

The average values for total organic carbon and soil pH for each soil location are shown in Table 5. [redacted] soil had the highest TOC of 3.35%, followed by [redacted] with a TOC of 2.8. Both of these values fall within the high soil health category and indicate a fertile and biologically active soil [8]. [redacted] soil had a very low TOC of 0.21%, indicating severely depleted soil organic matter with limited microbial life [8]. It is possible that the sample contained pipeline backfill rather than, or in addition to, native soil which would contribute to the low TOC.

The pH of [redacted] is near-neutral (6.92), which aligns with expectations for its Glacial Till parent material, typically composed of mixed clay, sand, and gravel [1]. The pH of [redacted] is slightly acidic (4.62), consistent with LandIS® data identifying the area as blanket bog peat soil [2]. This soil type is often anaerobic, slightly acidic, and rich in organic carbon. The pH of [redacted] is slightly alkaline, matching LandIS® data which categorises the local soil type as lime-rich [2].

Table 5: Soil analysis - TOC and pH.

Sample Location	TOC (%)	pH
[redacted]	2.80	6.92
[redacted]	3.35	4.62
[redacted]	0.21	8.29

3.2 Headspace Gas Analysis

3.2.1 H_2 Consumption

Figure 4 shows the amount of hydrogen measured in the headspace for the four different electron-acceptor treatments: iron, sulphate, carbon dioxide and nitrate. For each treatment, the hydrogen concentration is plotted for the live and killed soil samples from the three different sample locations: [redacted] [redacted] and [redacted] The headspace gas in each of these incubations was initially 10% hydrogen in a balance of nitrogen, meaning there was approximately 0.6 moles of hydrogen in each microcosm at the start of the incubation. Each value plotted is the average of data from three replicate microcosms at the same conditions, with the standard deviation shown as error bars. The amount of hydrogen in the headspace was measured every 7 days throughout the 28 day incubation period, starting from day 0, to monitor hydrogen consumption. Note, hydrogen was not measured in the microcosms starting with 100% nitrogen in the headspace [see Table 4].

© ROSEN
This document is classified as confidential

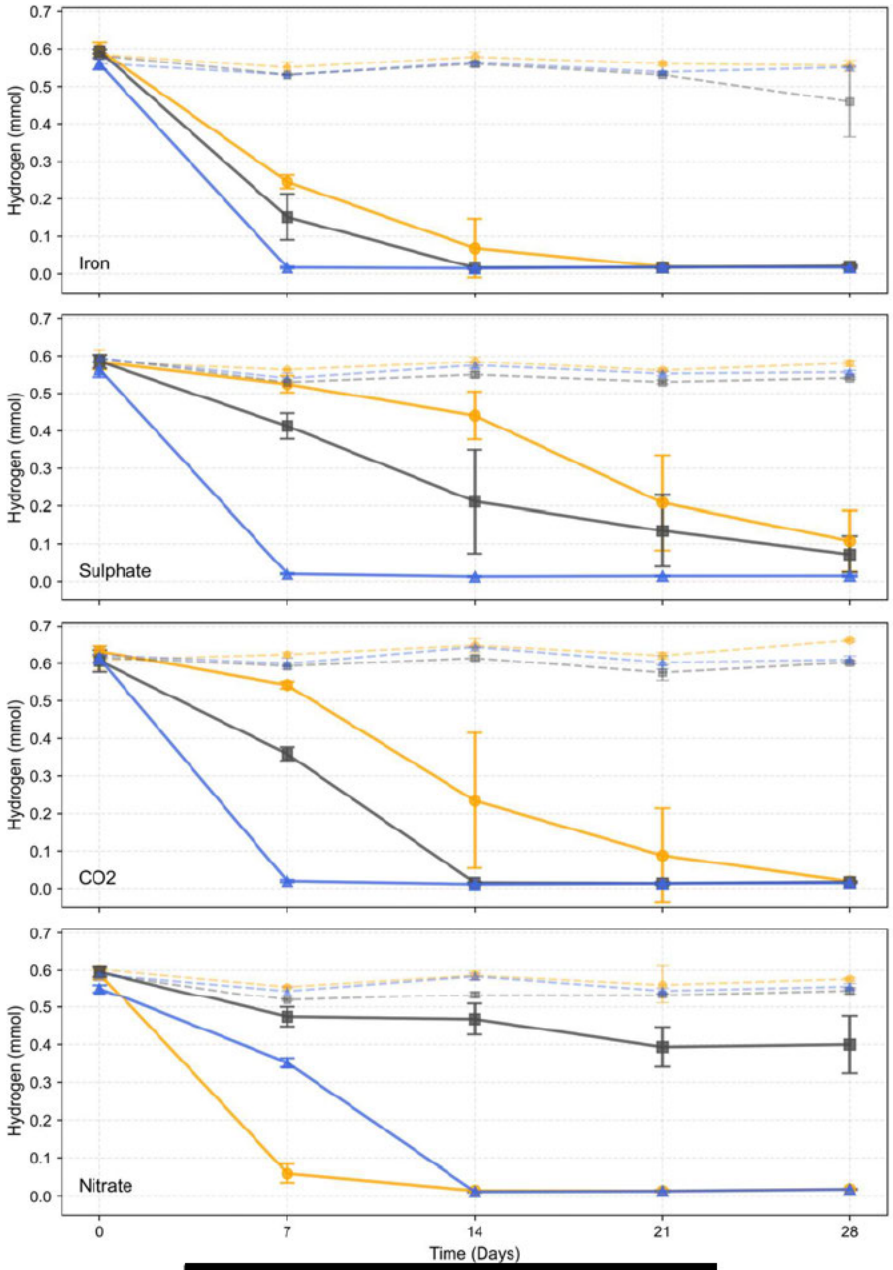

[redacted]

Figure 4: Total hydrogen (mmol) consumption across microcosms under Iron-, Sulphate-, CO_2 -and Nitrate-reducing conditions. Solid lines show data from live microcosms and dashed lines show data from abiotic microcosms sterilised with 2% formaldehyde to inhibit microbial activity.

All live soil samples demonstrated hydrogen during the experimental period, though consumption rates varied considerably between soil types and treatments [Figure 4]. In contrast, the amount of hydrogen stayed constant in abiotic kill controls, demonstrating the reduction in hydrogen concentration in live microcosms was due to microbial hydrogen consumption.

[redacted] soil demonstrated the most rapid hydrogen consumption, with complete depletion achieved by day 7 in the iron, sulphate, and carbon dioxide treatments. The nitrate treatment proceeded more slowly, 0.2 mmol consumed by day 7, but achieved complete consumption by day 14. This suggests the [redacted] soil sample contained an active and versatile community of hydrogenotrophic microorganisms.

[redacted] soil showed substantial hydrogen consumption in all treatments except nitrate. The Iron treatment exhibited rapid hydrogen consumption with 0.44 mmol of hydrogen consumed by day 7 and complete consumption by day 14, while the carbon dioxide treatment was slower with 0.24 mmol of hydrogen consumed by day 7 and complete consumption by day 14. The sulphate treatment results show steady hydrogen consumption through day 28, leaving 0.07 mmol residual hydrogen. Nitrate was the only treatment to have considerable hydrogen remaining in the headspace by day 28 with 0.39 mmol remaining.

[redacted] soil exhibited the slowest hydrogen consumption in all treatments except nitrate-treated microcosms. [redacted] soil exhibited rapid hydrogen consumption in the nitrate treatment with 0.53 mmol of hydrogen was consumed by day 7 with complete consumption by day 14. Iron was the next treatment to show complete hydrogen consumption, which occurred by day 21 and the carbon dioxide treatment by day 28. The sulphate treatment showed the slowest consumption, with 0.1 mmol residual hydrogen remaining at day 28. This suggests nitrate was the preferred electron acceptor in the [redacted] soil microbial community, and that the [redacted] soil had an active population of nitrate-reducing bacteria.

Overall, there are notable differences in hydrogen consumption by the three different soils, indicating variation in the composition and activity of their microbial communities. Generally, the soil microbial communities showed preferential hydrogen consumption under iron-reducing conditions, with microbial communities of all three soils achieving complete consumption of hydrogen by day 21.

3.2.2 Methane, Nitrous Oxide and Carbon Dioxide Production

In addition to hydrogen (H_2), methane (CH_4), carbon dioxide (CO_2) and nitrous oxide (N_2O) were measured in the gas headspaces during the incubation period.

3.2.2.1 Methane

Methanogens can convert carbon dioxide or organic carbon to methane through methanogenesis, which is linked to MIC through the cathodic depolarisation of metals, and in some cases, electrical MIC through the direct uptake of electrons from the metal surface. Figure 5 shows the concentration of methane measured in microcosms with hydrogen (left) and without hydrogen (right) in the gas headspace.

© ROSEN
This document is classified as confidential

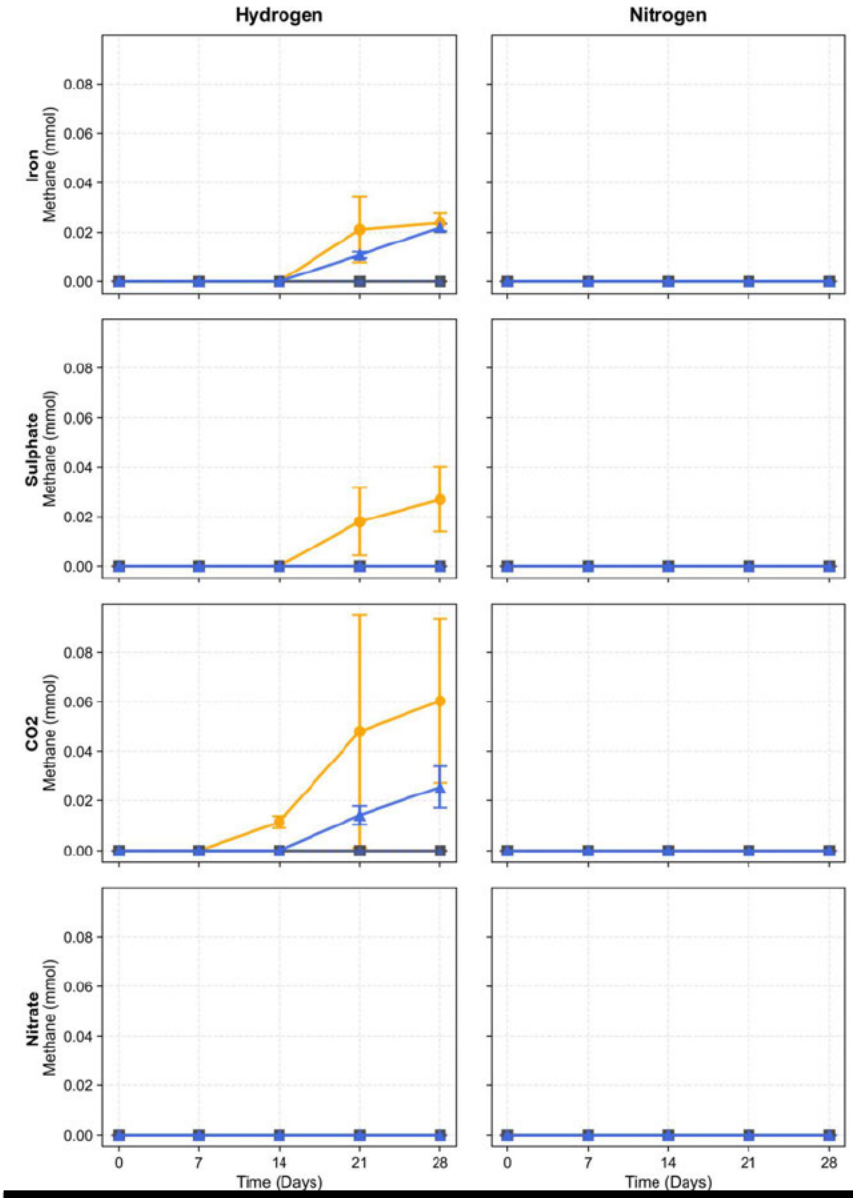

[redacted]

Figure 5: Methane (mmol) measured in the headspace of microcosms that initially contained 10% H_2 (left) or 100% N_2 (right). Solid lines show data from live microcosms and dashed lines show data from abiotic microcosms sterilised with 2% formaldehyde to inhibit microbial activity.

Methane was detected only in microcosms with hydrogen in the headspace, no methane was detected in any of the nitrogen headspace microcosms [Figure 5]. [redacted] soil microcosms produced 0.021 and 0.025 mmol of CH_4 in treatments of iron and CO_2 respectively by day 28. [redacted] soil microcosms produced 0.023 mmol, 0.027 mmol and 0.06 mmol of CH_4 in treatments of iron-, sulphate- and CO_2-treated microcosms respectively by day 28. [redacted] soil did not produce a measurable quantity of methane across any treatments under hydrogen or nitrogen headspace. If methanogenesis were the only pathway for hydrogen consumption, a maximum of 0.15 mmol of methane would be expected;

© ROSEN
This document is classified as confidential

however as a maximum of 0.06 mmol was measured, other hydrogen consumption pathways must also be active during this period.

3.2.2.2 Nitrous Oxide

Nitrous oxide (N_2O) is an and end-product or intermediate produced by different nitrate-reducing, denitrifying bacteria following the anaerobic denitrification pathway ($NO_3^- \rightarrow NO_2^- \rightarrow NO \rightarrow N_2O \rightarrow N_2$). While all microcosm gas headspaces were analysed, nitrous oxide was only detected in live microcosms with nitrate treatment, shown in Figure 6. No N_2O was detected in any of the killed control microcosms.

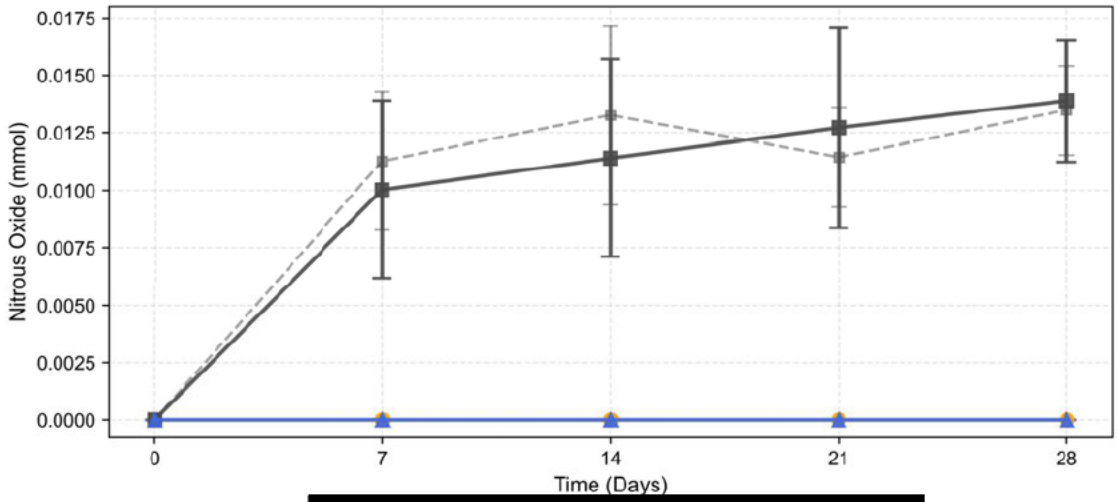

[redacted]

Figure 6: Nitrous oxide (mmol) measured in nitrate-treated microcosms. Solid lines show data from microcosms with hydrogen in the headspace and dashed lines show data from microcosms with no added hydrogen in the headspace.

Nitrous oxide was detected only in live microcosms with nitrate treatment, none was detected in CO_2, iron or sulphate treatments or any killed control microcosms. [redacted] soil produced approximately 0.013 mmol of N_2O by day 28 in both hydrogen and nitrogen gas headspaces [Figure 6]. Trace amounts of N_2O were also detected in [redacted] soil by day 21 and day 28, however the amount of N_2O was too low to be quantified using the GC-MS analysis employed. N_2O was not detected in the [redacted] soil microcosms.

[redacted] soil showed the slowest hydrogen consumption in nitrate treated microcosms [Figure 4] compared to [redacted] or [redacted] suggesting a lower affinity for nitrate as an electron acceptor compared to the other soils. This may explain why N_2O, an intermediate in microbiological nitrate reduction, is only measured in the headspace of this microcosm. It is possible that complete reduction of nitrate (NO_3^-) to N_2 occurred too quickly for the intermediate nitrous oxide to be measured in the [redacted] and [redacted] soils, that demonstrated a stronger affinity towards nitrate as an electron acceptor.

3.2.2.3 Carbon Dioxide

Carbon dioxide was measured in the gas headspace of the microcosms to analyse the uptake and production of CO_2 as a result of microbial activity, shown in Figure 7. The headspace of the microcosms with hydrogen (left) initially contained 10% hydrogen in 90% nitrogen except for the carbon dioxide treatment which contained 10% hydrogen, 10% carbon dioxide in 80% nitrogen. All of the microcosms without hydrogen (right) initially contained 100% nitrogen.

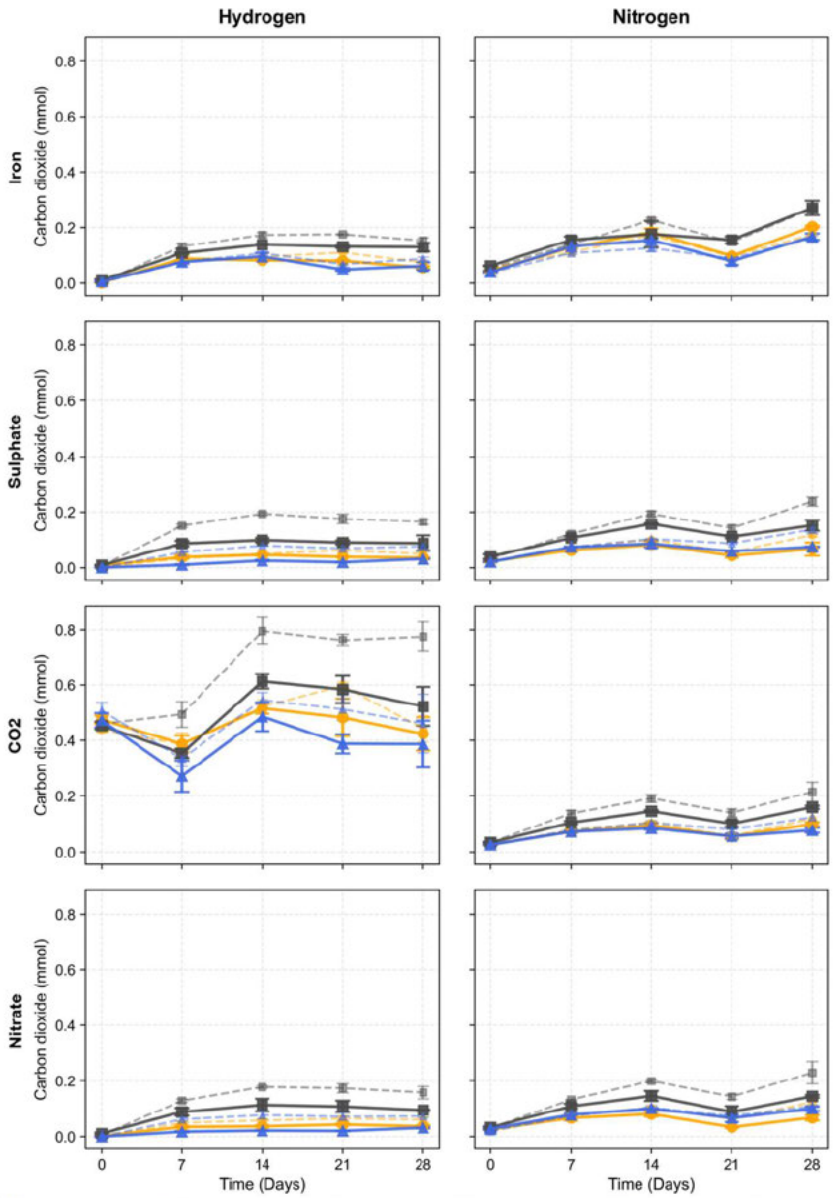

[redacted]

Figure 7: Carbon dioxide (mmol) measurement in gas headspace across the experiment period. Hydrogen headspace microcosms on the left with nitrogen on the right. The hydrogen CO_2 treatment started with 10% CO_2 in the headspace. Solid lines show data from live microcosms and dashed lines show data from abiotic microcosms sterilised with 2% formaldehyde to inhibit microbial activity.

© ROSEN
This document is classified as confidential

Carbon dioxide in the headspace of most microcosms, hydrogen, nitrogen and kill controls increased from day 0 to day 28 in all soil types [Figure 7]. The exception was the hydrogen CO_2 treatment where there was a net CO_2 decrease in [redacted] by 0.051 mmol and [redacted] by 0.086 mmol, while CO_2 in [redacted] soil increased by 0.068 mmol.

The overall increase of CO_2 in live microcosms can be down to the release of CO_2 into the headspace from decaying organic matter found naturally in the soils. Additionally, the pH buffer of sodium bicarbonate used to balance the pH of each system can also release CO_2 into the headspace. [redacted] across all microcosms is seen to hold the highest CO_2 in each treatment, while the starting pH of [redacted] soil is more acidic than [redacted] or [redacted] This may cause the bicarbonate solution to release more CO_2 into the headspace to maintain a more neutral system. The reduction in CO_2 in [redacted] and [redacted] in CO_2-treated live microcosms between day 0 and day 28 could be due to the production of methane by methanogenesis, demonstrated in Figure 5. However, the stoichiometry of methanogenic CO_2 reduction with hydrogen would suggest that there should be a one to one correspondence between CO_2 consumed (0.051 – 0.086 mol) and methane produced (0.02 – 0.06 mol) indicating that there may be another metabolic pathway for CO_2 consumption in these systems such as acetogenesis [Table 1]

3.2.3 pH Change

Changes in microcosm pH can indicate microbial activity, sulphate reduction, methanogenesis, nitrate reduction and iron reduction can all increase pH through the consumption of H^+ ions. The pH of each soil and medium was measured prior to microcosm set up (day 0) and immediately after the final headspace sampling on day 28. All pH measurements for all soil locations and all treatments containing hydrogen and nitrogen in the headspace and killed controls are shown in Figure 8.

© ROSEN
This document is classified as confidential

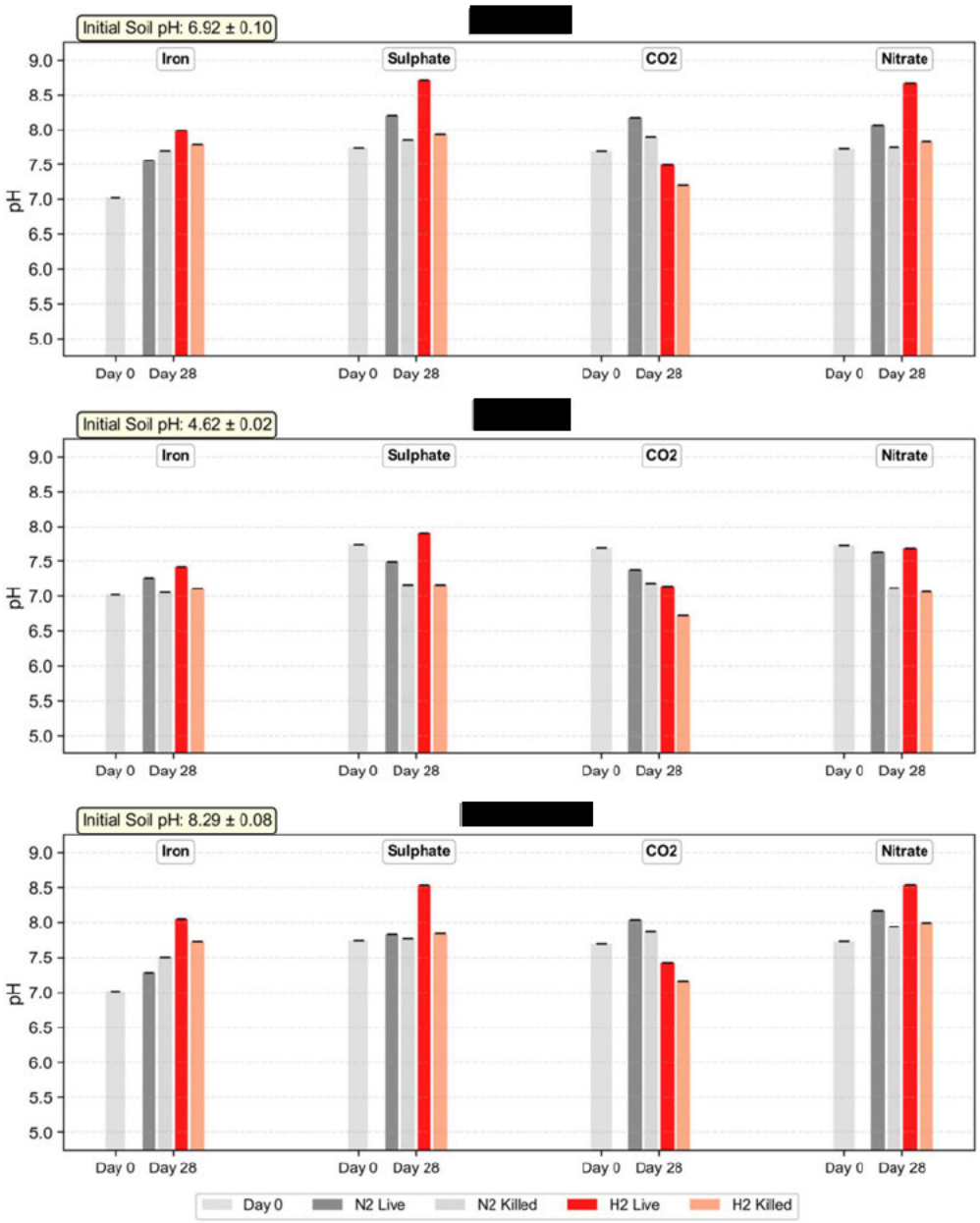

Figure 8: Microcosm Day 0 pH recorded prior to incubation and Day 28 recorded post-incubation. Average of three microcosms at the same conditions, with standard deviation shown as error bars. Soil pH for each sample location given in yellow box.

In microcosms inoculated with [redacted] soil, pH increased in live microcosms with hydrogen in the headspace under iron-, sulphate- and nitrate-reducing conditions [Figure 8] with pH increases of 0.97, 0.96 and 0.94 respectively. In live hydrogen microcosms with CO_2 in the headspace, the pH decreased by 0.2. The pH in microcosms with 100% nitrogen (no hydrogen) in the headspace increased less than in microcosms that contained hydrogen in the headspace. In these microcosms, pH increases were 0.53, 0.46, and 0.34 in iron, sulphate and nitrate treatments respectively. The pH increase was greater in live microcosms with hydrogen in the headspace under iron-, sulphate- and nitrate-reducing

conditions compared to the corresponding killed controls, suggesting that this increase in pH is likely due to hydrogen-stimulated microbial activity.

[redacted] soil showed less pronounced changes in pH compared to [redacted] soil. Hydrogen-containing microcosms treated with iron and sulphate showed an increase in pH of 0.40 and 0.16 respectively, while the pH in nitrate-treated microcosms with hydrogen in the headspace remained constant [Figure 8]. By contrast in microcosms with CO_2 in the headspace the pH decreased by 0.54. Microcosms with a 100% nitrogen headspace showed a pH increase of 0.24 in the iron treatment, while sulphate and nitrate treatments led to a decrease in pH of 0.25 and 0.09 respectively. By day 28 the pH was higher in all live microcosms than their equivalent killed controls in all treatments, and the pH increase in live hydrogen-containing microcosm was greater than in the corresponding killed controls, suggesting increased microbial activity.

Microcosms inoculated with [redacted] soil exhibited an increase in pH from day 0 to day 28 in live hydrogen-amended microcosms under iron-, sulphate- and nitrate-reducing conditions, with pH increases of 1.03, 0.79 and 0.80 respectively. By contrast the pH decrease by 0.27 in microcosms with CO_2 in the headspace [Figure 8]. A smaller pH increase is observed in microcosms with 100% nitrogen in the headspace under iron-, sulphate- and nitrate-reducing conditions, with pH increases of 0.26, 0.08 and 0.43 respectively. There was a consistently greater increase in pH in live hydrogen-containing microcosms compared to abiotic killed controls under iron-, sulphate- and nitrate-reducing conditions.

There is a consistent pattern of pH differences between treatments following 28 days of incubation independent of the soil inoculum used, with a higher pH in hydrogen-treated microcosms under the majority of conditions compared to nitrogen microcosms across all soil types. [redacted] and [redacted] experience greater changes in pH than [redacted] It is likely that the higher increase in pH is due to increased microbial activity in hydrogen microcosms compared to nitrogen microcosms, due to the consumption of H^+ ions in microbial reactions such as iron reduction, sulphate reduction and nitrate reduction.

For the CO_2 treatment, hydrogen microcosms initially contained 10% CO_2, 10% H_2 and 80% N_2 in the headspace. However, the corresponding nitrogen headspace microcosms initially contained 100% N_2 and no CO_2 [Table 4]. Consequently, the pH measured on Day 0 and Day 28 in the CO_2-treated microcosms are not directly comparable. This may explain the lower pH values measured in Day 28 samples compared to Day 0 samples in the majority of CO_2-treated microcosms while in the other treatments the pH generally increased following incubation [Figure 8]. The pH of live CO_2-treated microcosms with hydrogen in the headspace were generally lower over the incubation period, contrasting with the iron, sulphate, and nitrate treatments. The pH of corresponding killed controls with hydrogen in the headspace was also slightly lower than the value at Day 0. This was not observed with any of the other treatments tested. This suggests that the decrease in pH is more likely due to the chemical effect of dissolved CO_2 in the solution, rather than microbial activity.

3.3 General Corrosion Rate

The general corrosion rate was calculated from the mass loss of the steel coupons over the 28 day incubation period. The calculated corrosion rate with each soil inoculum and each electron acceptor treatment (iron, sulphate, CO_2 and nitrate) is shown in Figure 9, for both live and killed control microcosms under headspace with nitrogen and both nitrogen and hydrogen. The average corrosion rate was calculated from the weight loss of individual coupons from three replicate microcosms and the error bars show the standard deviation.

© ROSEN
This document is classified as confidential

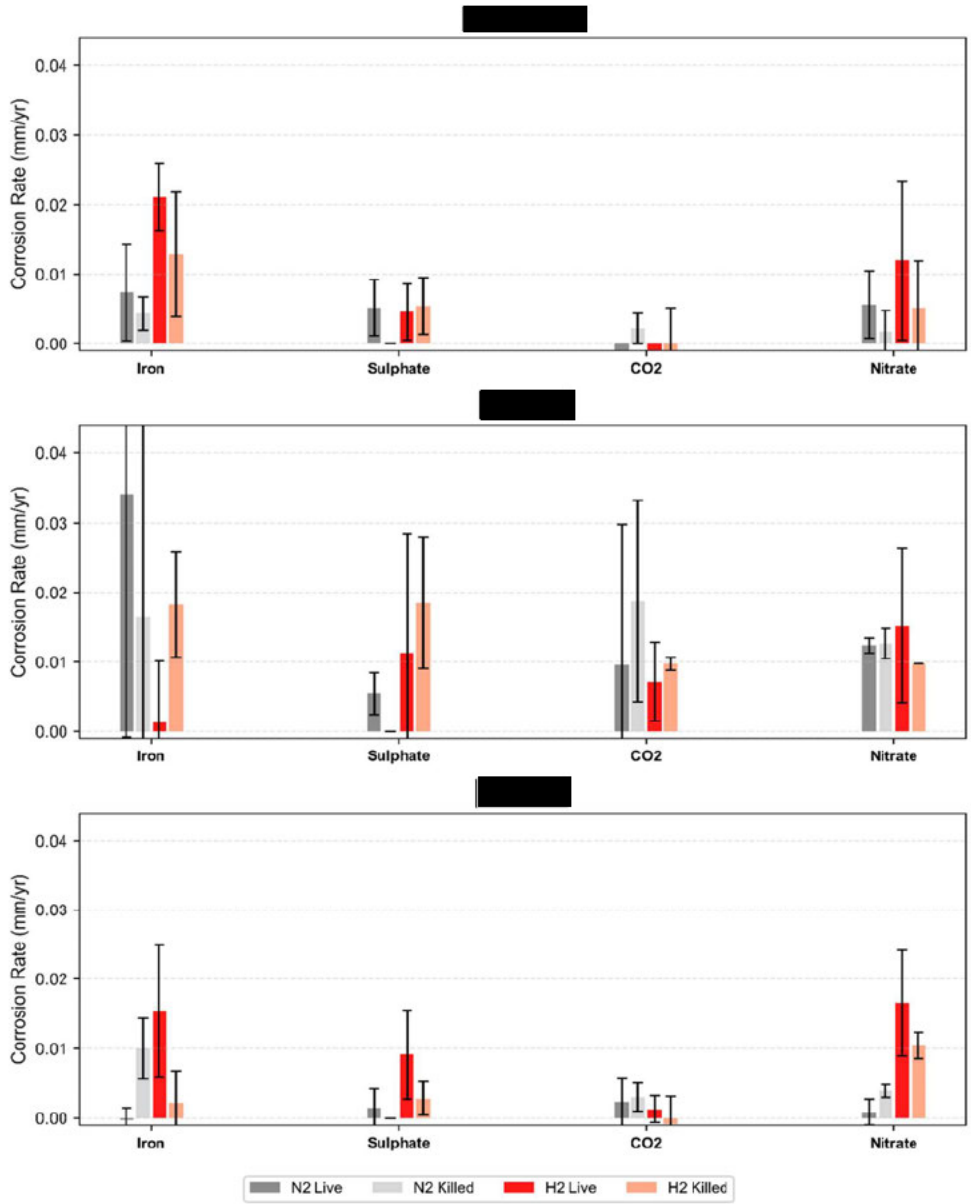

Figure 9: Corrosion rate of steel coupons in microcosms inoculated with different soils under four different electron accepting conditions.

Overall, the measured general corrosion rates were very low, typically less than 0.02 mm/year. The low weight loss values also contributed to the high variability seen in some of the data [Figure 9].

In microcosms inoculated with the [redacted] soil, the highest corrosion rates were observed in the live soil microcosms with hydrogen in the headspace, and iron or nitrate in the growth medium. In these treatments, the live soil microcosms show slightly higher corrosion rates than killed control soil microcosms, and the corrosion rates were higher with hydrogen in the headspace than with 100% nitrogen. In the microcosms with sulphate or CO_2, there was little difference in the corrosion rate between live and killed soil or between microcosms with hydrogen or nitrogen in the headspace [Figure 9].

© ROSEN
This document is classified as confidential

In [redacted] soil, hydrogen did not appear to increase the corrosion rate, and the corrosion rates were similar for the live and killed soil samples across all treatments [Figure 9].

In [redacted] soil, the highest corrosion rates were also observed in the live soil microcosms with hydrogen in the headspace, and iron, sulphate or nitrate in the growth medium. These microcosms had higher corrosion rates compared to the killed soil or microcosms with 100% nitrogen in the headspace [Figure 9].

Generally, higher corrosion rates in live microcosms that contained H_2 in the gas headspace compared to microcosms with 100% N_2 in the headspace could suggest that H_2 promotes MIC. However, all of the observed corrosion rates were very low, and in some cases the live and killed soils had similar corrosion rates. There is also large variation (and therefore standard deviation) between the experiments under the same conditions. Further testing over longer time periods would be required to conclusively determine whether hydrogen increases the rate of MIC.

To compare corrosion of the test coupons shown in Figure 9 to X52 pipeline material, some duplicate microcosms were prepared with coupons of X52 pipeline material inoculated with [redacted] soil. A comparison between the corrosion rate of the steel test coupons and the X52 pipeline material coupons under the same conditions are shown in Figure 10. The pipeline material samples show a negative corrosion rate, due to recording a mass increase during the incubation period. Though the same cleaning protocol was followed to remove corrosion products from all samples, it's likely the corrosion products were not adequately removed from the surface prior to reweighing. It is possible that the corrosion products were more strongly adhered to the pipeline material samples than the test coupons, but given the very low corrosion rates in both materials, it's likely within the range of experimental error and further testing over longer periods is required.

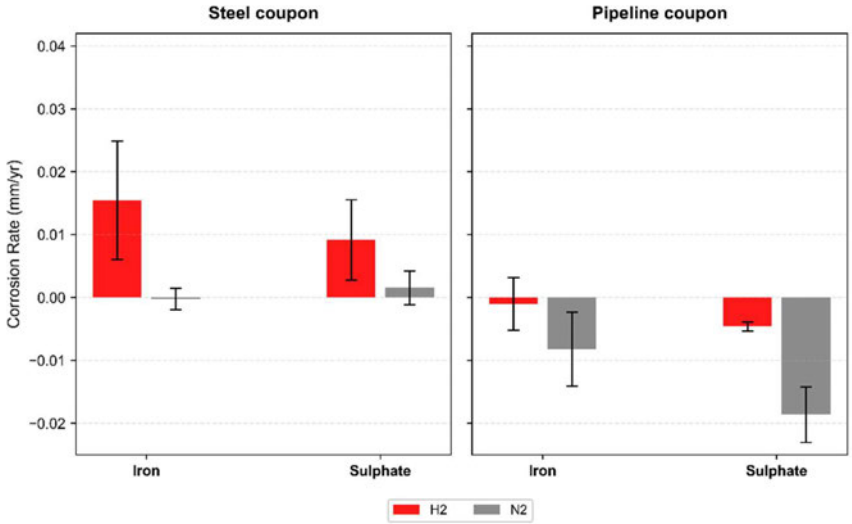

Figure 10: Comparison of corrosion rates of carbon steel test coupons (left) to coupons prepared from X52 pipeline material (right) in [redacted] soil under iron- and sulphate-reducing conditions with and without hydrogen in the headspace.

3.4 Scanning Electron Microscopy and Spectroscopic Analysis of Steel Coupons

All SEM and EDS images discussed in this section are presented in Appendix E. SEM imaging was used to examine the surface metal coupons and pipeline samples under 200x and 1000x magnification. EDS was used to analyse the elemental composition in these areas. EDS analysis measures a very small area (approximately 0.015 mm^2), so absence of corrosion products in the areas analysed with EDS does not rule out their presence elsewhere on the sample. EDS is also unable to detect very light elements with an atomic number less than 5, including hydrogen. The SEM and EDS data therefore represent subjectively identified corrosion features of the coupons and not a comprehensive quantitative analysis.

SEM images and EDS analysis of steel coupons and pipeline material samples prior to incubation are shown in Figure 11. Note, it was not possible to return to the same area for analysis post-incubation.

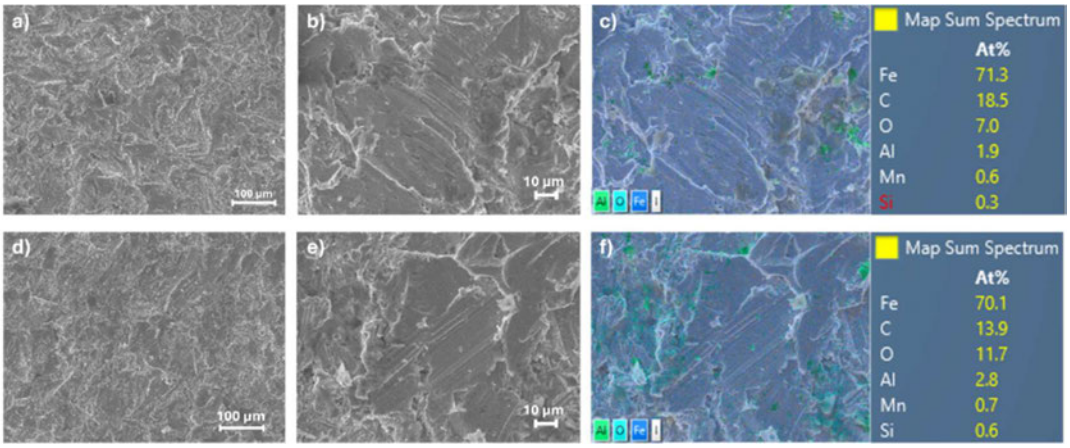

Figure 11: SEM and EDS analysis of steel coupon (a – c) and pipeline samples (d-f) prior to incubation. a) Coupon under 200x magnification, b) Coupon under 1000x magnification and c) EDS map and composition analysis of coupon. d) Pipeline sample under 200x magnification.

3.4.1 Iron-treated microcosms

EDS analysis of coupons and pipeline samples from live microcosms with iron treatment indicated that the main elements present were Fe, O, and C from the steel, as well as Si in samples from microcosms inoculated with [redacted] soil and a small amount of Ca in samples from both [redacted] and [redacted] soil [Appendix E]. The same elements were present in the equivalent killed control incubations. In addition small amounts of Al were identified in some samples. Si and Ca are likely to come from the clay-rich and sandy [redacted] soil inoculum, though Ca could also come from the Widdel and Bak growth medium. Al is likely to come from the steel, as it can also be seen on EDS maps of the samples prior to incubation [Figure 11]. In live soil microcosms incubated under iron-reducing conditions, coupons incubated with [redacted] soil as an inoculum show some evidence of metastable pitting corrosion which was more evident in live microcosms incubated with hydrogen compared to nitrogen microcosms or killed controls [Figure 12]. There was less evidence of possible metastable pitting corrosion on coupons from microcosms inoculated with [redacted] and [redacted] soil. There is some evidence of corrosion including deposits containing Fe and O on samples from all live microcosms

© ROSEN
This document is classified as confidential

and all killed controls, demonstrating corrosion under abiotic conditions as well as in live microcosms [Appendix E].

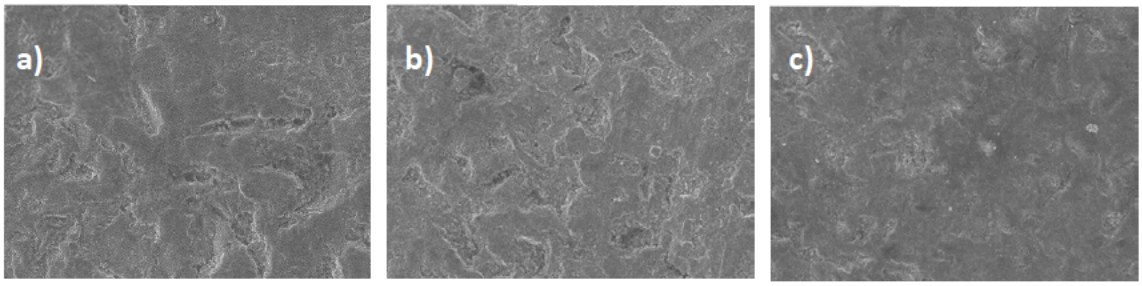

Figure 12: SEM Images of steel coupons under 200x magnification in live microcosm (a, b) and killed control (c), incubated with hydrogen in the headspace (a) or 100% nitrogen (b, c).

3.4.2 Sulphate-treated microcosms

EDS analysis of coupons from live microcosms with sulphate treatment indicated that the main elements present were Fe, O, and C from the steel as well as small amounts of P which is likely to come from the Widdel and Bak medium which contains potassium phosphate as a buffer. The low solubility of phosphate salts likely contributed to its presence on the coupons even after treatment to remove corrosion products. Si was detected on coupons incubated in microcosms inoculated with [redacted] soil under a nitrogen headspace. This is likely from the soil which is a clay-rich glacial till. S was detected on coupons from microcosms inoculated with [redacted] soil incubated with a nitrogen headspace and on samples of pipeline material from microcosms inoculated with [redacted] soil and incubated with hydrogen in the headspace. EDS of the killed controls revealed that Fe, O, C were the main elements present with small amounts of P and Al, no S was detected on any of the killed controls. The detection of S on the metal samples in live microcosms indicates activity of sulphate reducing bacteria which generate hydrogen sulphide and the S-detected is likely in the form of iron sulphide. Deposits containing Fe and O can be seen in SEM and EDS images from both live microcosms and killed controls, indicating corrosion that could be a result of abiotic and biotic mechanisms. There was more evidence of metastable pitting corrosion on coupons from live microcosms inoculated with [redacted] soil incubated with a headspace containing hydrogen or nitrogen, and in those inoculated with [redacted] soil incubated with hydrogen in the headspace, compared to coupons analysed from other microcosms, including killed controls [Appendix E].

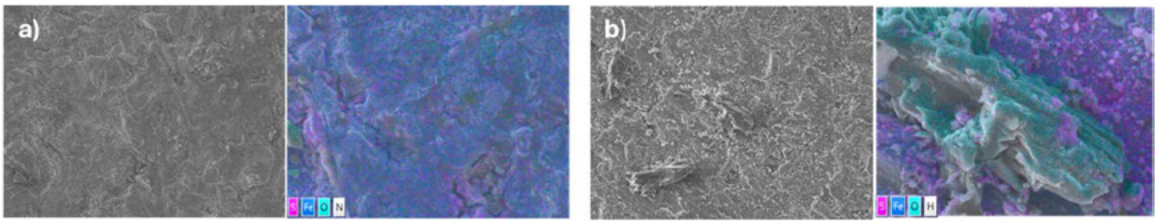

Figure 13: SEM and EDS of a) carbon steel coupons from microcosms inoculated with [redacted] soil and incubated under a 100% nitrogen headspace, and b) pipeline material sample from microcosms inoculated with [redacted] soil and incubated under a gas headspace initially containing 10% hydrogen

© ROSEN
This document is classified as confidential

3.4.3 CO_2-treated microcosms

EDS analysis of coupons from live microcosms with CO_2 in the headspace indicated that the main elements present were Fe, O, and C from the steel as well as small amounts of Ca from the Widdel and Bak growth medium or soil, and Si from the soil inoculum. In one coupon from a microcosm inoculated with [redacted] soil and incubated with a headspace containing 10% hydrogen and 10% CO_2, a clear deposit of S-containing material was identified, indicative of sulphate reducing bacteria activity. This was likely due to sulphate in the soil as no additional sulphate was added to the microcosms with CO_2 treatment. This coupon also appears to show strong evidence of metastable pitting corrosion in SEM images, more so than the other microcosms incubated with CO_2 in the headspace, including killed controls. EDS of the killed controls also mainly detected Fe, O, C and small amounts of P, Ca, and Si, no S was detected in any killed controls. Deposits containing Fe and O indicating corrosion can be seen on the surface of samples from both live microcosms and killed controls in SEM and EDS images [Appendix E].

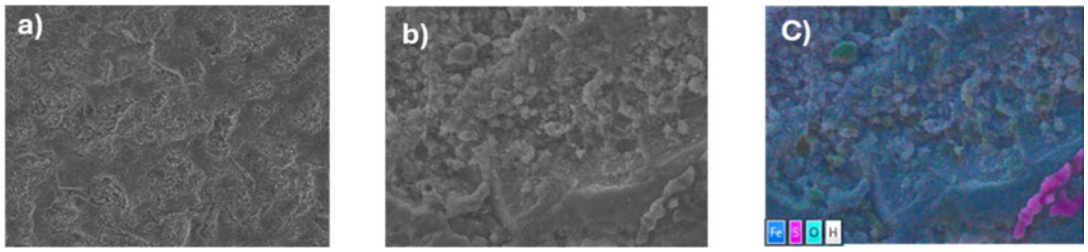

Figure 14: SEM and EDS analysis of steel coupon from microcosm inoculated with [redacted] soil incubated under a gas headspace initially containing 10% hydrogen. a) SEM image 200x magnification, b) SEM image 1000x magnification, c) EDS map showing sulphur-containing deposit

3.4.4 Nitrate-treated microcosms

EDS analysis of coupons from live microcosms with nitrate treatment showed that the main elements present were Fe, O, and C from the steel as well as trace amounts of Co and Cl likely from the Widdel and Bak growth medium or soil inoculum. EDS of the killed controls also detected Fe, O, C, and Al from the steel as well as small amounts of Ca and Si from the growth medium or soil. Compared to live microcosms with other treatments, there was less evidence of metastable pitting corrosion in the microcosms with nitrate treatment [Appendix E].

3.4.5 Summary of SEM and EDS analysis

Overall, there was evidence of corrosion in SEM images of coupons from live microcosms and killed controls for all treatments. There is evidence of increased metastable pitting corrosion in live microcosms compared to killed which is indicative of MIC. There is evidence of activity of sulphate reducing bacteria in live microcosms with sulphate treatment ([redacted] soil in nitrogen and [redacted] soil in hydrogen) and CO_2 treatment ([redacted] soil in hydrogen), and none on any coupons in adiabatic killed control microcosms. The morphology of the corrosion was similar for the pipeline samples and the carbon steel test coupons.

© ROSEN
This document is classified as confidential

3.5 Microbial Community Analysis

The microbial communities selected in microcosms under different incubation conditions were analysed by sequencing of 16S rRNA gene fragments amplified from DNA extracted from the different soil inocula and microcosm samples. Different 16S rRNA gene sequences represent different microbial taxa and the number of sequences of each different 16S rRNA gene gives an indication of the relative abundance of the different microorganisms present. The total number of 16S rRNA gene sequence reads obtained from each sample is shown in Appendix D.

For comparison between the treatments, count data was normalised to relative abundance within each sample. To analyse the diversity of the microbial community composition in different conditions, Principal Coordinate Analysis (PCoA) was used [Appendix F]. For visualisation of the microbial community profile, the 20 most abundant taxa in each sample were displayed in stacked bar charts.

3.5.1 Microbial Communities from [redacted] Soil Inoculated Microcosms

3.5.1.1 PCoA Analysis

Principle Coordinate Analysis (PCoA) of microbial communities from [redacted] soil and microcosms inoculated with [redacted] soil under different electron accepting conditions, either with 10% hydrogen in the headspace or incubated under a 100% nitrogen headspace, indicated that under all electron-accepting conditions distinct communities were selected depending on the presence of hydrogen in the headspace [Figure 15].

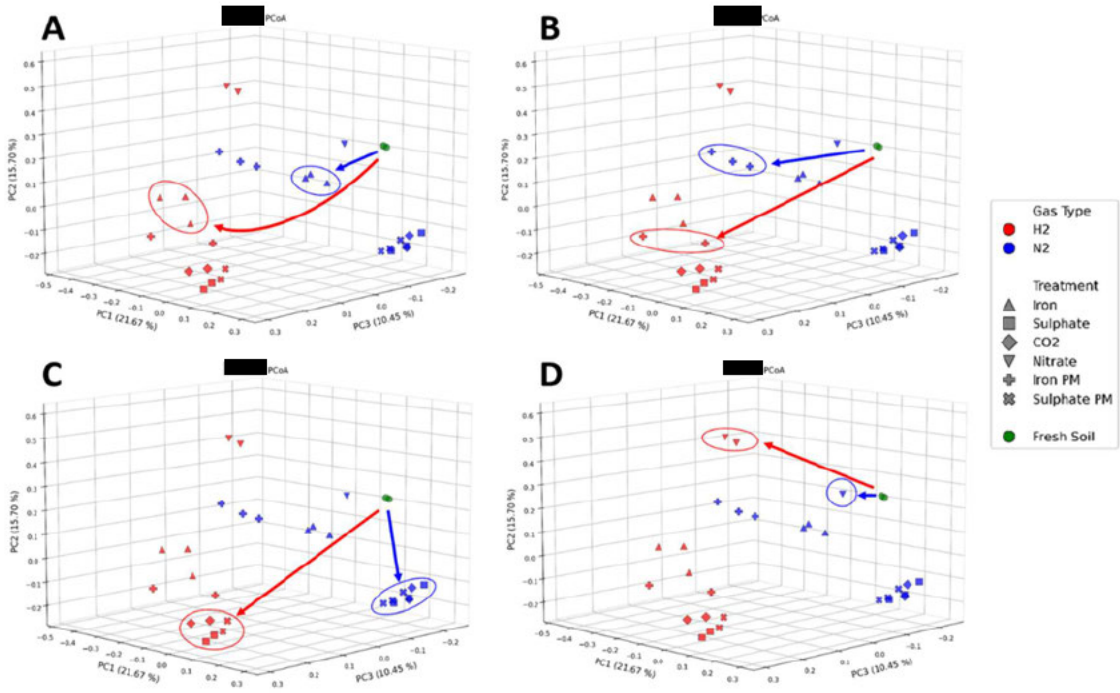

Figure 15: PCoA of microbial communities from [redacted] soil (green circles) and microcosms inoculated with [redacted] soil under different electron accepting conditions. Microbial communities from microcosms incubated with 10% hydrogen are red and those incubated under a nitrogen headspace are blue. The changes in community composition from that of the soil prior to incubation is illustrated for microcosms incubated under (A) iron-reducing conditions in the presence of carbon steel coupons, (B) under iron-reducing conditions in the presence of coupons of X52 pipeline material (C) under sulphate-reducing and CO_2-reducing conditions in the presence of carbon steel coupons and under sulphate-reducing conditions with coupons of X52 pipeline material, and (D) under nitrate-reducing conditions.

Under iron-reducing conditions distinct microbial communities were selected dependent on the presence of hydrogen in the microcosm headspace [Figure 15A and Figure 15B]. Interestingly, under iron-reducing condition different communities were selected when X52 pipeline material was present in the microcosms [Figure 15B] compared to the communities that developed when carbon steel coupons were present [Figure 15A]. This contrasted with microcosms incubated under sulphate-reducing conditions where the microbial communities selected were similar irrespective of the nature of the steel coupon present in the microcosms [Figure 15C]. The communities selected under sulphate-reducing and CO_2-reducing conditions were also similar to each other [Figure 15C]. The presence of nitrate in microcosms also selected for microbial communities that were distinct from those that developed under other electron accepting conditions and again were strongly influenced by the presence of hydrogen in the headspace [Figure 15D].

3.5.1.2 Microbial Community Composition Analysis

The changes in microbial community composition at a Family level, from soil starting composition to final composition following incubation in different electron acceptor treatments (iron-, sulphate-, CO_2- and nitrate-reducing conditions) with either 100% nitrogen or 10% hydrogen gas in the headspace, is shown in Figure 16.

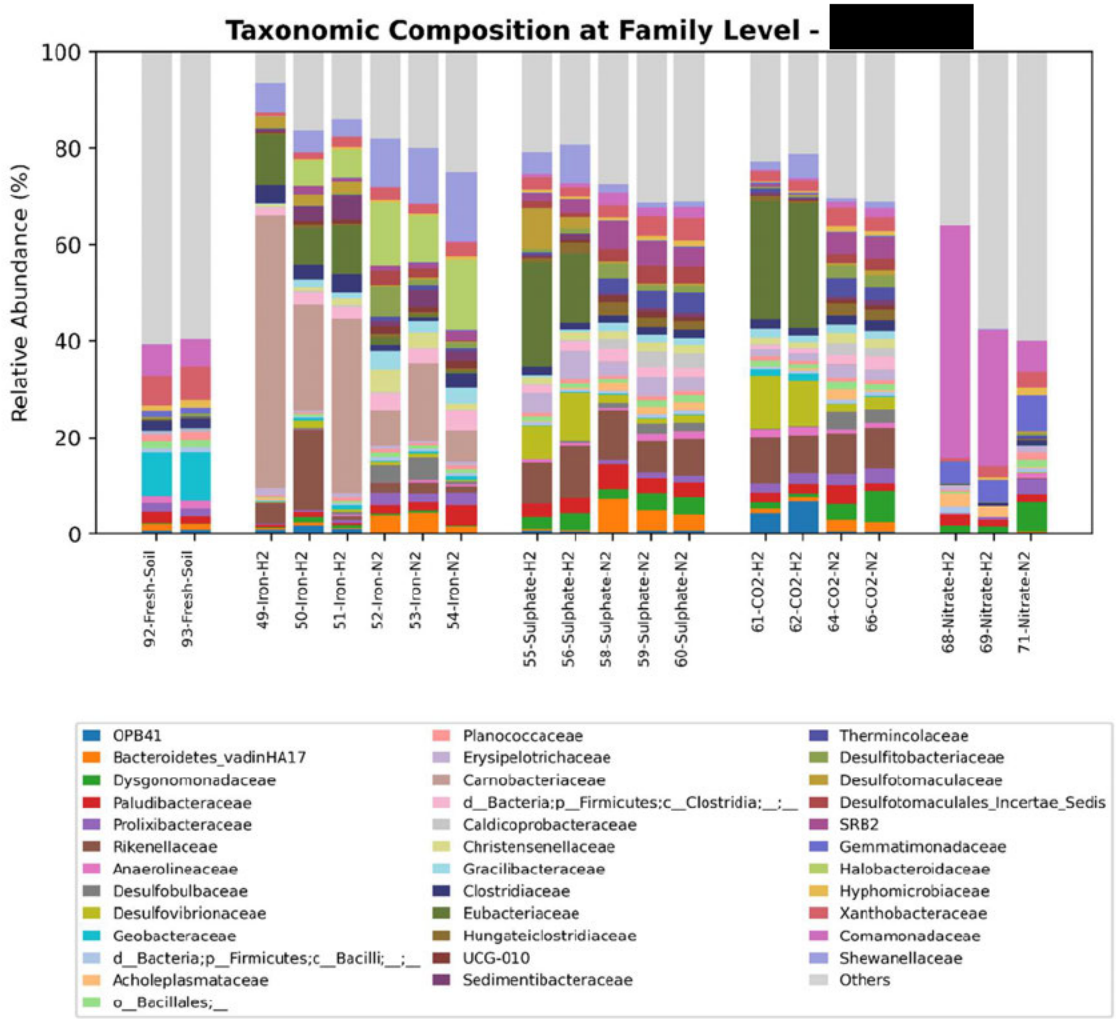

Figure 16: Microbial community composition in [redacted] soil prior to incubation and following incubation under iron-, sulphate-, CO_2- and nitrate-reducing conditions with nitrogen or 10% hydrogen gas headspace. Data represent the 20 most abundant taxa categorized at Family level.

Prior to incubation the predominant organisms in the [redacted] soil were members of the families *Geobacteraceae* (9% relative abundance), *Comamonadaceae* (6% relative abundance), *Xanthobacteraceae* (6% relative abundance), and *Plaudibacteraceae* (2% relative abundance) have the highest average relative abundances. Many members of the *Geobacteraceae* are anaerobic iron-reducing bacteria, but interestingly do not feature in the 20 most abundant taxa post-incubation, even when the soil was incubated under iron-reducing conditions. Members of the family *Comamonadaceae* are capable of nitrate reduction, and remained among the 20 most abundant taxa following incubation under sulphate-, nitrate- and CO_2-reducing conditions. They were particularly strongly selected under nitrate-reducing conditions [Figure 16]. *Xanthobacteraceae* and *Plaudibacteraceae* are both contain aerobic heterotrophic bacteria that utilise a range of organic substrates, and continue to feature in post-incubation microbial communities at comparative relative abundances despite anaerobic conditions.

Following incubation under iron-reducing conditions, the microbial community profiles were dominated by *Carnobacteriaceae,* which are capable of fermentative metabolism. Though not strongly associated

with MIC, their metabolic processes can produce organic acids which could contribute to metabolite MIC. In microbial communities from microcosms incubated with 10% hydrogen in the headspace members of the *Carnobacteriaceae* had an average relative abundance of 38% compared to 9% seen in microcosms with only nitrogen in the headspace. Bacteria from the family *Shewanellaceae* were strongly enriched under iron-reducing conditions particularly in microcosms with no hydrogen in the headspace (19.9-14.4% relative abundance). In microcosm with 10% hydrogen in the headspace they represented 3.7 to 6.1% if the microbial community. This is consistent with the known properties of this group of bacteria which includes well-characterized iron-reducing bacteria. Interestingly *Shewanellaceae* were also enriched in sulphate-reducing microcosms particularly when hydrogen was present in the headspace. Bacteria from the *Shewanellaceae* are not known to be capable of sulfate-reduction. With respect to MIC some *Shewanellaceae* are known to be capable of direct electron transfer to solid phase iron oxides for example and could potentially have a role in electrical MIC through direct electron transfer [9].

Bacteria from the family *Halobacteroidaceae* were unexpectedly selected under iron-reducing conditions particularly in microcosm with a 100% nitrogen headspace (9.9 to 14.5% relative abundance compared to 5.3 to 5.9% relative abundance in microcosms with 10% hydrogen in the headspace). Their presence was unexpected as these are organisms typically found in high salinity environments. They have a fermentative metabolism which is inhibited under high hydrogen conditions, which may explain their greater relative abundance when no hydrogen was present in the microcosm headspace). Fermentative organisms produce organic acids as metabolic products and could therefore contribute to chemical MIC. *Eubacteriaceae* had a higher relative abundance in microcosms with a 10% hydrogen headspace (9% relative abundance) compared microcosms with a nitrogen headspace (1% relative abundance). Despite being capable of acetogenesis, members of the *Eubacteriaceae* have not been associated with MIC.

A wide diversity of sulphate-reducing bacteria was present in microcosms inoculated with [redacted] soil these included *Desulfovibrionaceae, Desulfotomaculacea, Desulfobaccaceae, Thermodesulfovibrionia, Desulfomonilaceae. Desulfocapsaceae, Desulfomicrobiaceae, Desulfuribacillaceae, Desulfobulbaceae, Desulfatiglandaceae and Desulfarculaceae.* In addition elemental sulphur reducing *Desulfuromonadaceae* and sulphite-/thiosulphate-reducing *Desulfitobacteriaceae* were also detected at low relative abundances (typically less than 0.1%). However, when taken together the summed sulphate-reducing taxa represented as much as 19% of the microbial community in microcosms with 10% hydrogen in the headspace incubated under sulphate-reducing conditions. In the absence of hydrogen in the headspace the corresponding sulphate-reducing communities had a relative abundance of just over 9%. The majority of the sulphate-reducing bacteria in these cases comprised members of the *Desulfovibrionaceae* and the *Desulfotomaculaceae*. A similar pattern was seen in microcosms with CO_2 in the headspace. Interestingly in iron-reducing microcosms the opposite was seen with stronger selection for sulphate-reducers in the absence of hydrogen in the gas headspace.

Post-incubation in sulphate-reducing microcosms, *Desulfovibrionaceae,* capable of dissimilatory sulphate reduction and hydrogen oxidation, made up 9% of the microbial community in hydrogen containing microcosms compared to only 1% in microcosms with a nitrogen headspace. They are strongly associated with MIC and have the potential to produce highly corrosive H_2S. Acetogens from the *Eubacteriaceae* had a relative abundance of 17.5% in microcosms with 10% hydrogen in the headspace and were not detected in microcosms with a headspace of 100% nitrogen. Though capable of acetogenesis, they are not known to be capable of direct electron transfer which makes this type of acetogen a lower MIC risk than members of the *Sporomusaceae*.

© ROSEN
This document is classified as confidential

In CO_2-reducing microcosms, there was an increase in relative abundance of *Desulfovibrionaceae* (potentially highly corrosive sulphate reducers) to 10% in hydrogen microcosms compared to only 2% in nitrogen microcosms. This suggests the presence of natural sulphate in the soil, since no additional sulphate was added to the microcosms. Microcosms with CO_2 and H_2 in the headspace also saw an increase in acetogens *Eubacteriaceae* with a relative abundance (25%), while none were identified in nitrogen headspace microcosms, a trend similar to sulphate- and nitrate-treated microcosms.

Microbial communities in nitrate-reducing microcosms were dominated by nitrate-reducing bacteria from the *Comamonadaceae,* with a higher relative abundance of *Comamonadaceae* (38% average) found in microcosms with a 10% hydrogen headspace compared to microcosms a nitrogen headspace (6% relative abundance). These organisms could pose an MIC risk through the production of nitrite, which is highly oxidising towards steel [10]. Aside from the large increase in relative abundance of *Comamonadaceae,* the rest the microbial community was generally similar in composition to the starting community.

Overall, incubation under different electron acceptor and headspace conditions caused clear shifts in microbial community structure, with hydrogen frequently promoting microorganisms with potential relevance to MIC. Microcosms with hydrogen in their headspace generally favoured microorganisms associated with MIC compared to the microcosms with a 100% nitrogen headspace. These included bacteria from the *Carnobacteriaceae* (organic-acid producing fermenters) in iron-treated microcosms, *Desulfovibrionaceae* (sulphate reducers strongly associated with MIC) in sulphate and CO_2 treatments, and *Comamonadaceae* (nitrate-reducing bacteria) in nitrate-treated microcosms. One notable exception was the higher proportion of *Shewanellaceae* (iron reducing bacteria strongly associated with MIC) in microcosms with a nitrogen headspace (12% relative abundance) compared to microcosms with a 10% hydrogen headspace (4.5% relative abundance) in iron-treated microcosms..

3.5.2 Microbial Communities from [redacted] Soil Inoculated Microcosms

PCoA analysis of the soil microbial community indicated that under all electron-accepting conditions distinct communities were selected depending on the presence of hydrogen in the headspace [Appendix F]. The microbial community in [redacted] soil prior to incubation and post-incubation with different electron acceptors is shown in Figure 17. The starting soil microbial community was highly diverse, indicated by a Shannon index of 8. The community was dominated by Bacteria, and Archaea were not represented within the 20 most abundant taxa identified. Bacteria from the Class *Acidobacteriae* were present at the highest relative abundance and constituted 23% of the microbial community [labelled in Figure 17 as uncultured_2, as the microorganisms could not be identified at a Family level]. Bacteria from the Class *Acidobacteria* are commonly found in acidic soils, consistent with the low pH of the [redacted] soil (pH 4.62). Other abundant bacterial Families present in [redacted] soil were *Acidothermaceae* (9%) *Beijerinckiaceace* (6%) and *Xanthobacteraceae* (6%) which together represented about one fifth of the microbial community. Bacteria from these families are commonly encountered in terrestrial environments. Post-incubation, there was a decrease in relative abundance bacteria from all of these Families, reflecting the anoxic and reducing conditions in the microcosms.

© ROSEN
This document is classified as confidential

Figure 17: Microbial community composition in [redacted] soil prior to incubation and following incubation under iron-, sulphate-, CO_2- and nitrate-reducing conditions with nitrogen or 10% hydrogen gas headspace. Data represent the 20 most abundant taxa categorized at Family level.

Following incubation under iron-reducing conditions, the relative abundance of *Sporomusaceae* increased from less than 0.003% to 12% relative abundance in microcosms with 10% hydrogen in the headspace, and 5% relative abundance in microcosms with only nitrogen in the headspace. *Sporomusaceae* are acetogens which have been associated with electrical MIC through the direct uptake of electrons from steel [11]. Bacteria from the *Peptococcaceae* were present below the detection limit (0.001% relative abundance) in the [redacted] soil prior to incubation and increased to a maximum of 14% relative abundance and 21% relative abundance in iron-reducing microcosms with 10% hydrogen and 100% nitrogen in the headspace respectively. The family *Peptococcaceae* includes sulphate-reducing bacteria such as *Desulfotomaculum* which have been associated with MIC [12]. The relative abundance of members of the family *Desulfitobacteriaceae* increased to approximately 3% and 5% relative abundance in iron-reducing microcosms with 100% nitrogen and 10% hydrogen in the headspace respectively. The family *Desulfitobacteriaceae* includes sulphite- and thiosulphate-reducing bacteria which have been linked to MIC [13]. Other Families in the represented in the 20 most abundant taxa are not know to be linked to MIC.

It was only possible to obtain 16S rRNA gene sequence data from the sulphate-reducing microcosms incubated with 10% hydrogen in the headspace therefore direct comparison with communities selected with only nitrogen in the microcosm headspace was not available for comparison. The microbial

communities selected in incubated sulphate-reducing microcosms with 10% hydrogen headspace were dominated by *Sporomusaceae* (25% relative abundance). This family includes acetogens strongly linked to electrical MIC [11]. As in iron-reducing microcosms, the relative abundance of *Desulfitobacteriaceae* increased to 3% in sulphate-reducing microcosms with a 10% hydrogen headspace. While these bacteria with versatile respiratory metabolism including the capacity for sulphite and thiosulfate reduction were selected in the sulphate-treated microcosms, more typical sulphate reducers such as those that were detected in sulphate-reducing microcosms inoculated with [redacted] soil were absent.

Bacteria from the family *Sporomusaceae* (MIC related acetogenic bacteria) were strongly selected in microcosms with hydrogen and CO_2 in the headspace and reached a relative abundance of 20%. This contrasts with their relative abundance in microcosms with 100% nitrogen in their headspace, where their relative abundance was just 2%. *Sporomusaceae* are acetogenic bacteria that can use hydrogen to reduce CO_2 to acetic acid, explaining their high relative abundance under a headspace with nitrogen and CO_2. *Desulfobaccaceae*, *Thermodesulfovibrio*, *Desulfomonilaceae* were also detected in the [redacted] soil inoculum albeit at low relative abundance (typically less than 0.2%). However, in microcosms with hydrogen and CO_2 in the headspace *Desulfovibrionaceae* reached up to 6.7% relative abundance and when the headspace was 100% nitrogen a maximum relative abundance of 3.1% was seen. *Desulfitobacteriaceae* (sulphite- and thiosulfate-reducing bacteria) were also selected in microcosms with hydrogen and CO_2 in the headspace (6% relative abundance) and to a lesser degree in microcosms with a nitrogen headspace (3% relative abundance). *Gracilibacteraceae* also increased in relative abundance to 9% and 4% in microcosms a hydrogen and CO_2 and a nitrogen headspace respectively, though bacteria from the *Gracilibacteraceae* are not known to be linked to MIC.

Following incubation in nitrate treatment, there was a large increase in relative abundance of bacteria from the family *Paenibacillaceae* (12% and 19% in microcosms with hydrogen headspace and nitrogen headspace respectively). The family *Paenibacillaceae* includes some nitrogen-fixing species and nitrate-reducers. *Paenibacillaceae* could therefore be linked to MIC through reduction of nitrate to nitrite, which is highly oxidising towards steel [10]. Bacteria from the *Rhodocyclaceae* were present at a relative abundance of 16% in microcosms incubated with a hydrogen headspace but were not detected in microcosms with a nitrogen headspace. Members of the Family are capable of using hydrogen as an electron donor explains their growth in hydrogen-containing microcosms compared to those with a 100% nitrogen headspace. They are also known to be capable of nitrate reduction and therefore could constitute a potential risk of MIC through nitrite production.

Overall, incubation under different electron-accepting conditions and both in the presence and absence of hydrogen in the headspace led to substantial shifts in microbial community composition. Microcosms incubated under iron-reducing conditions with hydrogen in the headspace showed elevated relative abundances of *Sporomusaceae* (12%), a Family of acetogenic bacteria linked to electrical MIC via direct electron uptake from steel, compared to microcosms with a 100% nitrogen headspace. The relative abundance of *Peptococcaceae* and *Desulfitobacteriaceae* increased by a similar amount irrespective of the presence of hydrogen in the headspace. Under sulphate-reducing conditions in the presence of hydrogen *Sporomusaceae* were selected even more strongly than under iron-reducing conditions, reaching a relative abundance of 25%. The proportion of sulphate reducing bacteria was surprisingly low compared to [redacted] soil microcosms under the same conditions, suggesting the initial soil inoculum was lower in sulphate-reducing bacteria. The CO_2 treatments further demonstrated the stimulatory effect of hydrogen: *Sporomusaceae* reached 20% abundance under hydrogen compared to only 2% under nitrogen. Finally, in the nitrate treatments *Paenibacillaceae* increased to 12% in the presence of hydrogen and 19% when hydrogen was absent, and *Rhodocyclaceae*, reached 16%

© ROSEN
This document is classified as confidential

relative abundance in when hydrogen was present but were not detected when no hydrogen was present in the headspace of microcosms. Both of these Families may contribute to MIC through nitrate reduction to nitrite, a highly aggressive oxidant corrosive to steel.

3.5.3 Microbial Communities from [redacted] Soil Inoculated Microcosms

It was not possible to amplify 16S rRNA genes from DNA extracted from [redacted] soil and only 5 of 24 live microcosms inoculated with [redacted] soil yielded DNA from which 16S rRNA genes could be amplified.

Extraction and amplification of DNA from fresh samples of [redacted] soil (prior to incubation) proved ineffective and the composition of the microbial community could not be established. DNA extraction and PCR amplification of 16S rRNA genes was only successful following incubation in microcosms containing hydrogen in the gas headspace under iron-, sulphate- and nitrate-reducing conditions and this was not possible for all replicate microcosms. Microcosms inoculated with [redacted] soil with CO_2 in the headspace and all microcosms with a nitrogen headspace did not yield DNA from which 16S rRNA genes could be amplified. Failure to extract and amplify DNA can be caused by a low biomass or high ratio of clay minerals that can bind DNA reducing extraction efficiency. Given that amplification was successful only after incubation at optimum conditions for microbial growth for several weeks, it is likely that low biomass was the reason for unsuccessful amplifications in other conditions. This is consistent with the much lower initial TOC content of [redacted] soil (0.21%) compared to [redacted] (3.35%) and [redacted] (2.80%). It was demonstrated that DNA extracts from [redacted] soil did not inhibit amplification of 16S rRNA genes from DNA extracted from [redacted] soil, further indicating that it was low levels of DNA, rather than the presence of PCR inhibitors in the extracts from [redacted] soil that led to the lack of successful amplification of 16S rRNA genes.

The number of sequence reads obtained from a DNA sample can provide an indication of the quality and/or quantity of DNA in a sequencing reaction [Appendix D]. The small number of reads obtained from the few samples from microcosms inoculated with [redacted] soil from which 16S rRNA gene fragments could be amplified also supported the conclusion that low levels of DNA recovered from samples of [redacted] soil were the reason that it was not possible to obtain comprehensive microbial community data for the experiments inoculated with [redacted] soil.

Figure 18 displays the 20 most abundant microbial Families from the microcosms inoculated with [redacted] soil that yielded amplified 16S rRNA gene fragments. These are all from microcosms following 28 days of incubation with hydrogen in the gas headspace.

© ROSEN
This document is classified as confidential

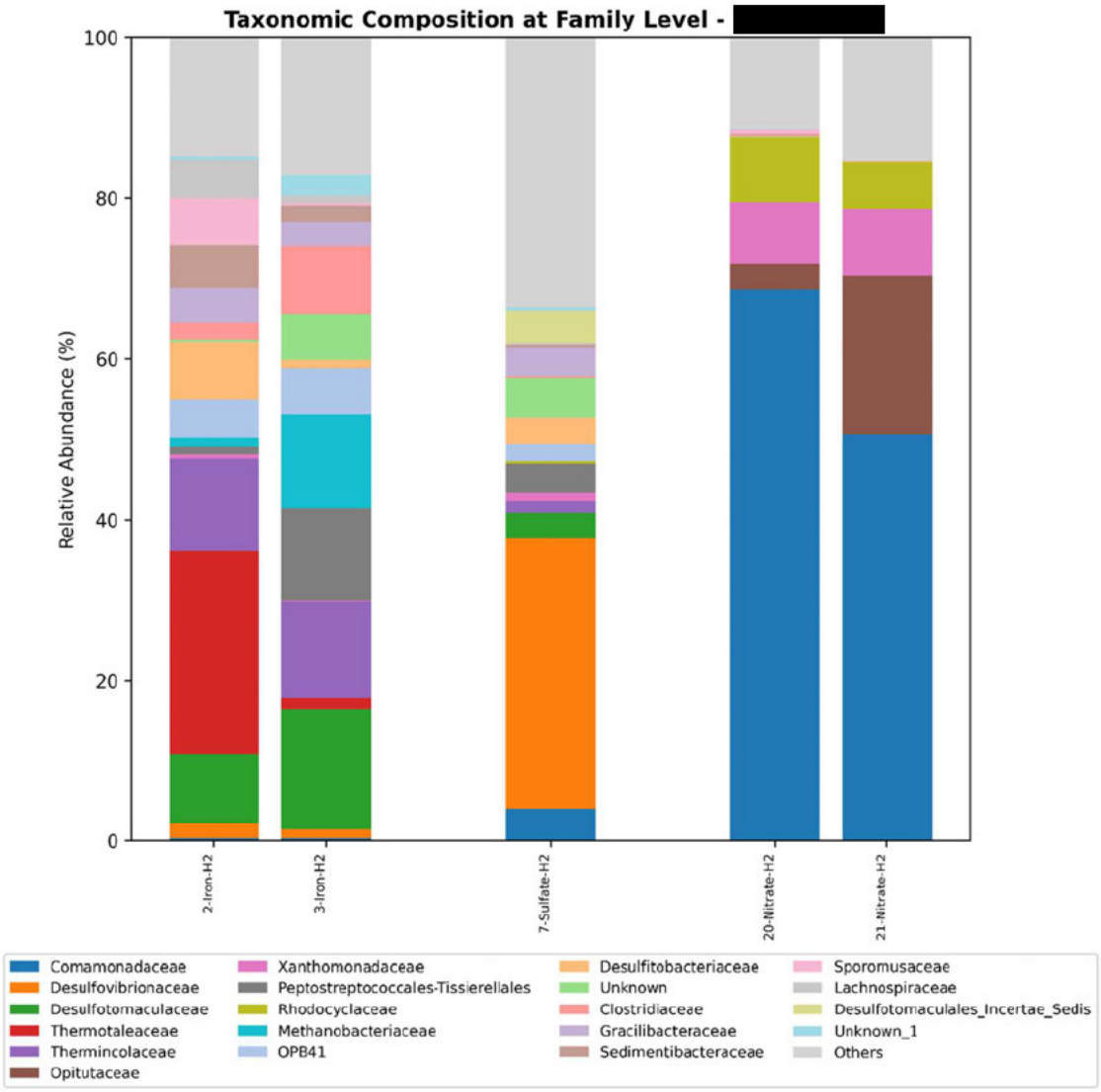

Figure 18: Microbial community composition in [redacted] soil microcosms after 28 days of incubation with a 10% hydrogen headspace, under iron-, sulphate- and nitrate-reducing conditions. Data represent the 20 most abundant taxa categorized at Family level.

Microbial community data was obtained from two of the three microcosms with hydrogen in the headspace incubated under iron-reducing conditions [Figure 18]. The microbial communities were predominantly bacteria, with bacteria from the families *Desulfotomaculaceae* and *Desulfovibrionaceae* among the taxa present at a high relative abundance (12% and 2% respectively), these are families containing predominantly sulphate-reducing bacteria with potential to contribute to MIC [14]. In addition to sulphate, a number of members of these families are also capable of using Fe^{3+} in the form of ferric (III) citrate as a terminal electron acceptor, which explains their abundance in the iron-reducing microcosms [15]. *Thermincolaceae*, which were also present at high relative abundance (approximately 12%) in both iron-reducing microcosms with hydrogen in the headspace are thermophilic bacteria capable of iron reduction. Methanogenic archaea from the family *Methanobacteriaceae,* were also detected in both iron-reducing microcosms with hydrogen in the headspace were detected at a relative abundance of 11% in sample 3 but were present at much lower abundance in sample 2. Some

methanogens from the *Methanobacteriaceae* have been implicated in MIC through the direct uptake of electrons from steel (electric MIC) [16]. The high proportion of *Methanobacteriaceae* corresponds with the detection of methane in the headspace of these microcosms [Figure 5]. Bacteria from the family *Thermincolaceae* were also detected in both iron-reducing microcosms with a hydrogen headspace with an average relative abundance of 12%. Bacteria from the family *Thermincolaceae* are anaerobic thermophilic fermentative microorganisms which have not been implicated in MIC.

Microbial community data was also obtained from one of the three microcosms with hydrogen in the headspace incubated under sulphate-reducing conditions [Figure 18]. The microbial community in this microcosm was dominated by sulphate reducers from the family *Desulfovibrionaceae* (33% relative abundance), with lower relative abundance of members of the *Desulfotomaculaceae* (3%), and *Desulfitobacteriaceae* a family including sulphite and thiosulfate-reducing bacteria with the ability to oxidize hydrogen (3% relative abundance). These are all bacteria capable of forming sulphide from sulphur oxyanions with a number linked specifically to MIC [14, 13].

Microbial community data was in addition obtained from two of the three microcosms with hydrogen in the headspace incubated under nitrate-reducing conditions [Figure 18]. *Comamonadaceae* have the highest average relative abundance of 59%, this is a diverse family of bacteria commonly found in soil habitats capable of oxidizing hydrogen and reducing nitrate. Their high relative abundance correlates with the rapid consumption of hydrogen by [redacted] soil microcosms [Figure 4]. Nitrate reduction has been associated with MIC through the production of nitrite, which is highly oxidising towards to steel [10, 17] this would be exacerbated by conditions that repress denitrification leading to greater accumulation of nitrite and other intermediates of denitrification. It is known that complete denitrification is inhibited by high pH which is characteristic of the [redacted] soil (pH 8.29). Other organisms prominent in the hydrogen-oxidizing nitrate-reducing microcosms included *Opitutaceae* (11% relative abundance), *Xanthomonadaceae* (7% relative abundance) and *Rhodocyclaceae* (6% relative abundance). Although bacteria from these families are not known to be associated with MIC, several genera within the families can reduce nitrate to nitrite, could potentially lead to a risk of corrosion.

Overall, the microbial communities selected post-incubation varied with different electron acceptors provided in the microcosms, with higher relative abundancies of microorganisms adapted to using the different electron acceptors present. A comparison between the communities with hydrogen and nitrogen in the headspace was not possible for the [redacted] experiments as DNA could only be amplified from microcosms incubated with hydrogen, this alone however suggests that hydrogen promoted the growth and metabolism of the microbial communities including some that have been associated with MIC. In microcosms with hydrogen in the headspace, iron treatment promoted the growth of methanogens, sulphate reducing bacteria and iron reducing bacteria; sulphate treatment strongly promoted sulphate reducing bacteria; and nitrate treatment strongly promoted nitrate reducing bacteria.

© ROSEN
This document is classified as confidential

4 DISCUSSION

4.1 [redacted]

[redacted] soil exhibited the highest rate of hydrogen consumption of the three soils, with complete depletion by Day 7 in the iron-, sulphate-, and CO_2-treated microcosms, and by Day 14 in the nitrate-treated microcosms. This rapid and consistent consumption across all four electron acceptor conditions suggests a highly active and metabolically versatile hydrogenotrophic community, capable of efficiently exploiting hydrogen as an energy source under a range of electron accepting conditions.

Methane was detected in the iron- and CO_2-reducing microcosms when hydrogen was present in the headspace, indicating methanogenic activity; however, when 16S rRNA gene sequence data were filtered at 0.5% relative abundance, no Archaea carrying the "Methano-" prefix exceeded this threshold. Despite their low relative abundance, these organisms were evidently metabolically active, producing a measurable change in headspace composition.

PCoA analysis [Figure 15], reveals substantial shifts in community composition relative to the initial soil inoculum, with clear separation between hydrogen and nitrogen microcosms. This divergence indicates that hydrogen availability exerted a strong selective pressure on the microbial community in [redacted] soil, enriching for microorganisms capable of hydrogenotrophic metabolisms. Hydrogen increased the relative abundance of several Families associated with MIC including sulphate-reducing bacteria from the family *Desulfovibrionaceae* which had higher relative abundance in hydrogen microcosms with both CO_2 and sulphate treatment.

Corrosion rate measurements support a hydrogen-driven MIC risk in [redacted] soil. Mass loss from steel coupons was higher in microcosms with hydrogen in the headspace compared to microcosms a headspace with no hydrogen under iron-, sulphate-, and nitrate-reducing conditions, consistent with the stimulation of corrosion-associated microbial activity in microcosms with hydrogen in the headspace. The CO_2 treatment was an exception, with very minor corrosion which was comparable between microcosms with and without hydrogen in the headspace. This may indicate that a specialised corrosion-associated community did not develop under those conditions within the experimental timeframe, despite the detection of methanogenic activity.

4.2 [redacted]

[redacted] soil exhibited rapid hydrogen consumption in the iron and CO_2 treatments, with complete depletion by day 14, suggesting an active and diverse hydrogenotrophic community capable of coupling hydrogen oxidation to multiple terminal electron acceptors [Figure 4]. The sulphate treatment showed a comparatively slower response with residual hydrogen remaining at the end of the incubation period, which may reflect a less abundant or less competitive sulphate reducing population, this was reflected in the microbial community composition with most sulphate reducers present at low relative abundance [Figure 17]. The nitrate treatment was the only soil treatment combination across the entire experiment to show considerable hydrogen remaining after 28 days, which might initially suggest a limited capacity for nitrate reduction in [redacted] soil.

However, the exclusive detection of nitrous oxide in [redacted] incubations both in microcosms with hydrogen in the headspace and with a nitrogen headspace, indicate that active denitrification was occurring. The accumulation of N_2O suggests that denitrification may have been incomplete. This also

© ROSEN
This document is classified as confidential

implies that sodium nitrate may have been preferentially utilised as an electron acceptor for oxidation of organic carbon in the soil over hydrogen, which could account for the comparatively low hydrogen consumption observed. This interpretation is supported by microbial community data that identified *Paenibacillaceae*, a Family known to include facultative denitrifiers, in both hydrogen and nitrogen microcosms. Additionally, *Rhodocyclaceae* which are capable of utilising hydrogen as an electron donor during denitrification were detected exclusively in microcosms with hydrogen in the headspace.

Microbial community analysis further supports these interpretations. Shifts in microbial community composition relative to the initial soil inoculum were evident after 28 days, with clear divergence between microcosms with and without hydrogen in the headspace [Figure 17]. PCoA [F.2] confirms that communities in each treatment clustered distinctly from the starting community, with hydrogen microcosms showing greater separation than nitrogen microcosms, indicating that hydrogen availability was a significant driver of community restructuring.

Corrosion rate data is inconclusive for [redacted] where there was high variability in the data obscuring any differences in corrosion rate between live and killed microcosms, and between hydrogen and nitrogen headspaces for all treatments. Microbial community analysis did however highlight higher relative abundancies of several microorganisms associated with MIC in microcosms with hydrogen gas headspace, including *Sporomusaceae* acetogenic bacteria associated with electrical MIC through direct electron transfer.

4.3 [redacted]

[redacted] soil is physically distinct from [redacted] and [redacted] soil, comprising large clumps of clay with gravel sized particles (0.2 cm to 3cm) and a notable absence of rootlets, which were present in both other soils. This coarser, less organic texture likely reflects differences in the microbial community structure and nutrient availability within [redacted] and may partially account for some of the divergent biological responses observed.

[redacted] displayed the slowest rates of hydrogen consumption of the three soils across the Iron, Sulphate, and CO_2 treatments, consistent with a less active or less abundant hydrogenotrophic community under these electron acceptor conditions. The nitrate treatment was a clear exception, with complete hydrogen consumption by Day 7, the fastest response observed in this soil. The starting community can therefore be considered broadly adapted to favour nitrate-reducing conditions, as further evidenced by the elevated sequence read counts recorded in 16S rRNA gene sequencing analysis in nitrate-treated microcosms (averaging 49,000 counts compared to 27,500 in Iron treatments), suggesting greater overall microbial growth under nitrate-reducing conditions [Appendix D]. This pattern also coincides with the low corrosion rates observed in the sulphate and CO_2 treatments, where slower microbial activity would be expected to limit biologically driven corrosion over the experimental timeframe. Corrosion rates of steel coupons was higher in microcosms with a 10% hydrogen headspace than in microcosms with a nitrogen headspace in the iron and nitrate treatments, consistent with hydrogen-stimulated microbial activity driving corrosion. Despite lower corrosion rates, sulphur was detected in SEM/EDS analysis of coupons incubated with CO_2 and hydrogen, demonstrating some activity of sulphate reducing bacteria in the soil microcosms.

DNA extraction and subsequent amplification and sequencing of 16S rRNA genes were only successful from microcosms incubated with a 10% hydrogen headspace, microcosms with a nitrogen headspace yielded insufficient DNA for analysis. While extraction difficulties from clay-rich soils are well documented due to the strong binding of DNA to clay particles [18], the failure to extract amplifiable

© ROSEN
This document is classified as confidential

DNA from nitrogen microcosms alongside successful extraction from hydrogen microcosms, suggests that hydrogen availability stimulated sufficient microbial growth to yield extractable DNA, while microbial activity in microcosms incubated under a nitrogen headspace remained below detection limits. This represents an important, if indirect, line of evidence for the role of hydrogen in promoting microbial proliferation in this soil.

Methane production was detected across the Iron, Sulphate, and CO_2 hydrogen microcosms [Figure 5], with rRNA gene sequencing identifying *Methanobacteriaceae* in the Iron treatment [Figure 18: Microbial community composition in [redacted] soil microcosms after 28 days of incubation with a 10% hydrogen headspace, under iron-, sulphate- and nitrate-reducing conditions. Data represent the 20 most abundant taxa categorized at Family level.Figure 18]. The presence of methanogenic Archaea is significant in the context of MIC risk, as members of this family are known to contribute to corrosion of steel infrastructure through the direct uptake of electrons from the metal surface, and cathodic depolarisation-mediated hydrogen consumption. Their detection here, even as a minor community fraction, is consistent with observations of methanogen-associated MIC in other pipeline environments [19], and underscores the potential for hydrogen enrichment to select for corrosion-relevant methanogenic activity over longer timescales.

© ROSEN
This document is classified as confidential

5 CONCLUSIONS AND FUTURE WORK

5.1 Conclusions

Hydrogen consumption was observed across all microcosms, with 80-100% consumed in all-but-one treatments tested. The sole exception was nitrate-treated microcosms inoculated with [redacted] soil. In microcosms with a hydrogen headspace, pH the increased across the iron, sulphate and nitrate treatments, while nitrogen microcosms exhibited comparatively minor changes in pH across all treatments, indicating higher microbial activity in microcosms with 10% hydrogen in the headspace.

Methane production was detected in the [redacted] and [redacted] soils across the iron-, sulphate- and CO_2-treated microcosms in the presence of hydrogen, but was absent in microcosms with no hydrogen in the headspace. Conversely, nitrous oxide was detected in nitrate-treated microcosms inoculated with [redacted] soil both in the presence and absence of in the headspace, indicative of active denitrification. Microcosms inoculated with [redacted] soil and treated with nitrate also showed nitrous oxide accumulation, but the levels were too low to allow reliable quantification.

DNA extraction and 16S rRNA gene sequencing were largely successful for [redacted] and [redacted] soils however, DNA extraction from [redacted] soil proved challenging and was unsuccessful for microcosms with nitrogen headspace. Sequencing of 16S rRNA genes from the microcosm samples revealed clear differences in microbial community composition between microcosms with and without hydrogen in the headspace. Hydrogenotrophic microorganisms were markedly more abundant in the hydrogen microcosms than in nitrogen microcosms, demonstrating the influence of headspace gas composition on community structure. Evidence of microorganisms associated with MIC was found across all soils and treatments, with notably higher abundance in hydrogen microcosms than in nitrogen microcosms, though MIC associated taxa were present in both. Key microorganisms identified include bacteria from the families *Shewanellaceae* (iron treatments), *Desulfovibrionaceae* (sulphate treatments), *Methanobacteriaceae* (CO_2 treatments) and *Paenibacillaceae* and *Rhodocyclaceae* (nitrate treatments).

Corrosion of steel coupons varied across soils and treatments. In microcosms inoculated with [redacted] and [redacted] soil greater corrosion rates were observed in microcosms with hydrogen in the headspace relative to microcosms with a 100% nitrogen headspace, while results from [redacted] were similar for either headspace gas. SEM analysis revealed limited quantifiable corrosion features, such as metastable pitting, but did confirm the precipitation of salts on coupon surfaces and activity of sulphate reducers in two sulphate-treated and one CO_2-treated microcosm.

Although the short experimental timeframe (28 day incubation) yielded some inconclusive corrosion rate data, the proliferation of microbial populations associated with MIC in the presence of hydrogen highlights the possibility that longer term corrosion risk, on the scale of months to years, cannot be excluded.

5.2 Limitations and Further Work

The experiments presented here represent a proof of concept for investigating the impact of hydrogen on MIC. It was conducted under conditions optimised for mesophilic microorganisms in order to generate a measurable response within a short timeframe. Measurements included headspace gas

© ROSEN
This document is classified as confidential

composition, microbial community analysis, and assessment of corrosion on steel coupons. However, the short duration of the study imposes inherent limitations on interpreting long-term MIC risk.

A key consideration is that short-term corrosion tests (≤30 days) do not reliably represent longer-term behaviour. In abiotic systems, short-duration tests often record higher initial corrosion rates because the steel surface is freshly exposed and has not yet stabilised; over extended exposure, corrosion rates typically decline as protective films develop on the metal surface. Frameworks such as the Planned Interval Test (PIT) demonstrate that corrosion behaviour varies significantly between early-stage and prolonged exposure, reinforcing that short-term data capture only part of the time-dependent corrosion profile.

However, MIC operates under biological kinetics, not purely electrochemical ones. Microbial communities require time for colonisation, biofilm maturation, succession, and the establishment of metabolically active consortia. As a result, short-term MIC experiments systematically underestimate long-term corrosion, capturing only the lag or early exponential growth phase rather than the more aggressive stages associated with mature sulphidogenic or hydrogenotrophic biofilms. Therefore, the low corrosion rates observed in this 28-day study should be considered conservative indicators, underscoring the need for extended testing (90–180 days or more) to capture the full corrosion potential under hydrogen-stimulated MIC conditions.

Several avenues exist for further investigation into the influence of hydrogen on microbial communities and the associated MIC risk to steel pipelines:

- **Long-term incubation/exposure experiments (months to years).**
  The short timeframe of this study limits the conclusions that can be drawn regarding corrosion risk. Extended experiments would allow assessment of whether cumulative microbial activity and sustained hydrogen exposure leads to increased corrosion of steel pipelines over operationally relevant timescales.

- **Temperature conditions reflecting location-specific environments.**
  This study was conducted at temperatures optimal for mesophilic conditions. Future work should consider incubations at lower temperatures to evaluate the activity of psychrophilic microorganisms and their potential contribution to corrosion under cold-climate or seasonal conditions. This would also reinforce the need for long-duration studies.

- **Experiments without supplementary growth media.**
  Removing additional growth media would restrict microorganisms to nutrients available solely from the soil inoculum, more closely replicating in-situ conditions. Under these conditions microbial activity will likely be lower, requiring longer-term experiments to observe measurable corrosion.

- **Alternative sources of inoculum from pipeline-adjacent environments.**
  Soils used in this study were sourced from terrestrial pipelines. Future work could explore inocula from more chemically and microbially diverse environments, such as estuarine sediments or subsea pipelines, where elevated salinity, anaerobic conditions, and distinct microbial communities may present a heightened or qualitatively different corrosion risk compared to terrestrial settings.

© ROSEN
This document is classified as confidential

- **Interaction between Cathodic Protection (CP) and MIC.**
  Cathodic Protection is a primary defence mechanism for buried steel pipelines, yet its interaction with MIC remains an area requiring deeper investigation. While CP can suppress electrochemical corrosion, it may also influence microbial activity by altering redox conditions, increasing hydrogen availability at the steel surface, or changing the community structure of hydrogenotrophic and sulphidogenic microorganisms. Conversely, MIC processes particularly those associated with biofilm formation, SRB activity and metabolic acid production may impact CP current demand or reduce CP effectiveness through local depolarisation or shielding effects. Future work should therefore include controlled experiments that examine **(i)** how varying CP potentials affect microbial community composition and hydrogen-driven metabolisms, and **(ii)** how established MIC biofilms influence CP performance, current distribution, and protective potential reach, particularly under hydrogen leakage scenarios.

5.3 Future Research Directions

5.3.1 Influence of CO_2 Leakage on Soil Microbiomes, MIC Processes and CP Performance

Findings from the CO_2-enriched microcosms indicate that elevated CO_2 levels can substantially alter soil chemistry and microbial behaviour, with potential implications for corrosion processes similar to those observed under hydrogen exposure. Dissolved CO_2 forms carbonic acid, lowering pH and shifting redox conditions in ways that may stimulate CO_2-utilising or acid-tolerant microbial groups, including acetogens and certain sulphidogenic or iron-reducing taxa. These changes could influence MIC pathways by promoting the formation of corrosive metabolites or by altering competitive interactions within the soil microbiome.

In the context of buried CO_2 pipelines, even low-rate fugitive CO_2 leakage may create localised conditions that accelerate external corrosion through both chemical acidification and biologically mediated mechanisms. Moreover, CO_2-driven changes in soil pH, buffering capacity, and microbial colonisation could impact cathodic protection (CP) performance by modifying current demand, altering potential distributions, or enabling biofilm development that restricts CP current flow.

Future investigations should therefore assess the combined chemical and biological effects of sustained CO_2 exposure on pipeline-adjacent soils to determine whether CO_2 leakage presents an MIC risk comparable to hydrogen. Such studies should also evaluate the potential impacts of CO_2 on CP effectiveness under field-realistic conditions.

© ROSEN
This document is classified as confidential

6 REFERENCES

[1] British Geological Survey, “ESB description of parent material,” UK Soil Observatory, 2001.

[2] T. Farewell, I. Truckell, K. C. and S. Hallett, “The derivation and application of Soilscapes: soil and environmental datasets from the National Soil Resources Institute,” https://www.landis.org.uk, Cranfield University, 2011.

[3] F. Widdel and F. Bak, “Chapter 183: Gram-negative mesophilic sulfate-reducing bacteria.,” in *The Prokaryotes*, 2nd ed., vol. IV, A. Balows, T. H.G., M. Dworkin, W. Harder and K. Schleifer, Eds., New York, Springer, 1992, pp. 3352-3378.

[4] QIAGEN, “DNeasy® PowerSoil® Pro Kit Handbook - For the isolation of microbial genomic DNA from all soil types, including difficult samples such as compost, sediment, and manure,” June 2025. [Online]. Available: https://www.qiagen.com/us/resources/resourcedetail?id=9bb59b74-e493-4aeb-b6c1-f660852e8d97&lang=en. [Accessed January 2025].

[5] J. G. CAPORASO, J. KUCZYNSKI, J. STOMBAUGH, K. BITTINGER, F. D. BUSHMAN, E. K. COSTELLO, N. FIERER, A. G. PEÑA, J. K. GOODRICH, J. I. GORDON, G. A. HUTTLEY, S. T. KELLEY, D. KNIGHTS, J. E. KOENIG, R. E. LEY, C. A. LOZUPONE and R. KNIGHT, “QIIME allows analysis of high-throughput community sequencing data,” *Nature Methods,* vol. 7, pp. 335-336, 2010.

[6] J. G. CAPORASO, C. L. LAUBER, W. A. WALTERS, D. BERG-LYONS, J. HUNTLEY, N. FIERER, S. M. OWENS, J. BETLEY, L. FRASER, M. BAUER, N. GORMLEY, J. A. GILBERT, G. SMITH and R. KNIGHT, “Ultra-high-throughput microbial community analysis on the Illumina HiSeq and MiSeq platforms.,” *The ISME Journal,,* vol. 6, pp. 1621-1624, 2012.

[7] B. J. CALLAHAN, P. J. MCMURDIE, M. J. ROSEN, A. W. HAN, A. J. A. JOHNSON and S. P. HOLMES, “DADA2: High-resolution sample inference from Illumina amplicon data.,” *Nature Methods,* vol. 13, pp. 581-583, 2016.

[8] R. Parvej, B. D. R. Myers, K. Nelson, G. Singh and T. Reinbott, “Soil organic carbon: A foundational indicator of soil health,” *University of Missouri, MU Extension,* 2025.

© ROSEN
This document is classified as confidential

[9] J. Philips, L. Procopio and I. Marshall, “Insights into the various mechanisms by which Shewanella spp.,” *njp materials degredation,* vol. 7, no. 95, 2023.

[10] T. Iino, “13 Microorganisms Inducing Microbiologically Influenced Corrosion,” in *Electron-Based Bioscience and Biotechnology*, Singapore, Springer, 2020, p. 169–19.

[11] S. Kato, I. Yumoto and Y. Kamagate, “Isolation of Acetogenic Bacteria That Induce Biocorrosion by Utilizing Metallic Iron as the Sole Electron Donor,” *Applied and Environmental Microbiology,* vol. 81, 2014.

[12] E. O. Imo, C. E. Ihejirika, A. G. Ndukaku and P. J. Misoni, “Effects of Desulfotomaculum sp on corrosion behaviour of mild steel,” *Zaštita materijala,* vol. 64, no. 2, pp. 190-197, 2023.

[13] L. R. Reddy, C. Egerter, N. Jehmlich, A. Fiskal, L. Helmholz, S. Castronovo, P. Schweyen, S. Wulf, T. Terenes and J. Meier, “New insights in the metabolic functions of freshwater sulfate reducing communities during steel corrosion by biophysicochemical, 16S rRNA gene sequence and metaproteomic analysis,” *International Biodeterioration & Biodegradation,* vol. 198, no. 105995, 2025.

[14] S. Lata, S. Chhaya and A. K. Singh, “Comparison of Biocorrosion due to Desulfovibrio desulfuricans and Desulfotomaculum nigrificans Bacteria,” *Journal of Materials Engineering and Performance,* vol. 22, p. 463–469, 2013.

[15] G. Yanf, J. Guo, L. Zhuang, Y. Yuan and S. Zhou, “Desulfotomaculum ferrireducens sp. nov., a moderately thermophilic sulfate-reducing and dissimilatory Fe(III)-reducing bacterium isolated from compost,” *International Journal of Systematic and Evolutionary Microbiology,* vol. 66, no. 8, pp. 3022-3028, 2016.

[16] S. Lahme and J. M. Aguas, “Development of an Immunoassay for the Detection and Diagnosis of Microbially Influenced Corrosion Caused by Methanogenic Archaea,” *CORROSION,* vol. 81, no. 1, p. 21–26, 2025.

[17] S. Lahme, D. Enning, C. M. Callbeck, D. Menendez Vega, T. P. Curtis, I. M. Head and C. R. J. Hubert, “Metabolites of an Oil Field Sulfide-Oxidizing, Nitrate-Reducing Sulfurimonas sp. Cause Severe Corrosion,” *Applied and Environmental Microbiology,* vol. 85, no. 3, 2019.

[18] P. Cai, Q. Huang, X. Zhang and H. Chen, “Adsorption of DNA on clay minerals and various colloidal particles from an Alfisol,” *Soil Biology and Biochemistry,* vol. 38(3), pp. 471-476, 2006.

© ROSEN
This document is classified as confidential

[19] C. C. Okoro, S. Olusegen and J. Lin, “Substrate Availability, pH, and Temperature Influence Methanogenesis and Mild Steel Corrosion.,” *Geomicrobiology Journal,* vol. 34(9), p. 729–736, 2017.

[20] Environment agency, “Decision document: National Grid Gas Plc,” 2017. [Online]. Available: https://assets.publishing.service.gov.uk/media/5a821deded915d74e3401d01/Decision_document.pdf.

[21] A. Spark, K. Wang, I. Cole, D. Law and L. Ward, “Microbiologically influenced corrosion: a review of the studies conducted on buried pipelines,” *Corrosion Reviews,* vol. 38, no. 3, 2020.

© ROSEN
This document is classified as confidential

APPENDIX A TOTAL ORGANIC AND INORGANIC CARBON

Sample	Mass	Carbon (%)	TOC (%)	TIC (%)
F1	0.1505	3.4468	3.2835	0.1633
F2	0.1518	3.5958	3.424	0.1718
B1	0.1511	2.7619	2.585	0.1769
B2	0.1512	3.1994	3.0174	0.182
H1	0.1521	3.1085	0.2224	2.8861
H2	0.1515	2.8242	0.1944	2.6298

Total organic content (TOC) and total inorganic content (TIC) was analysed on a Leco RC612. F = [redacted] B = [redacted] H = [redacted]

© ROSEN
This document is classified as confidential

APPENDIX B MATERIALS CERIFICATES

B.1 Steel Data Sheet

LIBERTY STEEL NEWPORT LIMITED

TEST CERTIFICATE

Corporation Road,
NEWPORT,
South Wales NP19 4XE
Tel: +44 (0) 1633 290 288
Fax: +44 (0) 1633 290 240

CUSTOMER : PHOENIX STEEL LTD
AMOS AYRE PLACE
SIMONSIDE INDUSTRIAL ESTATE
SIMONSIDE
SOUTH SHIELDS
TYNE & WEAR NE34 9PB
UNITED KINGDOM

4mm SOD
CAST No
BD001

SHIPPED TO : PHOENIX STEEL LTD
AMOS AYRE PLACE
NEWCASTLE RD ,SIMONSIDE IND EST
SOUTH SHIELDS, TYNE & WEAR
NE34 9PB

Specification : BS EN 10025:2004 Grade S355JR Size : 1250 x 4 mm Customer Order No : 61138-SIMA Despatch Date : 16/08/2017

Steelmaking Process : BOS / Concast Test Certificate to BS EN 10204 3.1 Despatch Note No : 663985 Liberty Steel Order No : 0024281/ 003

CAST NUMBER	COIL NUMBER	NOMINAL SIZE mm	YIELD STRENGTH (Re) N/mm2	TENSILE STRENGTH (Rm) N/mm2	% ELONG @ 80 mm	% ELONG @ 5.65vA	BEND TESTS
168538	AM3379	1250 x 4 mm	448	553		27.8	

CHEMICAL ANALYSIS %

C	Si	Mn	P	S	Cr	Mo	Ni	Cu	V	Al	Nb	N	CE
.13	.020	1.16	.012	.009	.040	.002	.010	.020	.072	.032	.001	.005	.348

CHARPY IMPACT TEST

Size	°C	Joules	Average
	0	0 / 0 / 0	0

HARDNESS TEST

Hardness Scale	Result 1	Result 2	Result 3	Average
HRB	0	0	0	0

Certified that the whole of the material hereon have been inspected and tested, and unless otherwise stated conforms with the requirements of the order.

CARES 1254 UKAS MANAGEMENT SYSTEMS 002

Signed: .....

For and on behalf fLIBERTY STEEL NEWPORT LIMITED

B.2 Laser Cutting Data Sheet

SETTING INFORMATION

```
MACHINE NAME      : Trumpf TruLaser 3030 Fiber (L49) Sinumerik
                    840D
DRAWING NAME      : P1 rsg4mm355 201025
DWG ISSUE         : 1
DWG DIRECTORY     : //192.168.0.220/Documents/ra.../ROSEN GROUP
DATE              : Mon Oct 20 14:15:51 2025
MATERIAL          : s355j2
THICKNESS         : 4 mm
STRATEGY          : Nitrogen/Standard - Performance Package/200
SHEET SIZE        : 1260 x 100 mm
CLAMP POSITIONS   :

RUN TIME          : UNKNOWN
SHEET UTILISATION : 15.7%

NUMBER OF SHEETS  : 1
```

TOOL LIST

TOOL	TYPE	SIZE	RADS	ANGLE	DIE/CL	EHL	Tool No.
1	Large Profiles	0.300 mm dia	-	-	-	-	100.3
2	Large lead-in	0.300 mm dia	-	-	-	-	700.3

NEST PARTS LIST

Item	Part Name	Num Off
1	8mm x 8mm 4mm s355	310

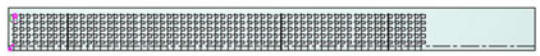

B.3 Pipeline Material Chemical Analysis

element

TEST CERTIFICATE

Element Materials Technology
Holwick Road, Riverside Park
Middlesbrough, Teesside
TS2 1QS, UK

P: +44 (0) 1642 250 336
F: +44 (0) 1642 250 337
info.teesside@element.com
element.com

ROSEN UK
FLOOR 2 Q5
QUORUM BUSINESS PARK
NEWCASTLE UPON TYNE
TYNE & WEAR
NE12 8BS
Attn: KARL BROWN

REF No X 554692 : Issue 1
Page 1 of 1
Ord No SEE BELOW
Date Tested 13/11/25
Date Reported 13/11/25

Item - REF: 20778 & 18086
2 OFF SAMPLES

Specification - PRODUCT SPECIFICATION NOT APPLICABLE

Chemical Analysis - ICP-OES,Combustion (C+S),See Below

	C [%]	Si [%]	Mn [%]	P [%]	S [%]	Cr [%]	Mo [%]	Ni [%]	Al [%]	Cu [%]	Nb [%]	Comments
001:	0.20	0.15	1.02	0.026	0.021	0.04	0.01	0.07	0.013	0.19	<0.010	20778
002:	0.20	0.13	1.00	0.020	0.021	0.03	<0.01	0.08	<0.010	0.16	<0.010	18086

	Ti [%]	V [%]	CEV [%]	Comments
001:	<0.010	<0.010	0.40	20778
002:	<0.010	<0.010	0.39	18086

Chemical Analysis Test Methods: Si,Mn,P,Cr,Mo,Ni,Al,Cu,Nb,Ti,V - ICP-OES. Inhouse Method TL CHEM03B
C,S - Combustion (C+S). Inhouse Method TL CHEM04B
CEV - See Below

Certificate Comments

$$CEV = C + \frac{Mn}{6} + \frac{Cr + Mo + V}{5} + \frac{Ni + Cu}{15}$$

---------- End of Text ----------

Tested by **ELEMENT CHEMISTRY**

EMMA STOWELL
CHEMISTRY MANAGER
For and on authority of
Element Materials Technology

67

APPENDIX C CHEMICAL COMPOSITION OF BAK AND WIDDEL GROWTH MEDIUM

Table 1: Basal media chemicals

Component	Chemical Formula	Concentration g/l or ml/l
Distilled water	H_2O	Up to 1000
Sodium Chloride	NaCl	1.0
Magnesium Chloride Hexahydrate	$MgCl_2$-$6H_2O$	0.5
Calcium Chloride Dihydrate	$CaCl_2$-$2H_2O$	0.15
Ammonium Chloride	NH_4Cl	0.3
Potassium Dihydrogen Phosphate	KH_2PO_4	0.2
Potassium Chloride	KCl	0.5

Table 2: Trace components

Component	Chemical Formula	Concentration g/l or ml/l
Distilled water	H_2O	987
Hydrochloric acid	HCl	12.5
Boric acid	H_3BO_3	30
Iron (II) sulphate Heptahydrate	$FeSO_4$-$7H_2O$	2.1
Manganese (II) chloride tetrahydrate	$MnCl_2$-$4H_2O$	0.1
Cobalt (II) chloride hexahydrate	$CoCl_2$-$6H_2O$	0.19
Nickel (II) chloride hexahydrate	$NiCl_2$-$6H_2O$	0.024
Copper (II) chloride dihydrate	$CuCl_2$-$2H_2O$	0.002
Zinc sulphate heptahydrate	$ZnSO_4$-$7H_2O$	0.144
Sodium molybdate dihydrate	Na_2MoO_4-$2H_2O$	0.018
Sodium selenite pentahydrate	Na_2SeO_3-$5H_2O$	0.004
Sodium tungstate dihydrate	Na_2WO_4-$2H_2O$	0.008

© ROSEN
This document is classified as confidential

Table 3: Vitamins

Component	Formula	Concentration
4-Aminobenzoic Acid	C7H7NO2	0.004
D(+)-Biotin	C10H16N2O3S	0.001
Nicotinic Acid	C6H5NO2	0.01
Calcium D(+)-pantothenate	C18H32CaN2O10	0.005
Pyridoxamine dihydrochloride	C8H12N2O2-2HCl	0.015
Thiamine Chloride hydrochloride	C12H18Cl2N4OS	0.01
Cyanocobalamin	C63H88CoN14O14P	0.005

Table 4: Bicarbonate Mixture

Component	Formula	Concentration
Distilled Water	H_2O	Up to 1000
Sodium Bicarbonate	$NaHCO_3$	84.0

Table 5: Sodium sulphide solution

Component	Formula	Concentration g/l or ml/l
Distilled water	H_2O	Up to 1000
Sodium Sulphide nonahydrate	$Na_2S\text{-}9H_2O$	48

Table 6: Electron acceptor treatments added to different microcosms

Component	Chemical Formula	Concentration g/l or ml/l
Ferric (III) Citrate	$C_6H_5FeO_7$	1.2247
Sodium Sulphate	Na_2SO_4	0.7102
Sodium Nitrate	$NaNO_3$	0.4249

© ROSEN
This document is classified as confidential

APPENDIX D SEQUENCING COUNTS

Sample ID		No. of Sequences	Sample ID		No. of Sequences	Sample ID		No. of Sequences
21	HNH.3	58,686	39	HCF.3	87,302	60	NSW.3	95,390
20	HNH.2	41,508	31	HSF.1	85,261	53	NIW.2	90,406
3	HIH.3	39,254	38	HCF.2	80,227	55	HSW.1	86,050
7	HSH.1	19,432	28	NIF.1	76,057	76	NIPM.1	80,819
2	HIH.2	14,529	45	HNF.3	75,511	52	NIW.1	77,248
			25	HIF.1	74,067	59	NSW.2	76,432
			90	F.3	71,907	79	HSPM.1	68,914
			40	NCF.1	66,083	58	NSW.1	67,880
			30	NIF.3	65,450	80	HSPM.2	67,389
			44	HNF.2	63,375	66	NCW.3	67,194
			32	HSF.2	62,984	71	NNW.2	65,915
			37	HCF.1	62,421	83	NSPM.2	64,590
			47	NNF.2	60,846	78	NIPM.3	62,761
			42	NCF.3	56,323	93	W.3	60,830
			33	HSF.3	54,561	54	NIW.3	60,291
			29	NIF.2	53,665	51	HIW.3	60,254
			46	NNF.1	53,098	84	NIPM.3	59,334
			48	NNF.3	51,811	64	NCW.1	56,296
			43	HNF.1	47,579	61	HCW.1	53,456
			26	HIF.2	47,032	50	HIW.2	53,124
			41	NCF.2	46,586	92	W.2	50,843
			88	F.1	43,956	82	NSPM.1	50,639
			89	F.2	41,041	62	HCW.2	49,481
						56	HSW.2	48,000
						77	NIPM.2	45,931
						49	HIW.1	40,842
						68	HNW.2	33,392
						74	HIPM.2	31,011
						75	HIPM.3	17,132
						69	HNW.3	1,094

© ROSEN
This document is classified as confidential

APPENDIX E SEM AND EDS ANALYSIS

Live Microcosms				
	SEM		EDS	
	x200 magnification	x1000 magnification	Map	Analysis
Iron				
[redacted] H_2, coupon (HIH2, HIH3)	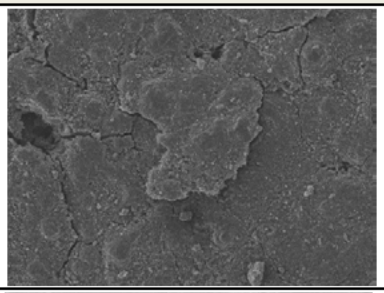	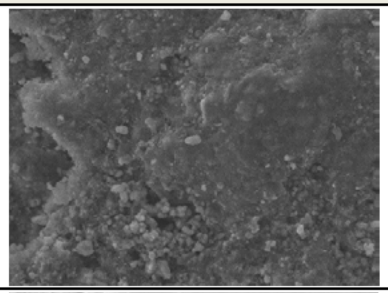	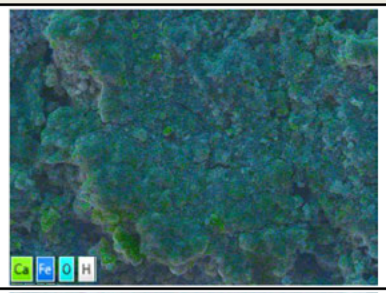	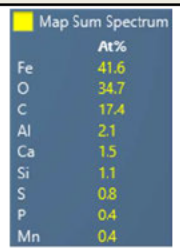 Map Sum Spectrum At% Fe 41.6 O 34.7 C 17.4 Al 2.1 Ca 1.5 Si 1.1 S 0.8 P 0.4 Mn 0.4
[redacted] N_2, coupon (NIH3)	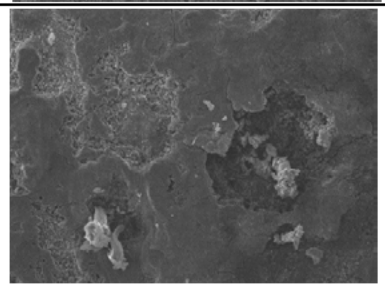	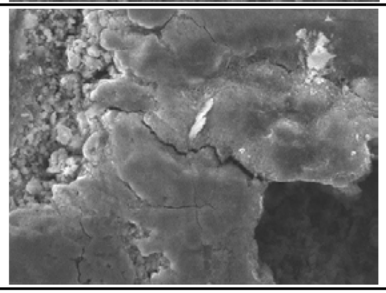		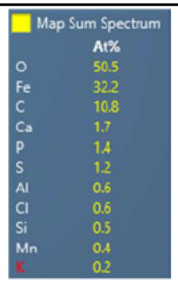 Map Sum Spectrum At% O 50.5 Fe 32.2 C 10.8 Ca 1.7 P 1.4 S 1.2 Al 0.6 Cl 0.6 Si 0.5 Mn 0.4 K 0.2
[redacted] H_2, coupon (HIF2)	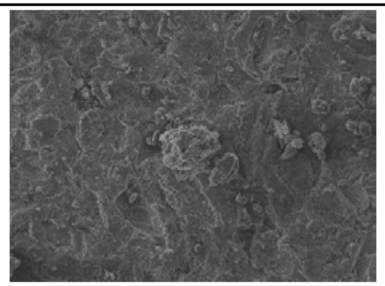	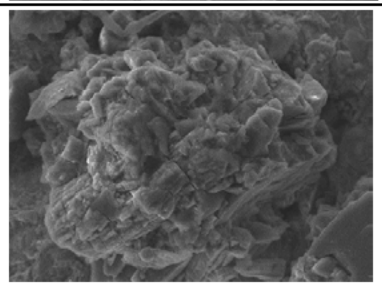	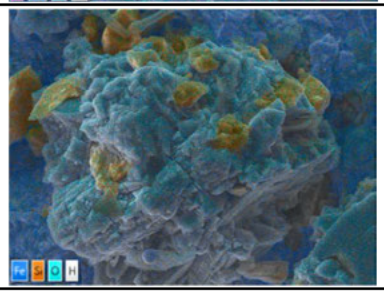	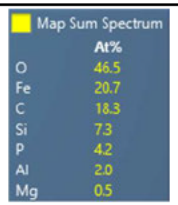 Map Sum Spectrum At% O 46.5 Fe 20.7 C 18.3 Si 7.3 P 4.2 Al 2.0 Mg 0.5

© ROSEN
This document is classified as confidential

[redacted] N_2, coupon (NIF1)	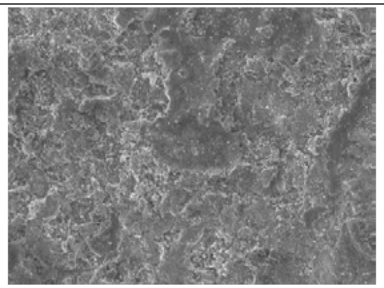	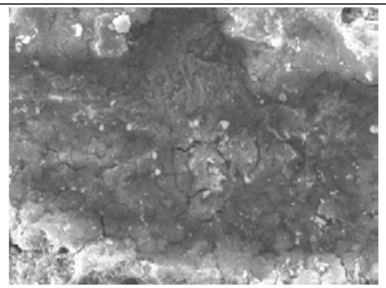	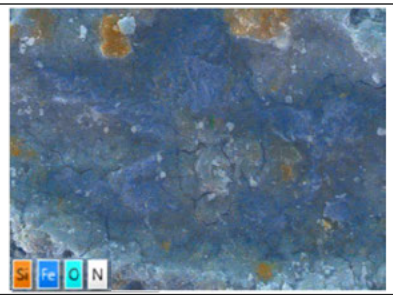	Map Sum Spectrum At% O 43.7 Fe 35.3 C 13.3 Si 3.1 Al 2.1 Na 0.8 Cl 0.4 Mn 0.3 P 0.2 K 0.2
[redacted] H_2, coupon (HIW2)	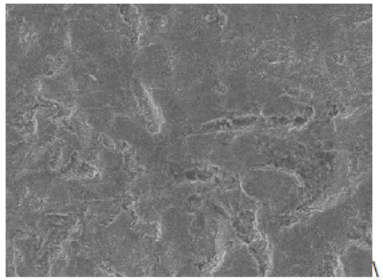	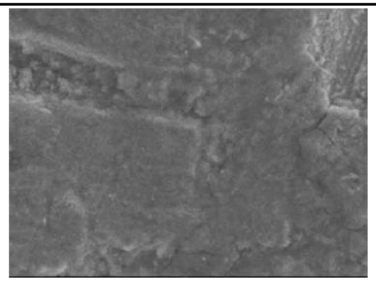	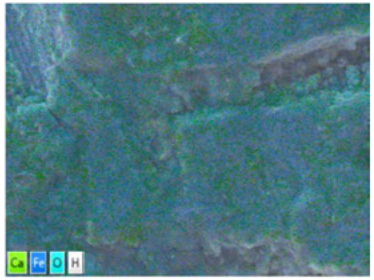	Map Sum Spectrum At% O 40.9 Fe 38.5 C 15.3 Al 1.9 Si 1.2 Ca 0.9 S 0.5 Mn 0.4
[redacted] N_2, coupon (NIW3)	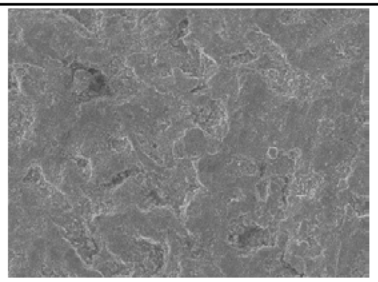	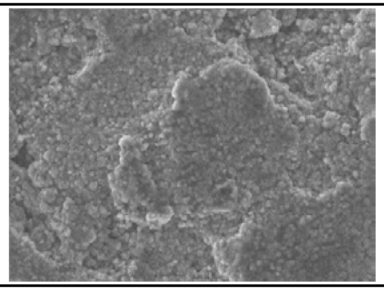	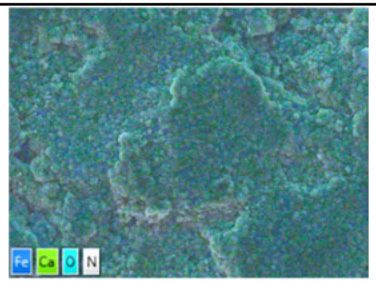	Map Sum Spectrum At% O 49.8 C 23.1 Fe 22.9 Ca 1.9 Al 0.8 Si 0.7 P 0.4 S 0.3 Mn 0.3

© ROSEN
This document is classified as confidential

[redacted] H_2, pipeline sample (HIPM3)	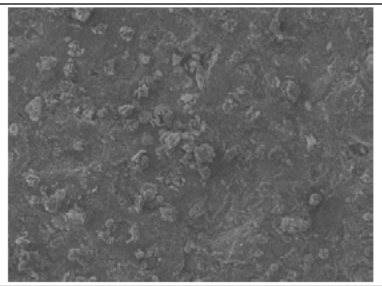	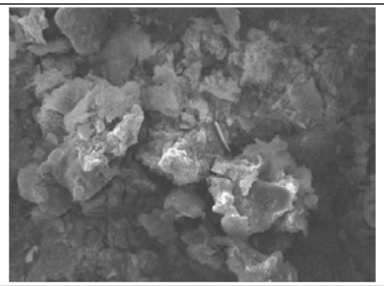	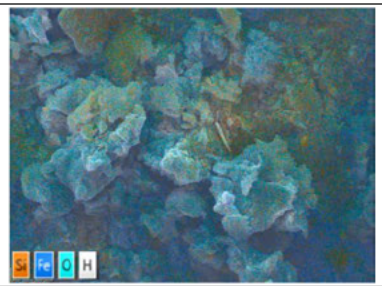	Map Sum Spectrum At% O 47.6 Fe 28.6 C 12.7 Si 4.8 Al 4.5 S 0.5 Mn 0.4 P 0.2 K 0.2
[redacted] N_2, pipeline sample (NIPM1)	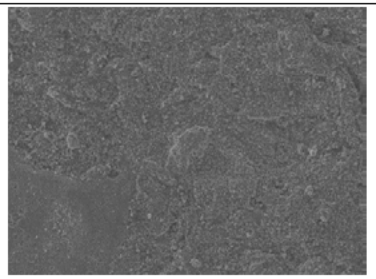	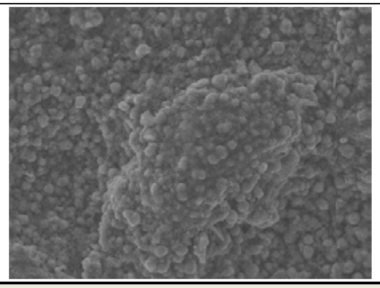	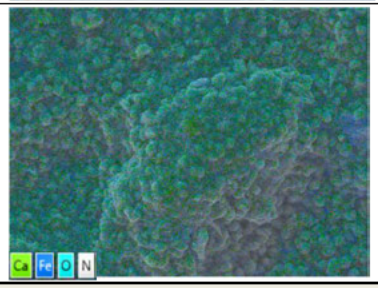	Map Sum Spectrum At% O 50.1 Fe 25.4 C 19.7 Ca 1.9 Al 1.1 Si 0.7 S 0.4 P 0.4 Mn 0.3
Sulphate				
[redacted] H_2, coupon (HSH2)	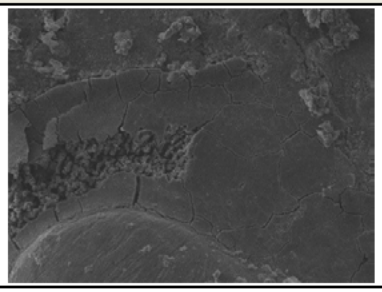	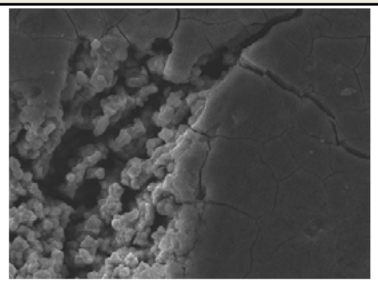	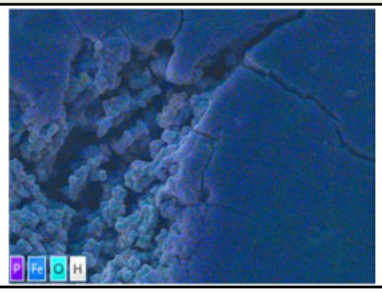	Map Sum Spectrum At% O 55.2 Fe 26.8 C 10.2 P 4.0 Ca 1.9 Mg 0.9 Al 0.4 Si 0.3

© ROSEN
This document is classified as confidential

[redacted] N_2, coupon (NSH3)	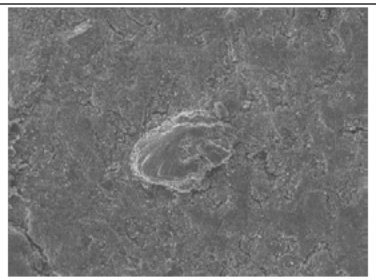	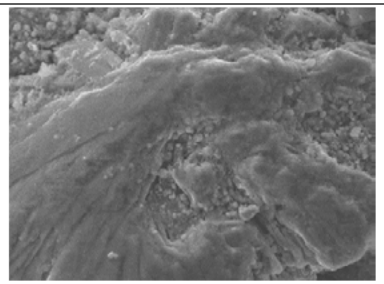	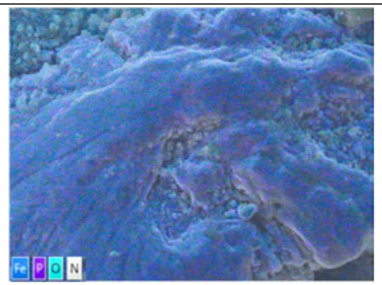	Map Sum Spectrum At% O 61.2 Fe 14.6 C 14.4 P 6.9 Mg 0.9 S 0.8 Ca 0.5 Si 0.4 Br 0.2
[redacted] H_2, coupon (HSF3)	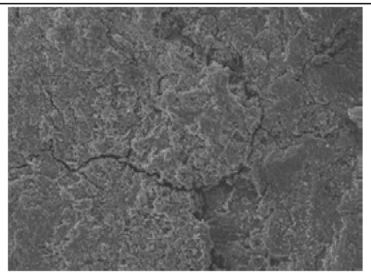	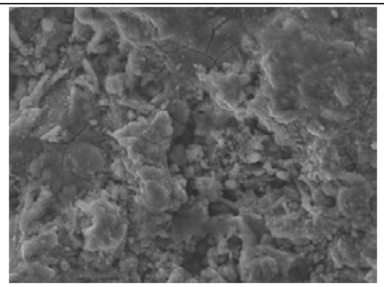	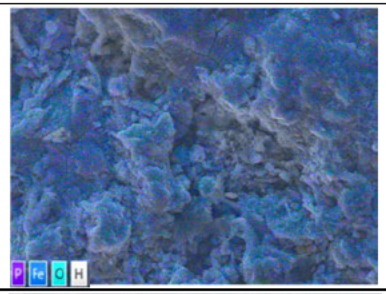	Map Sum Spectrum At% O 46.7 Fe 29.4 C 18.2 P 3.4 Ca 0.6 Mg 0.5 Al 0.5 Si 0.3
[redacted] N_2, coupon (NSF3)	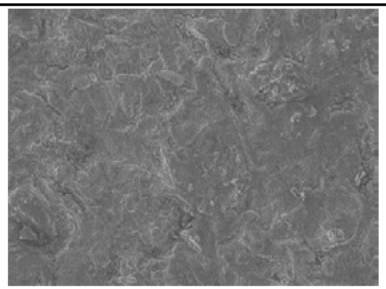	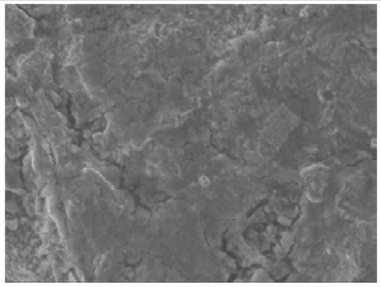	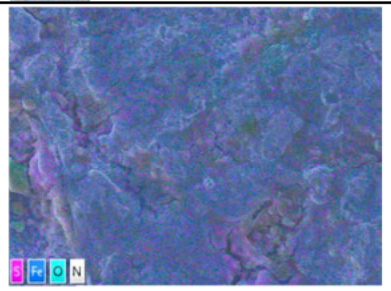	Map Sum Spectrum At% Fe 37.7 O 31.9 C 22.8 S 2.3 Al 2.2 Si 1.3 P 0.5 Mg 0.4 Ca 0.3 Mn 0.3

© ROSEN
This document is classified as confidential

[redacted] H_2, coupon (HSW1)	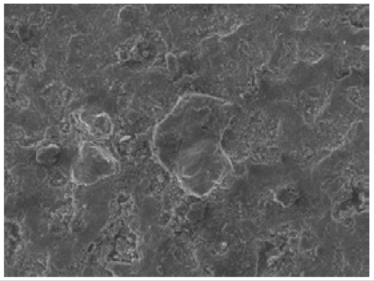	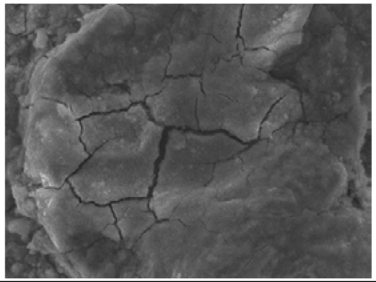	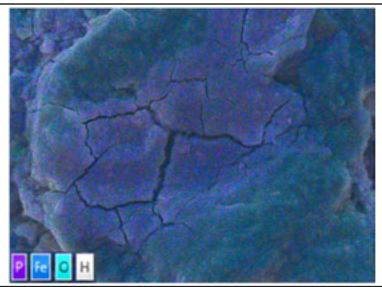	Map Sum Spectrum At% O 51.2 Fe 19.0 C 18.4 P 3.2 Si 3.2 Ca 1.8 S 1.5 Mg 1.0 Al 0.3
[redacted] N_2, coupon (NSW1)	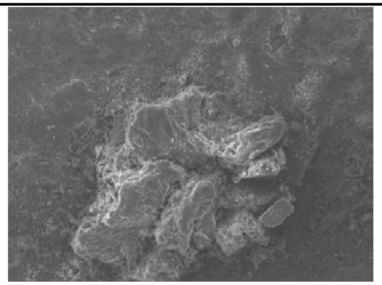	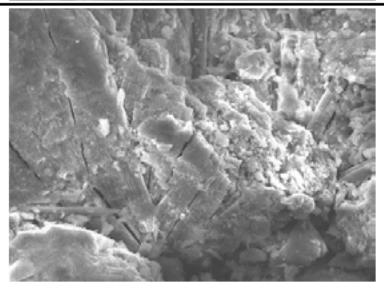	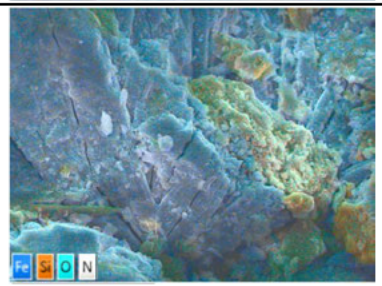	Map Sum Spectrum At% O 53.8 C 15.7 Fe 10.1 Si 7.0 P 5.6 Al 3.8 Mg 1.7 Na 0.8 Ca 0.4 K 0.3 S 0.3
[redacted] H_2, pipeline sample (HSPM1)	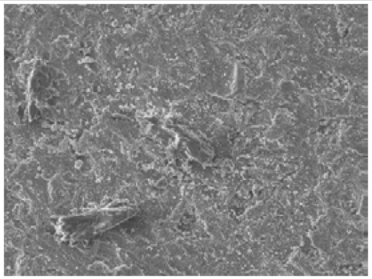	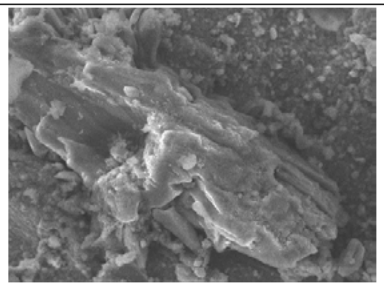	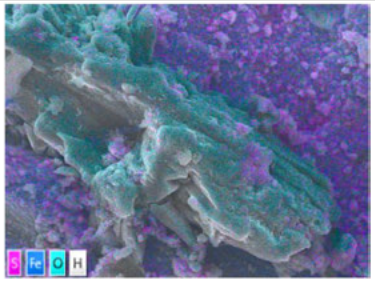	Map Sum Spectrum At% O 48.2 Fe 19.7 C 17.3 P 4.2 S 4.2 Mg 3.5 Si 1.1 Al 1.0 Ca 0.3 Mn 0.2

© ROSEN
This document is classified as confidential

[redacted] N_2, pipeline sample (NSPM2)	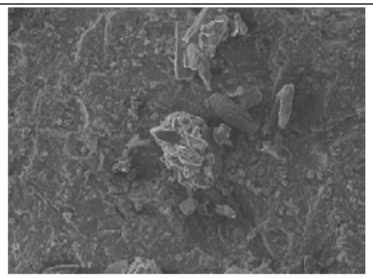	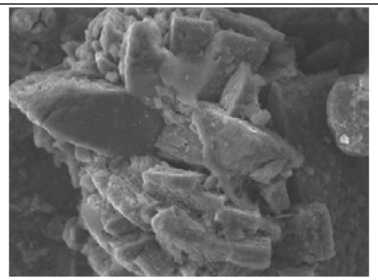	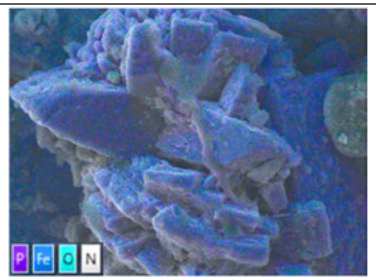	Map Sum Spectrum At% O 52.1 Fe 18.8 C 17.0 P 6.1 Mg 1.5 Si 1.5 Al 1.5 S 0.7 Mn 0.3 Ca 0.2 K 0.2
CO_2				
[redacted] H_2, coupon (HCH3-LC)	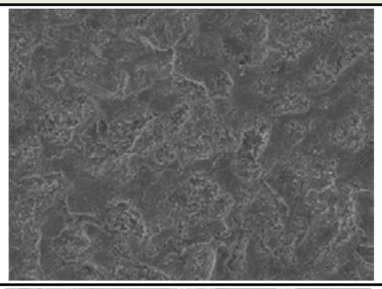	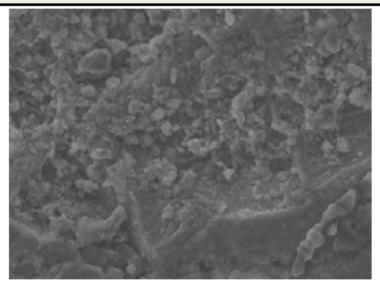	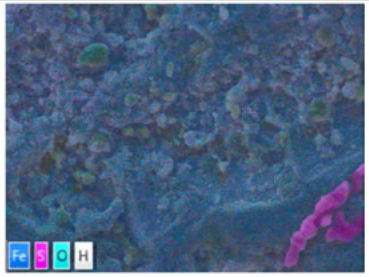	Map Sum Spectrum At% O 39.1 Fe 26.7 C 18.9 S 10.0 Ca 1.5 Al 1.4 Si 1.4 P 0.5
[redacted] N_2, coupon (NCH3)	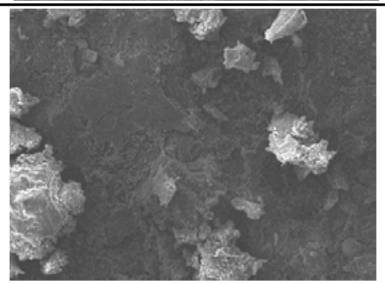	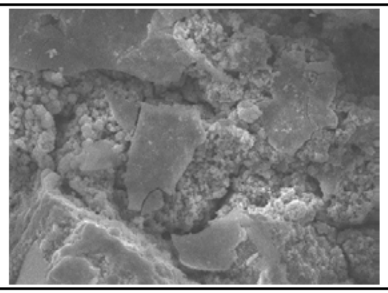	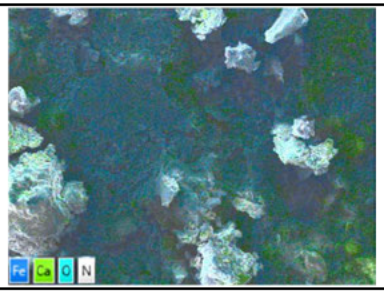	Map Sum Spectrum At% O 53.3 Fe 25.0 C 9.7 Ca 3.6 Si 3.0 Al 1.3 Cl 1.3 S 1.1 Mg 0.7 P 0.7 K 0.2

© ROSEN
This document is classified as confidential

[redacted] H_2, coupon (HCF2)	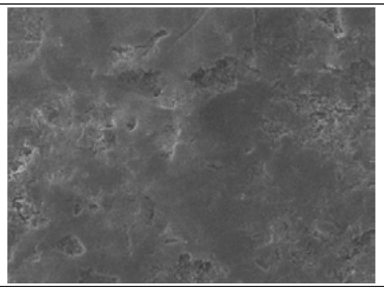	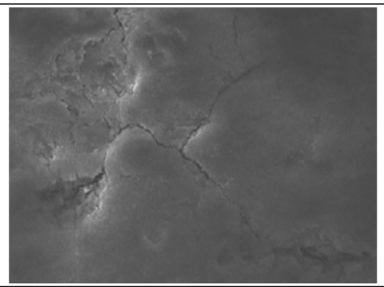	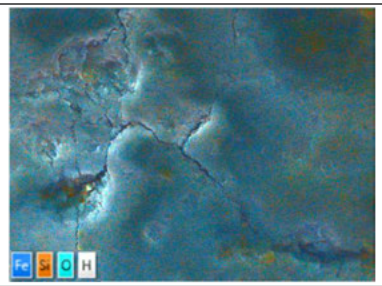	Map Sum Spectrum At% O 51.7 Fe 18.0 C 15.7 Si 6.0 Al 4.6 S 2.0 Mg 0.6 K 0.5 P 0.3
[redacted] N_2, coupon (NCF2)	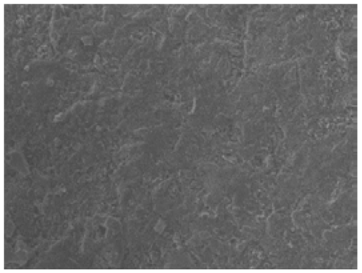	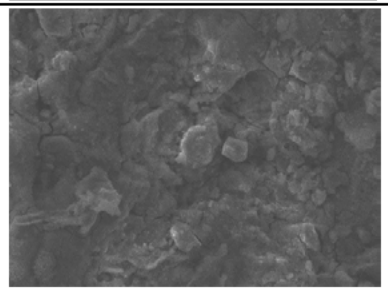	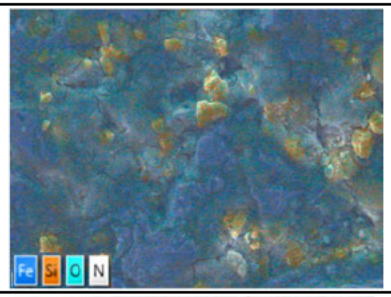	Map Sum Spectrum At% O 41.5 Fe 29.0 C 16.1 Si 6.5 Al 2.7 S 2.6 K 0.4 Ti 0.4 Cl 0.3
[redacted] H_2, coupon (HCW1)	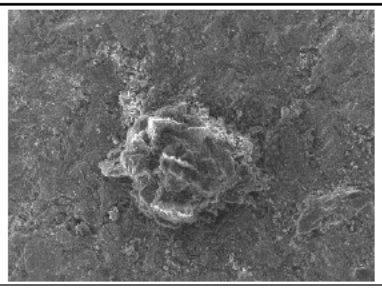	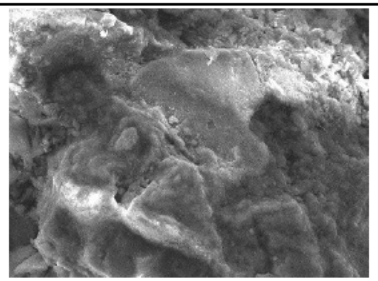	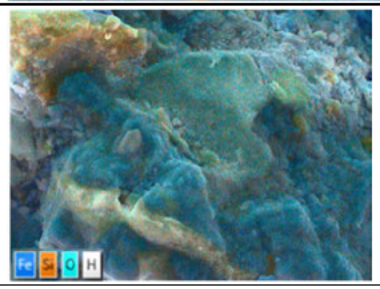	Map Sum Spectrum At% O 50.6 C 29.9 Fe 6.1 Si 5.2 Al 3.4 P 2.2 Mg 1.4 Ca 0.4 K 0.3 S 0.2

© ROSEN
This document is classified as confidential

[redacted] N_2, coupon (ICW1)	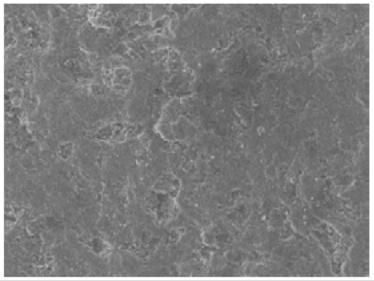	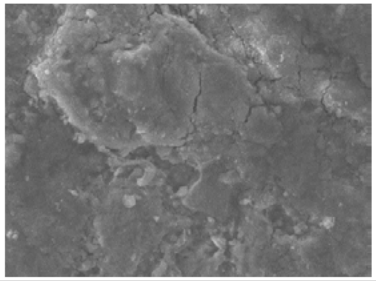	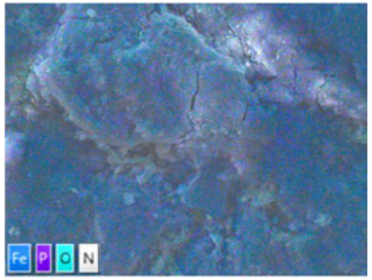	Map Sum Spectrum At% O 43.0 Fe 27.2 C 20.6 Al 2.4 P 2.2 S 1.2 Ca 1.1 Si 1.1
Nitrate				
[redacted] H_2, coupon (HNH3)	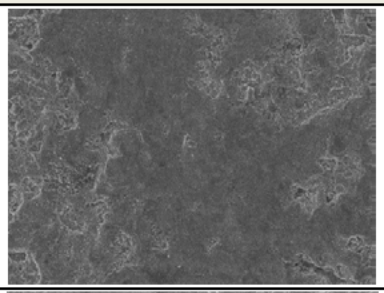	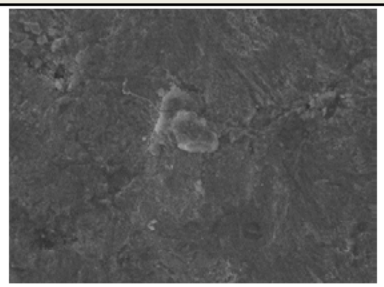		Map Sum Spectrum At% Fe 49.4 O 27.9 C 14.3 P 2.6 Al 1.9 Mg 1.2 Ca 1.1 Mn 0.5 Na 0.4 Si 0.4
[redacted] N_2, coupon (NNH1)	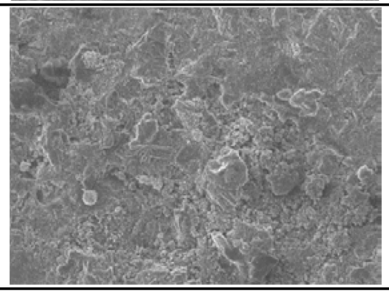	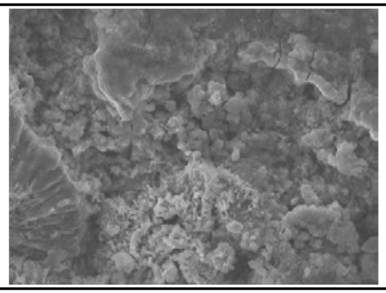	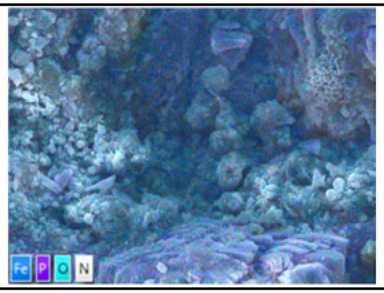	Map Sum Spectrum At% O 53.5 Fe 27.0 C 11.7 P 3.2 Al 1.4 Si 0.9 Mg 0.8 Ca 0.6 Cl 0.3

© ROSEN
This document is classified as confidential

[redacted] H_2, coupon (HNF1)	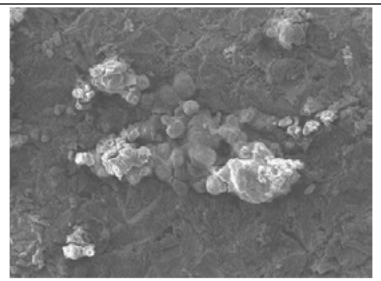	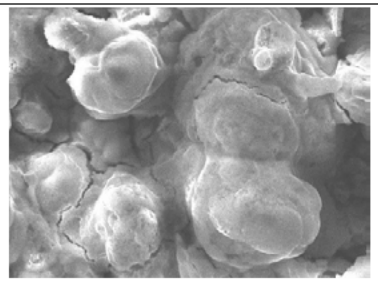	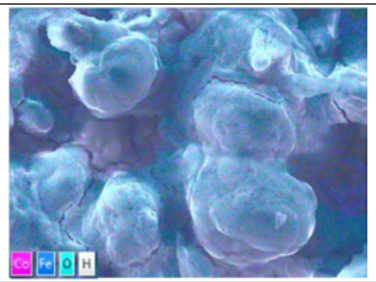	Map Sum Spectrum At% O 51.0 Fe 38.3 C 9.4 Mn 0.4 Al 0.3 Co 0.2
[redacted] N_2, coupon (NNF1)	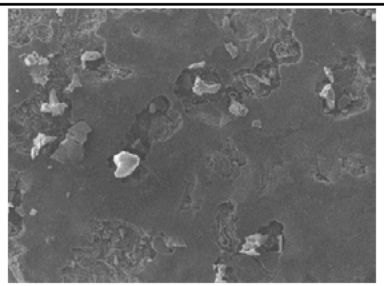	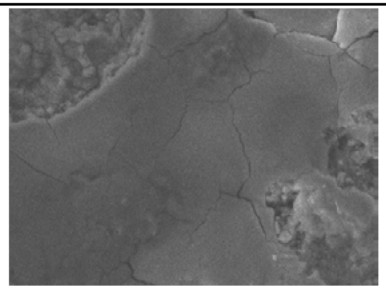	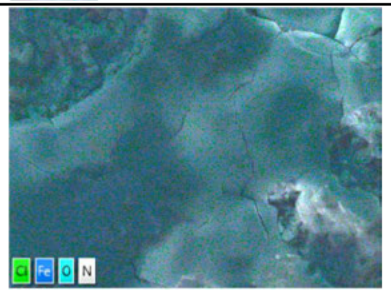	Map Sum Spectrum At% O 53.3 Fe 34.0 C 9.1 Al 0.9 Cl 0.9 Si 0.7 P 0.4 Mn 0.3 Ca 0.2
[redacted] H_2, coupon (HNW3)	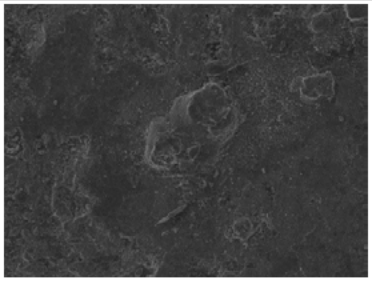	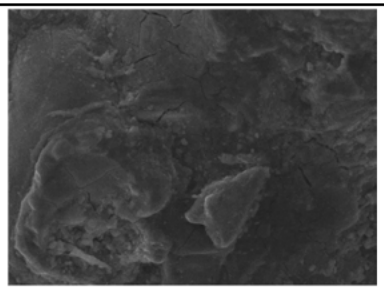		Map Sum Spectrum At% O 40.5 Fe 29.5 C 22.2 P 2.5 Ca 1.5 Si 1.1 Mg 1.1 Al 0.9

© ROSEN
This document is classified as confidential

[redacted] N_2, coupon (NNW1)	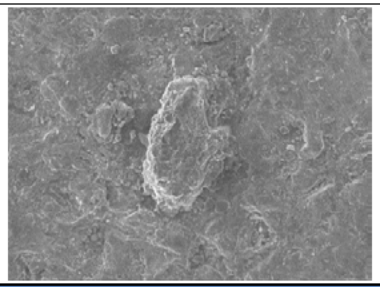	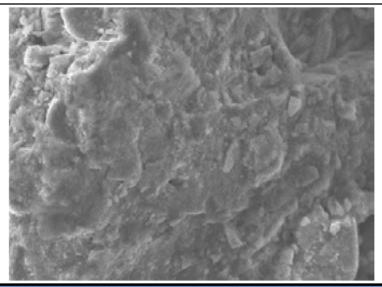	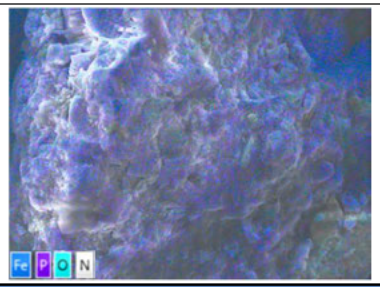	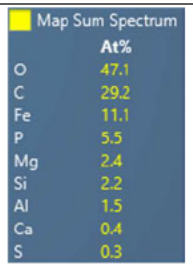
Killed Microcosms				
	SEM		**EDS**	
	x200 magnification	**x1000 magnification**	**Map**	**Analysis**
Iron				
[redacted] H_2, coupon (HIHK3)	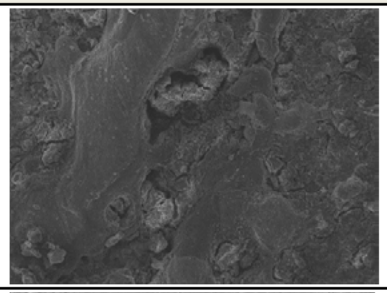	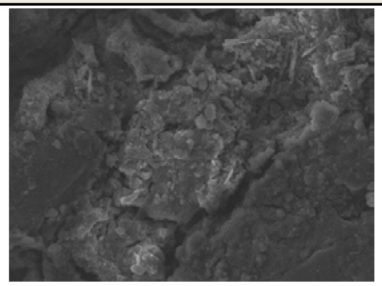	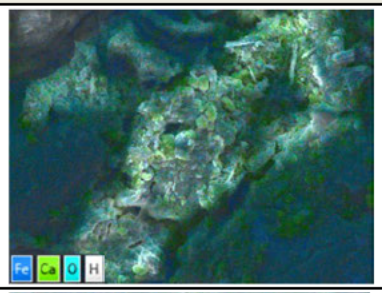	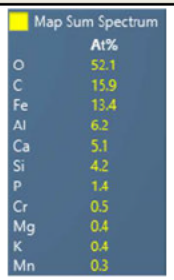
[redacted] N_2, coupon (NIHK3)	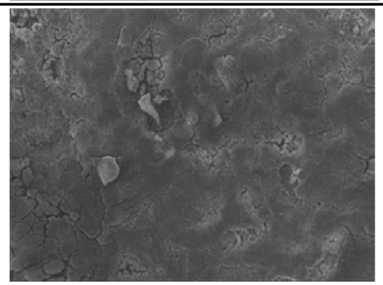	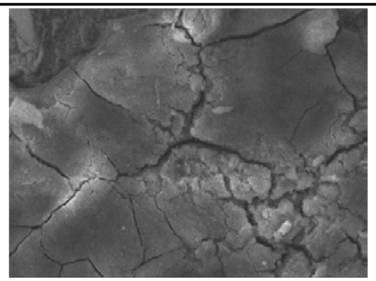	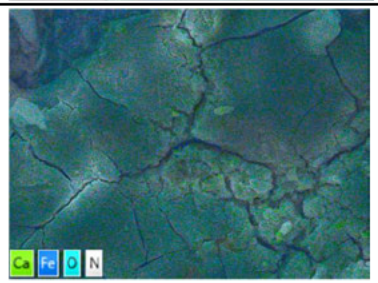	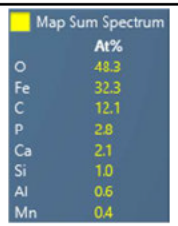

© ROSEN
This document is classified as confidential

[redacted] H_2, coupon (HIFK1)	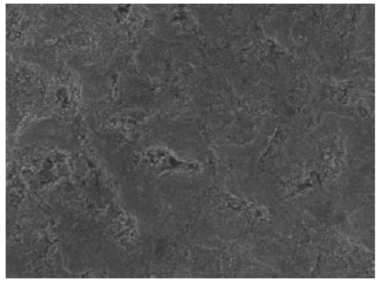	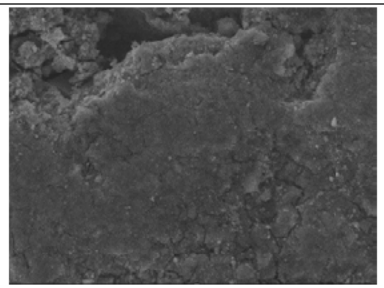	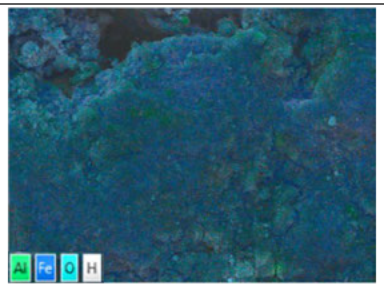	Map Sum Spectrum At% O 38.7 Fe 31.5 C 23.5 Al 2.8 Si 1.1 P 0.5 Mg 0.5 Ti 0.5 S 0.4 Mn 0.3 Ca 0.2
[redacted] N_2, coupon (NIFK3)	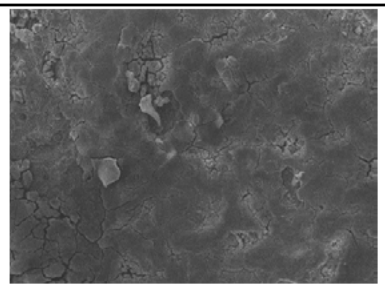	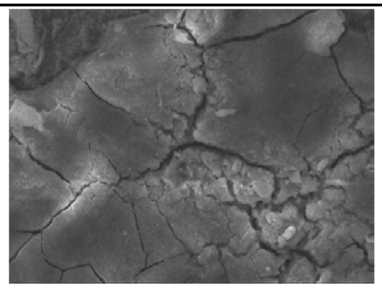	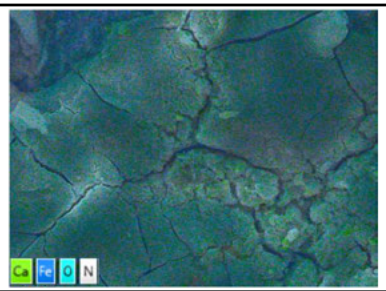	Map Sum Spectrum At% O 48.3 Fe 32.3 C 12.1 P 2.8 Ca 2.1 Si 1.0 Al 0.6 Mn 0.4
[redacted] H_2, coupon	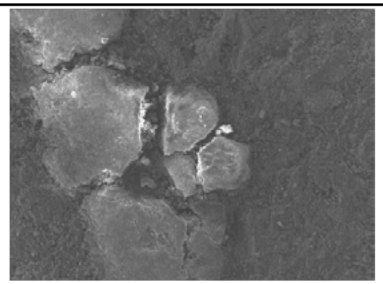	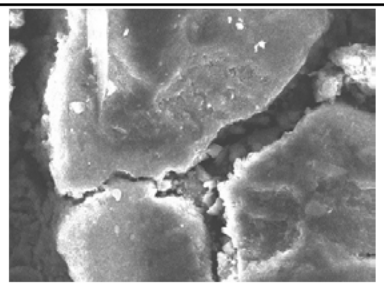	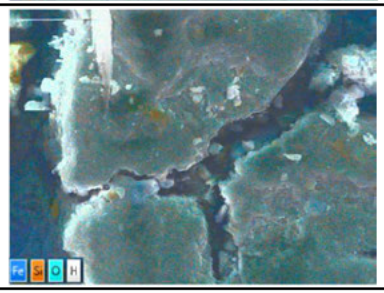	Map Sum Spectrum At% O 53.1 C 20.0 Fe 11.4 Si 6.0 Al 4.8 P 2.5 Ca 0.8 Na 0.4 Mg 0.4 K 0.3

© ROSEN
This document is classified as confidential

[redacted] N_2, coupon (NIWK3)	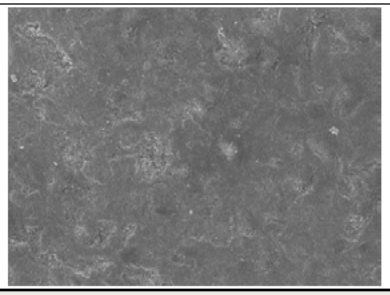	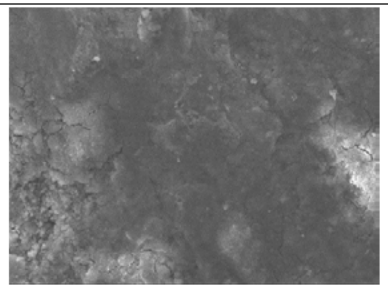	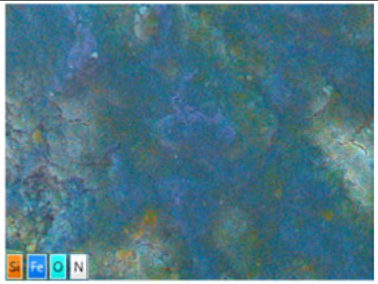	Map Sum Spectrum At% O 44.9 Fe 25.0 C 16.7 Si 4.2 Al 4.1 P 2.7 Na 0.8 Ca 0.7 K 0.3
Sulphate				
[redacted] H_2, coupon (HHSK3)	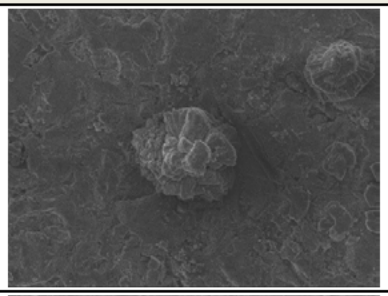	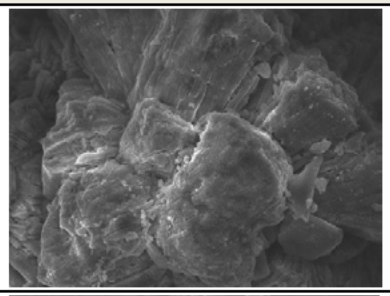	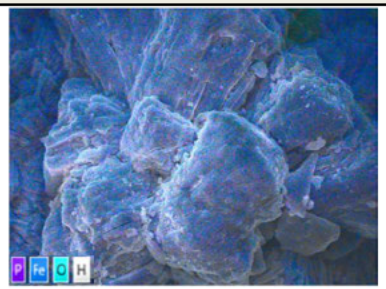	Map Sum Spectrum At% O 55.6 C 15.4 Fe 12.7 P 9.6 Mg 4.7 Si 0.9 Ca 0.5 Al 0.3 Mn 0.3
[redacted] N_2, coupon (NSHK1)	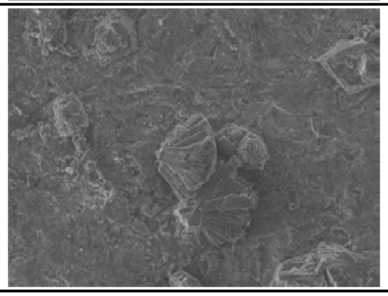	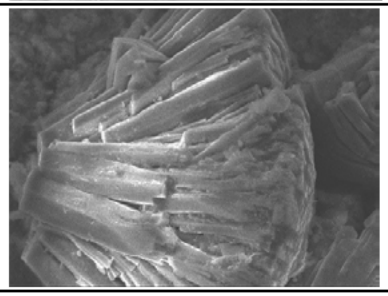	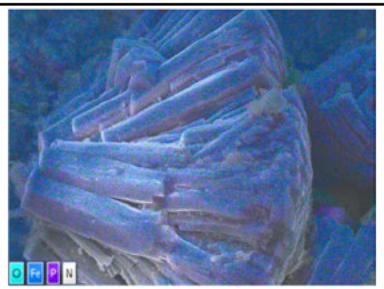	Map Sum Spectrum At% O 57.7 C 17.9 Fe 12.0 P 6.2 Mg 4.4 Si 0.7 Ca 0.4 Al 0.3 Mn 0.2

© ROSEN
This document is classified as confidential

[redacted] H_2, coupon (HSFK1)	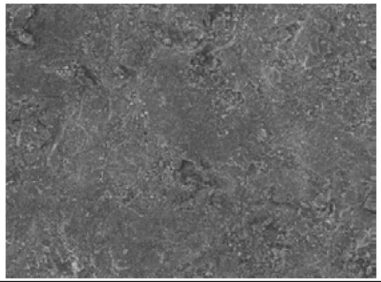	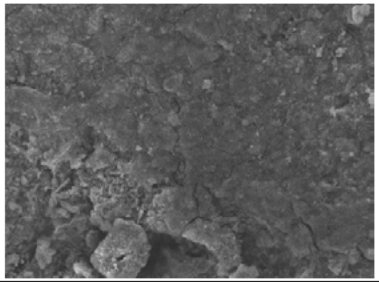	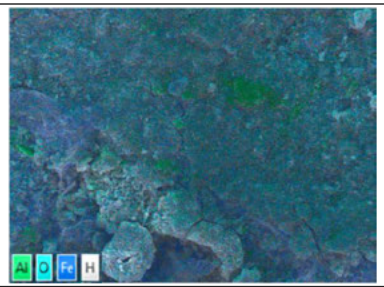	Map Sum Spectrum At% O 42.3 Fe 33.0 C 18.5 Al 3.5 P 0.9 Si 0.7 Ca 0.3
[redacted] N_2, coupon (NSFK1)	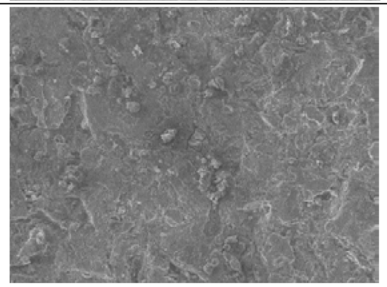	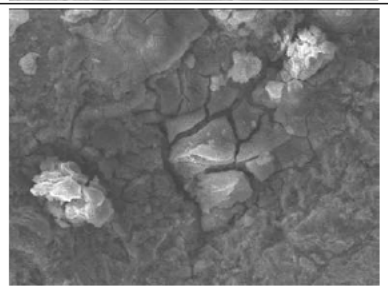	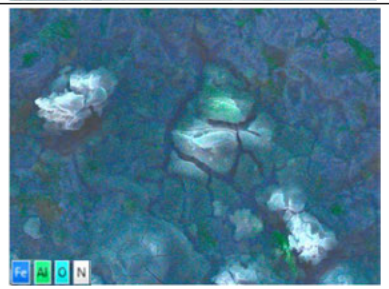	Map Sum Spectrum At% O 40.6 Fe 37.1 C 15.3 Al 3.1 Si 0.9 P 0.7 Ti 0.6 Na 0.5 Mn 0.3 Mg 0.2 S 0.2 Ca 0.2
[redacted] H_2, coupon (HSWK1)	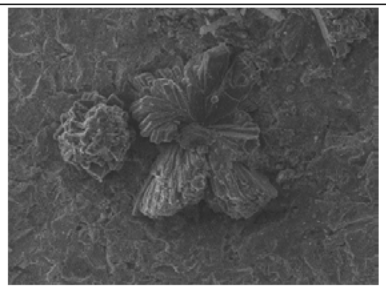	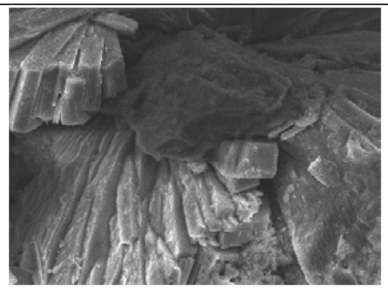		Map Sum Spectrum At% Fe 52.3 O 22.2 C 17.6 Al 3.7 P 1.4 Si 0.8 Ca 0.7 Mn 0.5

© ROSEN
This document is classified as confidential

[redacted] N_2, coupon (NSWK2)	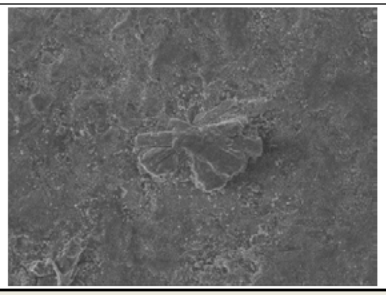	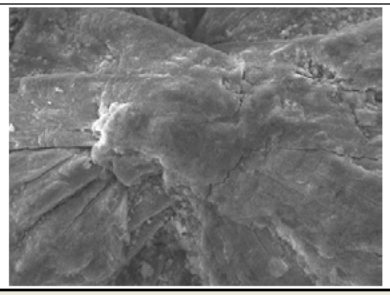	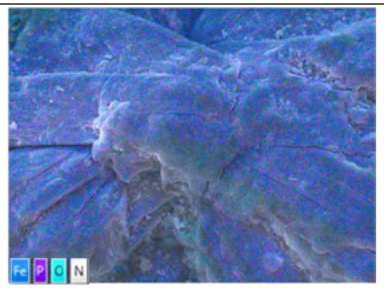	Map Sum Spectrum At% O 55.4 Fe 15.1 C 14.7 P 9.6 Mg 4.0 Si 0.3 Al 0.3 Mn 0.2 Ca 0.2
CO_2				
[redacted] H_2, coupon (HCHK2)	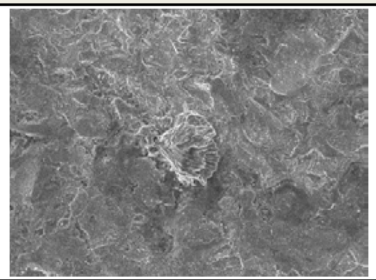	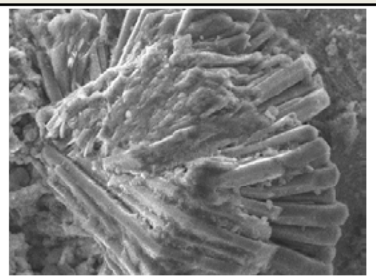	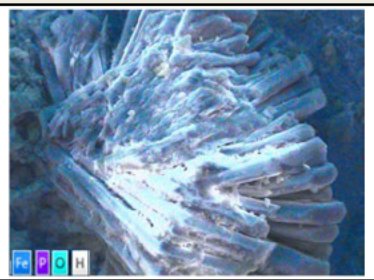	Map Sum Spectrum At% O 55.7 Fe 16.8 C 15.9 P 6.3 Mg 2.9 Ca 0.8 Al 0.7 Si 0.6 Mn 0.4
[redacted] N_2, coupon (NCHK2)	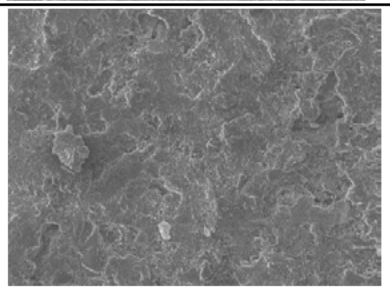	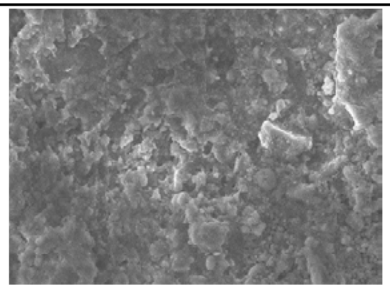	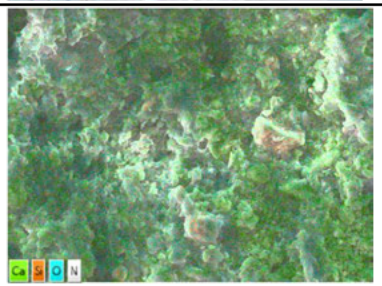	Map Sum Spectrum At% O 58.9 C 12.3 Fe 9.7 Ca 8.4 Si 6.2 Al 3.1 K 0.6 Mg 0.4 P 0.3

© ROSEN
This document is classified as confidential

[redacted] H_2, coupon (HCFK2)	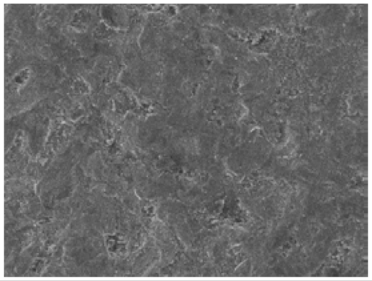	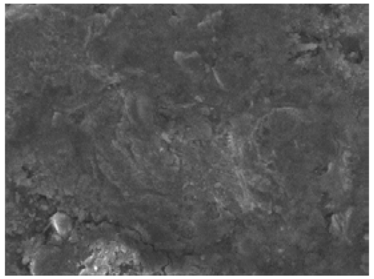	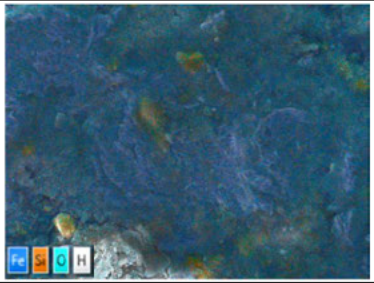	Map Sum Spectrum At% O 36.3 Fe 35.8 C 20.5 Al 2.5 Si 2.4 Ca 0.6 P 0.6 S 0.3 Mn 0.3 Cl 0.3
[redacted] N_2, coupon (NCFK2)	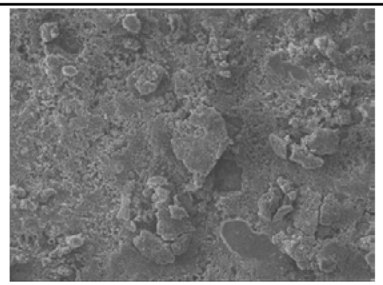	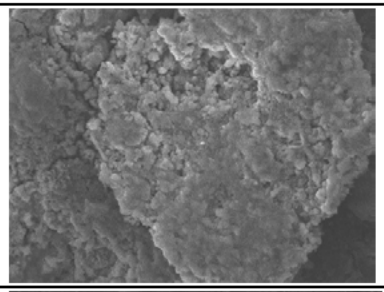		Map Sum Spectrum At% O 49.9 Fe 35.9 C 11.4 Si 1.1 Al 0.9
[redacted] H_2, coupon (HCWK1)	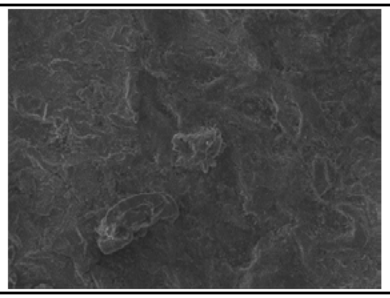	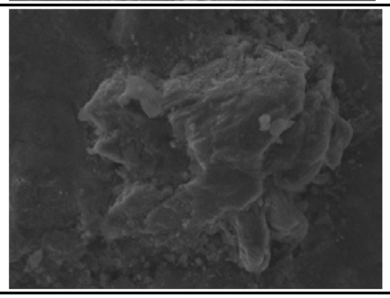	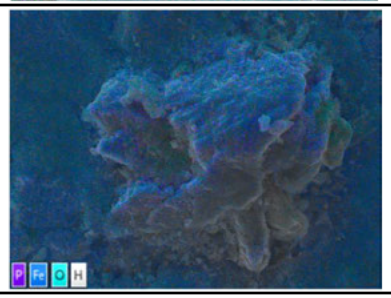	Map Sum Spectrum At% O 43.1 Fe 32.8 C 16.8 P 2.9 Si 1.3 Al 1.2 Mg 0.9 Mn 0.4 Ca 0.3 Cl 0.2

© ROSEN
This document is classified as confidential

[redacted] N_2, coupon (NCWK3)	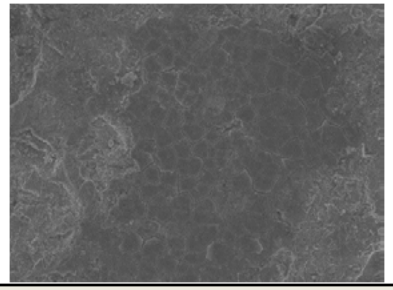	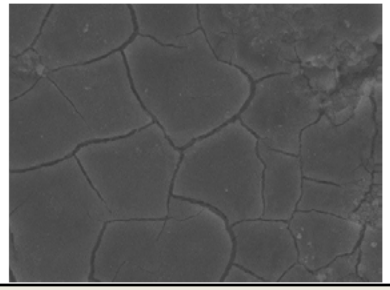	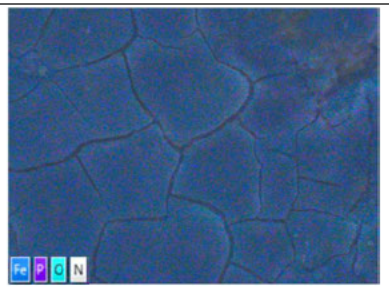	Map Sum Spectrum At% O 51.9 Fe 26.2 C 10.2 P 7.2 Ca 2.5 Mg 0.9 Al 0.6 Mn 0.3
Nitrate				
[redacted] H_2, coupon (HNHK2)	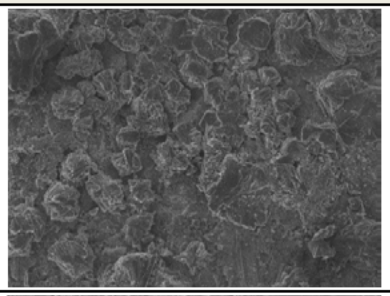	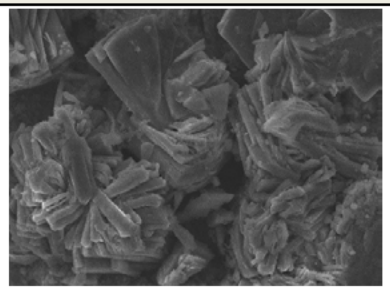	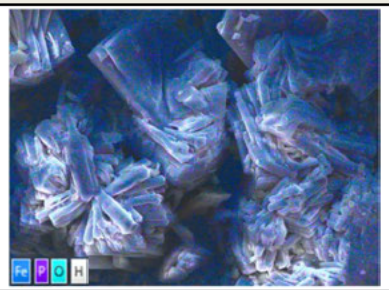	Map Sum Spectrum At% O 61.9 Fe 14.4 C 8.6 P 8.2 Mg 5.3 Ca 0.9 Al 0.4 Si 0.3
[redacted] N_2, coupon (NNHK2)	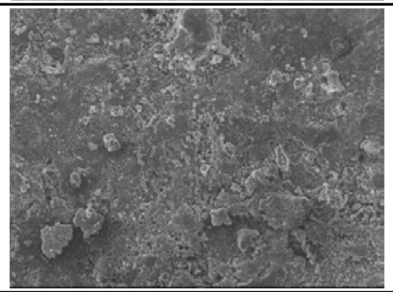	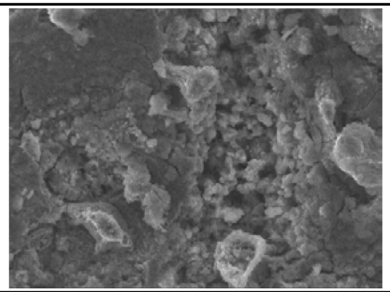	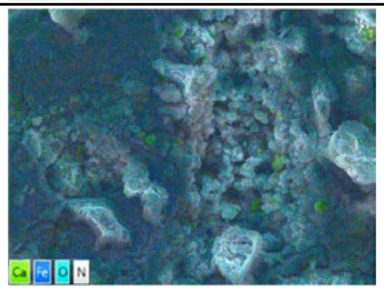	Map Sum Spectrum At% O 44.6 Fe 39.7 C 12.5 Al 0.7 Ca 0.6 Cl 0.6 Si 0.5

© ROSEN
This document is classified as confidential

[redacted] H_2, coupon (HNFK1)	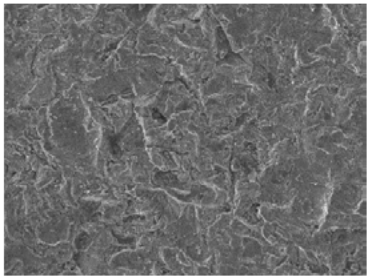	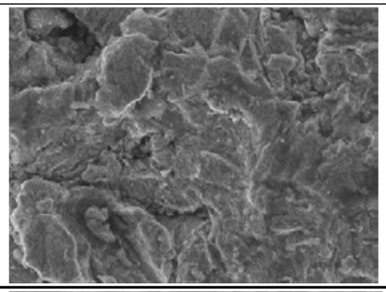	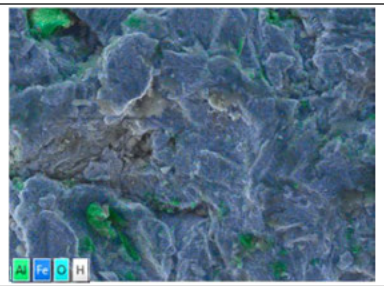	Map Sum Spectrum At% Fe 48.5 C 22.8 O 21.5 Al 4.2 Si 0.6 P 0.6 Mn 0.4 Mg 0.4 Ti 0.3 Ca 0.3 S 0.3
[redacted] N_2, coupon (NNFK2)	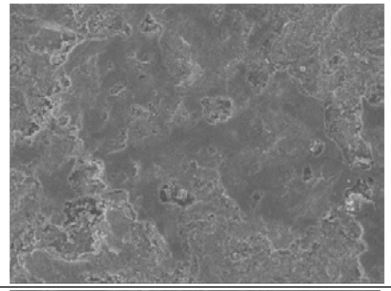	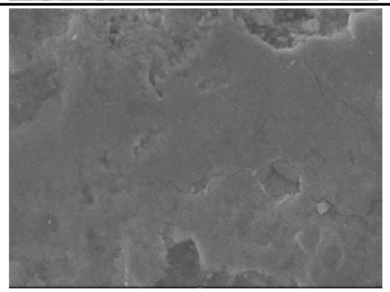	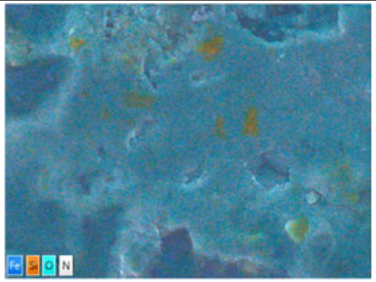	Map Sum Spectrum At% O 53.8 Fe 32.8 C 9.2 Si 1.8 Al 1.4
[redacted] H_2, coupon (NWK2)	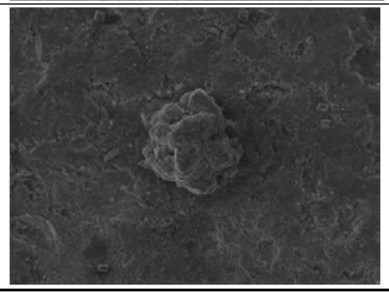	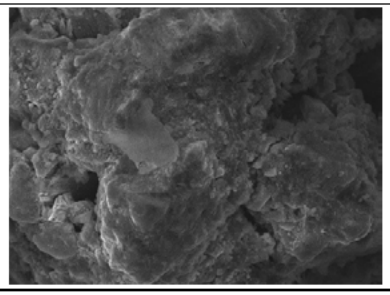	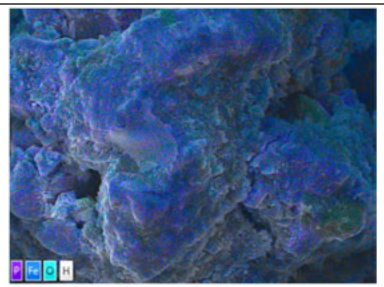	Map Sum Spectrum At% O 46.8 C 25.2 Fe 15.4 P 5.3 Mg 2.6 Si 2.3 Al 1.1 Ca 0.6 Mn 0.3 S 0.3

© ROSEN
This document is classified as confidential

[redacted] N_2, coupon	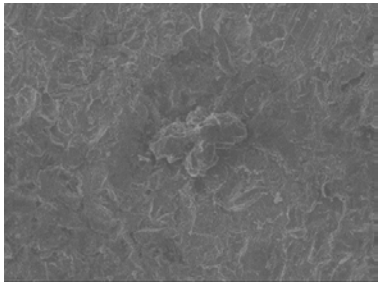	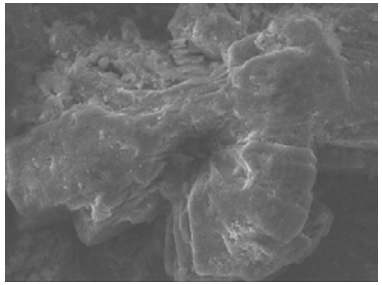	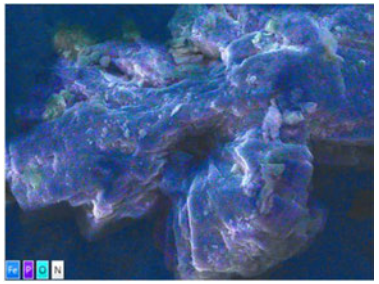	Map Sum Spectrum At% O 52.5 Fe 17.8 C 15.1 P 6.5 Mg 3.7 Si 2.4 Al 1.2 Mn 0.4 Ca 0.2

© ROSEN
This document is classified as confidential

APPENDIX F PRINCIPAL COORDINATE ANALYSIS ON SOIL TREATMENTS

F.1 [redacted] PCoA

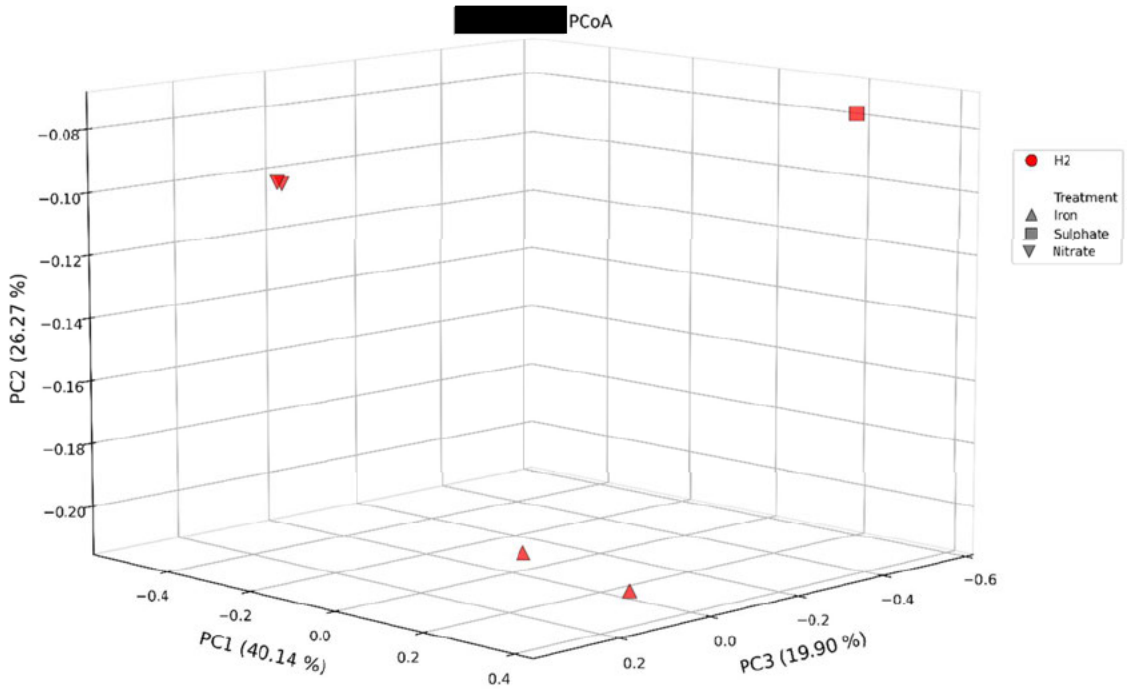

Figure 1. [redacted] PCoA

F.2 [redacted] PCoA

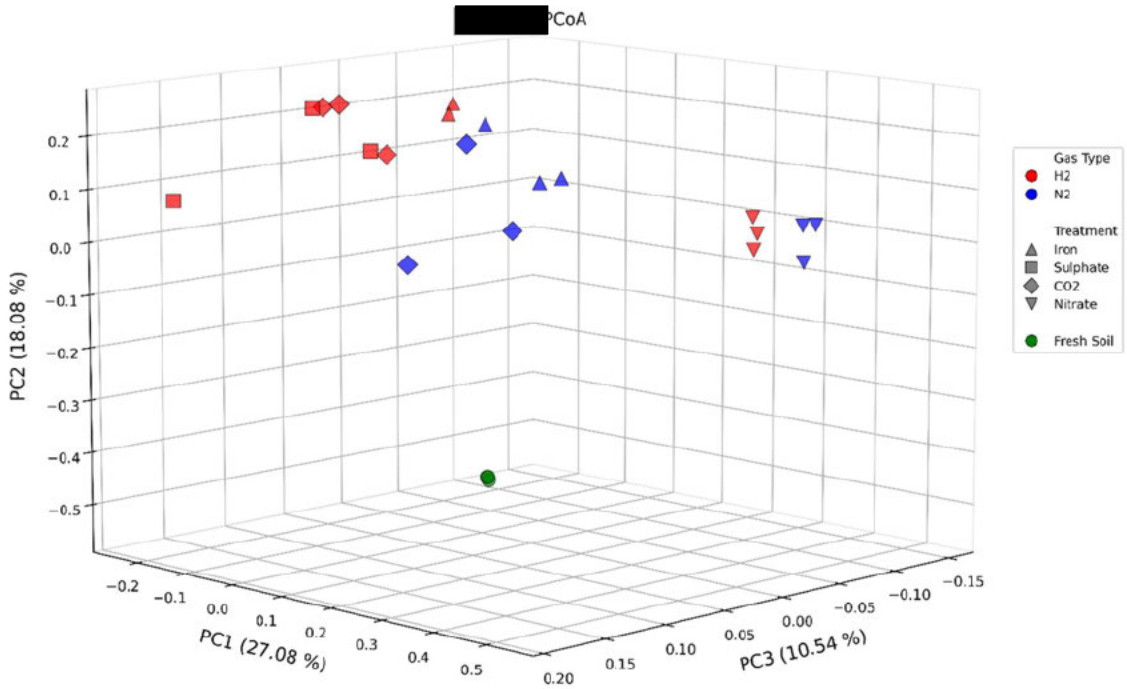

Figure 2. [redacted] PCoA

F.3 [redacted] PCoA

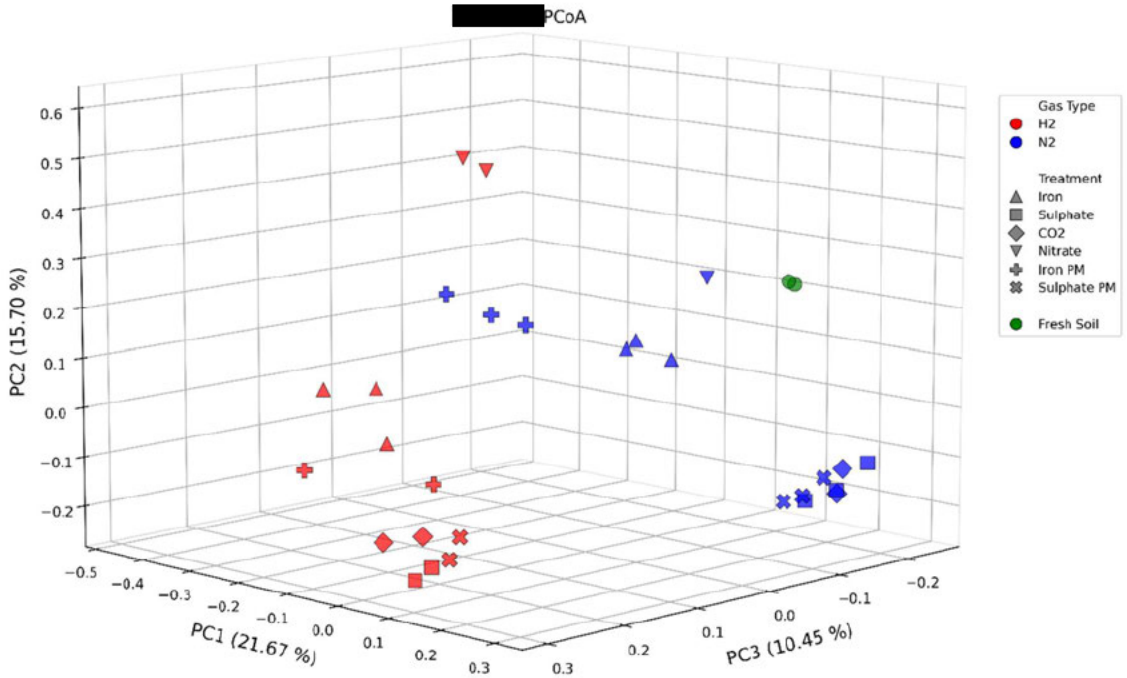

Figure 3. [redacted] PCoA

© ROSEN
This document is classified as confidential